GEORGIA INSTITUTE OF TECHNOLOGY — OFFICE OF CONTRACT ADMINISTRATION

PROJECT ADMINISTRATION DATA SHEET

[X] ORIGINAL [ ] REVISION NO. ____

Project No. E-21-638 (R5991-0A0) GTRC/~~GIT~~ DATE 7/ 25/ 85

Project Director: K.R. Davey School/~~Dept~~ EE

Sponsor: Argonne National Lab
Argonne, Illinois 60439

Type Agreement: Agreement 51772401 under Prime Contract 31-109-ENG-38 (DOE)

Award Period: From 7/15/85 To ~~9/30/85~~ ~~9-30-86~~ 12-31-85 (Performance) 9/30/86 (Reports)

Sponsor Amount:	This Change ~~9-30-86~~ 9-30-87	Total to Date
Estimated: $		$
Funded: $	8,000	$ 8,000

Cost Sharing Amount: $ N/A Cost Sharing No: N/A

Title: Transient Electromagnetic Analysis

ADMINISTRATIVE DATA OCA Contact Ralph Grede x4820

1) Sponsor Technical Contact:

2) Sponsor Admin/Contractual Matters:
Ms. Dianne Hutchinson
Senior Contract Specialist
Argonne National Laboratory
4700 South Cass Ave.
Argonne, Ill 60439
(312) 972-7955

Defense Priority Rating: N/A Military Security Classification: N/A
(or) Company/Industrial Proprietary: ____

RESTRICTIONS

See Attached N/A Supplemental Information Sheet for Additional Requirements.

Travel: Foreign travel must have prior approval – Contact OCA in each case. Domestic travel requires sponsor approval where total will exceed greater of $500 or 125% of approved proposal budget category.

Equipment: Title vests with U.S. Government - Article x-(c)-(3)

COMMENTS:

This is a fixed price instrument.

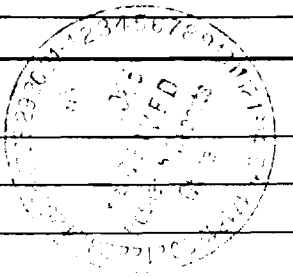

COPIES TO:

SPONSOR'S I. D. NO. 02.240.008.85.002

Project Director
Research Administrative Network
Research Property Management
Accounting
Procurement/GTRI Supply Services
Research Security Services
Reports Coordinator (OCA)
Research Communications (2)
GTRC
Library
Project File
Other A. Jones

FORM OCA 65:285

GEORGIA INSTITUTE OF TECHNOLOGY OFFICE OF CONTRACT ADMINISTRATION

SPONSORED PROJECT TERMINATION/CLOSEOUT SHEET

Date 5/19/88 ~~12/29/87~~

Project No. E-21-638 School/~~Lab~~ EE

Includes Subproject No.(s) N/A

Project Director(s) K. Davey GTRC / ~~GIT~~

Sponsor Argonne National Lab Argonne, Illinois 60439

Title Transient Electromagnetic Analysis

Effective Completion Date: 9/30/87 (Performance) 9/30/87 (Reports)

Grant/Contract Closeout Actions Remaining:

- [ ] None
- [X] Final Invoice or Final Fiscal Report
- [X] Closing Documents
- [X] Final Report of Inventions
- [X] Govt. Property Inventory & Related Certificate
- [ ] Classified Material Certificate
- [ ] Other

Continues Project No. Continued by Project No.

COPIES TO:

Project Director
Research Administrative Network
Research Property Management
Accounting
Procurement/GTRI Supply Services
Research Security Services
Reports Coordinator (OCA)
Legal Services

Library
GTRC
Research Communications
Project File
Other Duane Hutchison
Angela DuBose

FORM OCA 69.285

E-21-638

GEORGIA INSTITUTE OF TECHNOLOGY
SCHOOL OF ELECTRICAL ENGINEERING
ATLANTA, GEORGIA 30332

TELEPHONE: (404) 894-2961

January 21, 1986

Ms. Dianne Hutchinson
Senior Contract Specialist
Argonne National Laboratory
4700 South Cass Ave.
Argonne, IL 60439

SUBJECT: Contract No. 31-109-ENG-38, Project Director - Dr. K. R. Davey, Monthly Reports

Dear Ms. Hutchinson:

Enclosed please find Monthly Reports for the periods 10/1/85 - 10/31/85 and 11/1/85 - 11/30/85 for the above referenced project per contract specifications. If you have any questions or comments, please do not hesitate to contact Dr. Davey at 404/894-2925.

Sincerely,

Cindy Meyer
Administrative Assistant

CM
Enclosures

GEORGIA INSTITUTE OF TECHNOLOGY
SCHOOL OF ELECTRICAL ENGINEERING
ATLANTA, GEORGIA 30332
TELEPHONE: (404) 894- 2925

January 10, 1986

To: Argone National Labs

From: Kent Davey

Subject: Monthly Progress Report on Contract E21-638; 12/15/85

In unraveling eigenvalues to the short cylinder, we have found that the shorter cylinder has a multiplicity of eigenvalues; compressed considerably more as the length distends. How does one determine the relative importance of each eigenvalue in governing the total field? In linear algebra, we find eigenvectors and weight them appropriately according to their initial conditions. In our problem, we use the initial fields and the integral relations (not all null fields) to dictate this weighting. It appears that we must assume the field to be a superposition of components each with its own decay, $c_i e^{-\lambda_i t}$. Only one choice of c's will be consistent with the initial field at time t=o+. One then convolves this impulse response field with the true external field time profile as was done in the 2-d case. We shall attempt this analyis in the coming months.

KRD/mjc

GEORGIA INSTITUTE OF TECHNOLOGY
SCHOOL OF ELECTRICAL ENGINEERING
ATLANTA, GEORGIA 30332

TELEPHONE: (404) 894- 2925

January 10, 1986

To: Argonne National Labs

From: Kent Davey

Subject: Monthly progress report on contract E21-638 for 11/15/85

The solution of boundary integral equations using the null field approach was the focus of activity this month. Meaningful solutions are generally insensitive to the placement of the null points only to a limited extent. For every interface (and for each basis function) one must use 2 null points (one on either side of the interface). The 2-d cylinder is a 3 region problem; the identification matrix governing the solution of the 3-D problem is never full for a 3 region problem. When one attempts to force the regions to be connected (i.e., via an air bridge) and thus make the matrix full, an incorrect solution results. The effect is witnessed in the 3-D problem as well. One can view the short cylinder as a 3 region problem (outside, conductor, inside) with an air-air interface at the cylinder ends. In doing so, it is possible to arrange the matrix so that it is not full and arrive at a correct solution for eigenvalues. The full matrix is rather unstable it appears in generating eigenvalues. This problem will be examined further in the coming months.

KRD/mjc

MONTHLY PROGRESS REPORT FOR ARGONNE CONTRACT E21-638

by

Kent Davey
Georgia Institute of Technology

Period Covered: January 1986

During this period, research was focused on the completion of the two-dimensional (2-D) code and the analysis of the three-dimensional (3-D) problem. It is noted that the transient field response for the large, medium, and small FELIX cylinders were in good agreement with experimental data. The eigenvalue approach seems to be a sound and appropriate method of analyzing the fields in the time domain. No marching via an implicit or explicit Crank-Nicholson scheme was necessary. In changing from 2-D to 3-D, we simply interchanged our Green's function substituting what was formally our 2-D Hankel function for an exponential function. No success at all for predicting what we thought was the correct eigenvalue for the short 3-D FELIX cylinder was realized. It was during this time that we suspected trouble either with the second order vector potential method utilized to break the vector Helmholtz problem into two scaler problems, or the assumed basis functions that we were using. We completed the month of January with more analysis of the 2-D problem. In particular, we examined what happens if one works the 2-D problem as if it were a two region problem connected by a bridge between the inner air region and the outer air region. We noted that this effectively loaded the eigenvalue matrix with nonzero values where formally zeros existed. This change appeared to yield considerable errors in terms of our predictive capability into the matrix. Springboarding from this knowledge, we suspected that perhaps an appropriate way to address the 3-D problem was by considering it as three separate regions having an artificial boundary on the inner cylinder air to outside air interface at the ends of the cylinder.

MONTHLY PROGRESS REPORT FOR ARGONNE CONTRACT E21-638

by

Kent Davey
Georgia Institute of Technology

Period Covered: February 1986

During this month, the focus of research was entirely on the three-dimensional (3-D) code. We continued to consider the FELIX cylinder as a three region problem. A breakthrough occurred towards the beginning of the month when we realized the source of much of our former error lie in the integration routine being used. We were using a Gauss-Legendre integration quadrature scheme with 32 points. When integrating over the entire length of the cylinder, we found that was not accurate; we then switched to a 96 Gauss-Legendre scheme and as a second check multiple integrations over the region employing a 32 points Gauss-Legendre algorithm. During this process, the inner air region was considered separate from the outer air region. The correction and the integration seems to have stabilized the prediction of eigenvalues considerably. The prediction of those values for the first few modes in the axial direction appears to agree well with the quasi 2-D limit which we discussed in our former progress report.

MONTHLY PROGRESS REPORT FOR ARGONNE CONTRACT E21-638

by

Kent Davey
Georgia Institute of Technology

Period Covered: March 1986

Having realized some success through the improvement of our integration scheme, we were able to predict eigenvalues that agreed reasonably well with limiting cases that we knew to be correct in the two-dimensional (2-D) realm. It was during this month that we began to question the meaning of the eigenvalues which we were predicting. The interpretation that seems to be most sound is that for every axial mode of the field whose shape can fit into a sinusoid of argument $(n\pi/\ell)$ there exists a unique and well defined eigenvalue representing the characteristic decay time of a magnetic field having that shape. The different modes are delineated only by their axial dependence. By the nature of the initial field excitation, it appears that only magnetic fields having a sinusoidal dependence in the θ direction can be excited. For every axial mode therefore, there exists really a number of characteristic decay times. However, for each mode the first decay time is well removed from the hierarchical times; these secondary or hierarchical eigenvalues represent diffusion through the thickness of the cylinder preserving the axial dependence characteristic of that mode. The total number of eigenmodes characterizing a problem is totally defined by the initial field excitation. For the FELIX cylinder, the initial excitation is nearly uniform at time $t = 0$; thus, the Fourier decomposition of that flat field dependence at $t = 0$ is a sum of sinusoids, each having the weighting $\frac{4}{n\pi}$, where n is odd. One can, of course, envision an initial field excitation which would excite only selected modes, and thus we would expect to see very precise decay times for each one of those modes.

It was at this time that we discovered the work that Larry Turner was conducting at Argonne seemed to substantiate our findings. The conclusion on both fronts was that one could not characterize the data being measured with only one or two characteristic decay times. Theoretically, this of course follows from the fact that the initial field excitation cannot be decomposed into only two eigenmodes.

MONTHLY PROGRESS REPORT FOR ARGONNE CONTRACT E21-638

by

Kent Davey
Georgia Institute of Technology

Period Covered: April 1986

Based on discussions both at the Rutherford Appleton Laboratory and the International Conference on Mathematical Modeling with Dick Shaw, it was thought that addressing the three-dimensional (3-D) problem with the artificial boundary as if it had three regions was indeed unnatural and perhaps unnecessary. In the mid 60s, many researchers, using the null field technique that we are employing, discovered that often the prediction of resonances in scattering problems was not accurate. There is a way of making that prediction sound however. In scattering theory, the solution is to place the points characterizing unknowns on the surface itself, but in addition to those points, we place extra null field points outside the surface. Using this trick, we end up with more equations than there are unknowns; the total problem is thus solved as a least squares minimization of the total error incurred by all of the equations. Upon applying this technique, we found that considerable success was realized in that the three region artifice was no longer necessary. Considering all the air to be region one and all the conductor to be region two, and the twain having only one interface between them; a solid and correct eigenvalue prediction was realized for the short cylinder. The curious case in point is that for the large cylinder and medium cylinder, an additional eigenvalue seems to have appeared, one that we had not reckoned with using the null field approach only. At present we are attempting to resolve the dilemma to see whether or not the second eigenvalue predicted really has any bearing on the problem. The method of resolution we

are attempting is to predict the eigenvectors associated with these two eigenvalues for a given mode.

ARGONNE NATIONAL LABORATORY-GEORGIA TECH CONTRACT E21-638

PROGRESS REPORT/ASSESSMENT OF FUTURE DIRECTIONS

August 4, 1986

The major work thus far has concentrated on an eigenvalue prediction of the transient fields generated in the FELIX experiments. These eigenvalues, which dictate the temporal evolution of the field, are predicted using a combination of integral equations with points both on the object interface and in the null field zone. The integral equations are written for the 3-D problem using a second order vector potential representation. Global basis functions are used to represent the spatial field character.

The most promising aspect of this work is the accuracy of field prediction achievable with only a few unknowns. Results for the 2-D and 3-D cylinder show this approach to be quite accurate. With more complicated structures, we observed that for each field shape or mode assumed, more than one significant eigenvalue was observed. This, of course, suggests that the shapes assumed were not true eigenvectors, in the sense that it is used in linear algebra. Inclusion of the higher order eigenvalues gives a very close agreement with data.

One begins to question whether or not the advantages of the eigenvalue approach are worth the effort in more complicated geometries. The second question being raised is how difficult will a prediction of eigenmodes become as the geometry becomes more complex? It is clear that use of model shapes is quite an advantage in any computation since it reduces the number of unknowns significantly. Scaled experimental data may offer some insight as to the most dominant modes (those that stay around the longest), but not the others. It may, therefore, be expeditious to seek a method which capitalizes on known

experimental data at different snapshots in time to realize a "smart" global basis set. Note, this global set will not be an eigenmodel set, so an alternate technique must not be dependent on eigenmodes as such, only general shapes.

The use of time/space Green's functions may be one such technique that allows this distinction while still utilizing a small number of "smart" global basis functions. This equation characterizing vector potential $\underline{A}$ in a 2-D problem is

$$C\,A(p,t) = \int_{t_o}^{t} d\tau\left[\iint G(P-Q,t-\tau)\mu_s J_s ds\right] - \sigma \iint G(P-Q,t-\tau)A(Q,t_o)ds$$

$$- \int_{t_o}^{t} d\tau\left[\int \left(H(P-Q,t-\tau)A(Q,\tau) - \frac{1}{\mu_o} G(P-Q,t-\tau)\,\frac{\partial A(Q,\tau)}{\partial n}\, d\ell\right]\right] .$$

where

$$G(P-Q,t-\tau) = \frac{-\mu_o}{4\pi(t-\tau)} \exp \frac{-\mu_o \sigma |r_{pq}|^2}{4(t-\tau)}$$

$$H(P-Q,t-\tau) = \frac{\mu_o \bar{\sigma r}_{pq} \cdot \hat{n}_Q}{8\pi(t-\tau)^2} \exp \frac{-\mu_o \sigma |r_{pq}|^2}{4(t-\tau)}$$

$$C = \begin{cases} 1 & P \text{ in domain of interest} \\ 1/2 & P \text{ on interface} \\ 0 & P \text{ out of the domain of interest (null field)} \end{cases}$$

Note, if the interval $(t-\tau)$ is fixed, the spatial integral over the region of interest need be performed only once. Furthermore, μ and σ can be adjusted

piecewise in space/time if need be. I think the procedure can be made more stable if both null field and interface points are used, based on previous work this year. I propose that this variation of the space/time Green function approach be examined on the FELIX problems to estimate its applicability for the more complicated tokomak structures.

GEORGIA INSTITUTE OF TECHNOLOGY
SCHOOL OF ELECTRICAL ENGINEERING
ATLANTA, GEORGIA 30332

TELEPHONE: (404) 894-7337

March 3, 1987

Ms. Dianne Hutchinson
Senior Contract Specialist
Argonne National Laboratory
4700 South Cass Avenue
Argonne, IL 60439

Subject: Contract No. 51772401 under Prime Contract 31-109-ENG-38 (DOE)

Dear Ms. Hutchinson:

Enclosed please find copies of the Status Report for the period 1/1/87-3/1/87 on the above noted contract, "Transient Electromagnetic Analysis."

If you have any questions, please feel free to contact me.

Sincerely yours,

Pam Majors
Administrative Assistant

pm
Enclosures

Bi-monthly report on Argonne Contract E21-638
March 2, 1986
Kent Davey

This is the first report on the revised contract; because the funds were only recently released, no formal work was begun and will not begin until spring quarter. Some additional thought was given to the use of the time-space Green's function approach. Among the difficulties with this approach is the fact that one of the terms involves a temporal integration over all time from the start of the transient. Not only is this bothersome numerically, but it can be quite prone to numerical instability the further into the transient one gets. One approach to this problem is to approximate this integral as a Gauss-Legendre sum and solve implicitly for the coefficients of the sum as part of the matrix solution. In this regard the approach parallels the Crank-Nicholson scheme. What is preserved is the simplicity of the global basis functions. The effect of multiple eigenfunctions is accounted for implicitly. This will be the focus of activity as of April 1.

GEORGIA INSTITUTE OF TECHNOLOGY
SCHOOL OF ELECTRICAL ENGINEERING
ATLANTA, GEORGIA 30332

TELEPHONE: (404) 894-7337

May 11, 1987

Ms. Dianne Hutchinson
Senior Contract Specialist
Argonne National Laboratory
4700 South Cass Avenue
Argonne, IL 60439

Subject: Contract No. 51772401 under Prime Contract 31-109-ENG-38 (DOE)
Project Director: K. R. Davey

Dear Ms. Hutchinson:

Enclosed please find copies of the Status Report for the period 3/1/87-5/1/87 on the above noted contract, "Transient Electromagnetic Analysis."

If you have any questions, please feel free to contact me.

Sincerely yours,

Pam Majors
Administrative Assistant

pm
Enclosures

GEORGIA INSTITUTE OF TECHNOLOGY
SCHOOL OF ELECTRICAL ENGINEERING
ATLANTA, GEORGIA 30332

TELEPHONE: (404) 894-

Bi-monthly report on Argonne Contract E21-638
May 8, 1986
Kent Davey

Significant progress was made on the project over the past two months. A formulation of the time - space Green's formulation was completed showing several errors of omission or commission in the paper by Alain Nicholas ("A boundary Integral Equation Approach ..",IEEE Mag, vol MAG-19,no.6, November 1983, pp 2453f) on which this approach is based. The most serious difficulty is that the Green's function is singular at the end points in time; thus, no finite difference Crank - Nicholson scheme is suitable as was originally thought. Instead a rather unique approach using the Gauss - Laquerre integration method is employed. The problem becomes an integral equation in time and a boundary integral equation in space. Global basis functions are employed in space for the vector potential and its normal derivative. The temporal weighting constants are solved consecutively based on all previously calculated values.

The approach has been implemented to date on the infinite (2D) FELIX cylinder. The general decay appears to match that predicted by the eigenvalue approach. It should be noted that this approach is not penalized with more complicated structures as is the eigenvalue technique which must sort out higher order eigenvalues for every spatial mode shape.

GEORGIA INSTITUTE OF TECHNOLOGY
SCHOOL OF ELECTRICAL ENGINEERING
ATLANTA, GEORGIA 30332

TELEPHONE: (404) 894-7337

July 7, 1987

Ms. Dianne Hutchinson
Senior Contract Specialist
Argonne National Laboratory
4700 South Cass Avenue
Argonne, IL 60439

Re: Contract No. 51772401 under Prime Contract 31-109-ENG-38 (DOE)
Project Director: K,R. Davey

Dear Ms. Hutchinson:

Enclosed please find copies of the Status Report for the period 5/]/87-6/30/87 on the above noted contract, "Transient Electromagnetic Analysis."

If you have any questions, please feel free to contact me.

Sincerely

Pam Majors
Administrative Assistant

PM
enclosures

Bimonthly Project Report on Contract #E21-638

Prediction of Transient Electromagnetic Fields Using the Time Space Green's Function Technique

by

Kent Davey
School of Electrical Engineering
Georgia Institute of Technology
Atlanta, Georgia 30332-0250

June 1987

The time space Green's function technique has been successfully implemented in the two-dimensional FELIX cylinder experiment. Although the field predictions are slightly higher by about 15% over the experimental measurements, they are quite well in line with the eddy net predictions. As implemented now, the program calculates the spatial matrices generic to the problem at hand once. The progression of the solution in time is realized extremely quickly and efficiently. One is essentially solving the matrix equation $\mathbf{Ax} = \mathbf{b}$, where $\mathbf{A}$ is constant for all time and $\mathbf{b}$ is dependent on previously calculated time values. With the stipulation that one keeps the time step Δt constant throughout the process, only the right hand side of the matrix equation changes as one progresses. This fast algorithm has indeed been checked and verified for accuracy with a two-dimensional analog of the FELIX cylinder experiment.

The three-dimensional equivalent for the cylinder experiment has been coded and is now being debugged. The same approach calculating the entire time sequence evolution of the field is being adopted. Thus, although the spatial matrix calculations are "n" times faster, once accomplished the temporal solution progresses as quickly as in the two-dimensional case. Calculations thus far indicate that integration points in close proximity to selected field points are extremely important during the integration calculation procedure. Although it's too soon to tell, preliminary calculations suggest that some shortcuts can be realized in the calculation of the governing matrix due to this effect.

The objective in the next bimonthly period will be to complete the debugging of the three-dimensional program and begin to sort out how to generalize the technique for arbitrary geometries.

GEORGIA INSTITUTE OF TECHNOLOGY
SCHOOL OF ELECTRICAL ENGINEERING
ATLANTA, GEORGIA 30332

TELEPHONE: (404) 894-7337

October 19, 1987

Ms. Dianne Hutchinson
Senior Contract Specialist
Argonne National Laboratory
4700 South Cass Avenue
Argonne, IL 60439

RE: Contract No. 51772401 under Prime Contract 31-109-ENG-38 (DOE)
Project Director: K. R. Davey

Dear Ms. Hutchinson:

Enclosed please find copies of the Status Report for the periods 6/1/87-7/30/87 and 8/1/87-9/30/87 on the above referenced contract, "Transient Electromagnetic Analysis."

If you have any questions, please feel free to contact me.

Sincerely,

Pam Majors
Research Administrator

pm
Enclosures

Bimonthly Report to

Argonne National Laboratory

for

Contract E21-638

covering

June and July 1987

by

Kent Davey
School of Electrical Engineering
Georgia Institute of Technology
Atlanta, Georgia 30332-0250

During these two months, focus of attention was on the implementation of the two-dimensional code and the checking of its accuracy. The code was checked by comparing results with those recorded at the First International Eddy Current Workshop at the Rutherford Appleton Laboratory, March 1987, at Oxford, England. The results indicate that the predictions via the time space Green's function approach are quite good in comparison to other two-dimensional codes. The solution was implemented using only four unknowns taking care to represent azimuthal falloff in the field with the sinusoidal variation. The full usefulness of the technique it is felt must be seen after its implementation in a three-dimensional problem. It is for this reason that the three-dimensional calculations have begun. How much flexibility the code allows in the choice of time step is still an unknown.

Bimonthly Report to

Argonne National Laboratory

for

Contract E21-638

covering

August and September 1987

by

Kent Davey
School of Electrical Engineering
Georgia Institute of Technology
Atlanta, Georgia 30332-0250

During these months, the three-dimensional codes have been successfully implemented and tested. Results are being compared to the data worked out by Thomas Summers in August 1985 for the FELIX cylinder experiments. The results indicate reasonably accurate prediction of the three-dimensional field. The results are, however, both encouraging and discouraging. The encouraging aspect of the work lies in the fact that even a three-dimensional field solution can be obtained using only four unknowns. The accuracy of the solution is, however, increased by incorporating additional eigenmodes to represent the axial field dependence. Of course, sinusoidal variation in the azimuthal correction is assumed throughout. A second aspect which is encouraging is seen in the fact that although a rather coarse time step was used, reasonably accurate results followed. The negative aspects of the work appear to be in the choice of the time step, that is, the solution is sensitive to one's choice of time step. Too coarse a time step yields unreliable field

predictions as one would suspect intuitively. On the other hand, pressing the time step to the other limit, making it too small, yields numerical problems. The integration in time is unbounded in one direction; this is handled quite well by the Gauss-Laguerre integration quadrature formula. When one makes the time step too small, however, the unknown which is embedded at this infinite time integration takes on a rather large weighting constant. The result is in numerical instability which yields poor results. It appears that we ought to seek an optimum choice based on the magnetic relaxation time characteristic of the problem. The accuracy of the method using such sparse number of unknowns does suggest and argue quite well for the usefulness of the approach.

THE CALCULATION OF TRANSIENT EDDY CURRENT FIELDS USING NULL FIELD INTEGRAL TECHNIQUES

by

Kent R. Davey
and
Hsiu Chi Han
School of Electrical Engineering
Georgia Institute of Technology
Atlanta, Georgia 30332-0250

July 1985

ABSTRACT

The transient eddy current problem is characteristically computationally intensive. The motivation for this research was to realize an efficient, accurate, solution technique involving small matrices via an eigenvalue approach. Such a technique is indeed realized and tested using the null field integral technique. Using smart (i.e., efficient, global) basis functions to represent unknowns in terms of a minimum number of unknowns, homogeneous eigenvectors and eigenvalues are first determined. The general excitatory response is then represented in terms of these eigenvalues/eigenvectors. Excellent results are obtained for the Argonne Felix cylinder experiments using a 4 x 4 matrix. Extension to the 3-D problem (short cylinder) is set up in terms of an 8 x 8 matrix.

Introduction

Approaches to transient eddy current solutions to date tend to fall into one of two categories [4-7]:

(1) Time domain developed by forward difference albeit explicit or implicit. Spatial discretizations are pursued in much the same way as present time harmonic problems.

(2) Time domain developed via the characteristic eigenvalues/eigenvectors of the system. The spatial domain is characteristically pursued via either finite difference or finite element techniques.

The first approach is computationally intensive, involving the solution of the entire spatial domain recursively throughout the time period of interest. The second approach is theoretically more efficient, but is frought with many other problems. To obtain an accurate spatial discretization, one must necessarily employ a sufficiently large number of nodal points. For every modal point there will result an eigenvalue and related eigenvector. It is the author's experience that most real world problems have only a handful of dominant eigenvalues; by far most of the eigenvalues generated by a finite element technique are both spurious and (hopefully) subdominant. High accuracy in the spatial field representation is bought with the price of generating a host of important eigenvalues, a potential source of considerable error. It is with the intent of capitalizing on the positive features of the eigenvalue approach while minimizing the size of matrices (and thus number of eigenvalues) that the present research was undertaken.

The general theory involving the use of the null field integral equations in determining eigenvalues is first developed. The theory is applied to the Argonne Felix cylinder experiments [1-3]. Predictions are compared to the

exact analytical expressions for the problem. Extension of the technique to the short cylinder is discussed briefly, such an extension being realized through an 8 x 8 matrix rather than through the 4 x 4 matrix used for the long cylinder.

General Theoretical Development

The solution of the general matrix equation

$$\underline{X}' = \underline{\underline{A}}\,\underline{x} + \underline{b} \tag{1}$$

is found by first assuming

$$\underline{x} = e^{\lambda t} \tag{2}$$

and solving the homogeneous eigenvalue problem

$$\underline{\underline{A}}\,\underline{x} = \lambda\,\underline{x} \tag{3}$$

for eigenvalues $\underline{\lambda}$ and eigenvectors $\underline{u}$, where

$$\underline{\lambda} = \begin{bmatrix} \lambda_1 & & & \\ & \lambda_2 & & \\ & & \ddots & \\ & & & \lambda_N \end{bmatrix}$$

$$\underline{u} = [\underline{x}_1 \quad \underline{x}_2 \quad \cdots \quad \underline{x}_N]$$

$\underline{x}_n$ = nth eigenvector

The temporal solution is written in terms of the particular solution $\underline{x}_p(t)$ as

$$\underline{x}(t) = \sum_{i=1}^{N} C_i \underline{x}_i e^{\lambda_i t} + \underline{x}_p(t) \ , \tag{4}$$

the C_i's being chosen to satisfy initial conditions.

Assuming temporal dependence $e^{-\lambda t}$ for all unknowns, the source-free magnetoquasistatic vector Helmholtz equation becomes

$$\nabla^2 \vec{A} + k^2 \vec{A} = 0 \tag{5}$$

where $k^2 = \lambda\mu\sigma$.

It is convenient from a pedagogical perspective to focus attention on the two dimensional object shown in Fig. 1, which has only a z-directed vector potential (the vector/subscript on $\vec{A}$ being henceforth dropped). The integral equation for A in each region can be written

$$\oint \left(\frac{\partial A_1'}{\partial n} G_1 - A_1' \frac{\partial G_2}{\partial n}\right) ds' = \begin{cases} A(r) & ; \ r \in \text{Domain 1} \\ A(r)/2 & ; \ r \text{ interface} \\ 0 & ; \ r \in \text{Domain 2} \end{cases} \tag{6}$$

$$-\oint \left(\frac{\partial A_2'}{\partial n} G_2 - A_2' \frac{\partial G_2}{\partial n}\right) ds' = \begin{cases} A(r) & ; \ r \in \text{Domain 2} \\ A(r)/2 & ; \ r \text{ interface} \\ 0 & ; \ r \in \text{Domain 1} \end{cases} \tag{7}$$

where

$G_1 = -\frac{j}{4} H_o^{(2)}(kr)$

$G_2 = -\ln(r)/2\pi$

$H_o^{(2)}$ = modified Hankel function of second kind, order zero.

Solution is realized by first assuming values for A_1 and $\partial A_1/\partial n$ in terms of a global basis set.

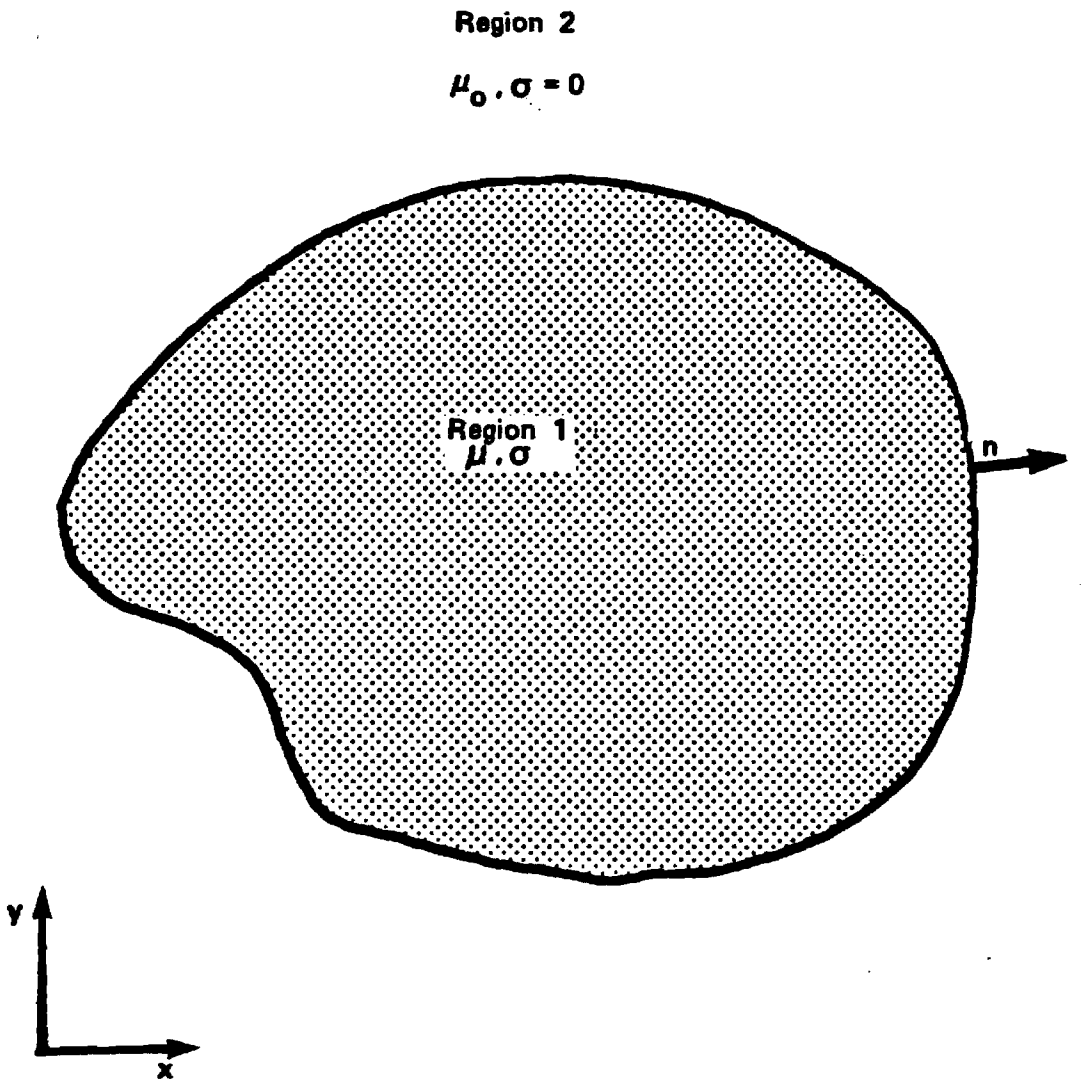

Figure 1. General two dimensional object characterized by a z - directed vector vector potential.

$$A_1 = \sum_{i=1}^{N} C_i \psi_i(\vec{r}) \tag{8}$$

$$\frac{\partial A_1}{\partial n} = \sum_{i=1}^{N} D_i \psi_i(\vec{r}) \tag{9}$$

(The basis functions in (8) and (9) will in general be identical but need not be for the analysis.) Boundary conditions on tangential $\vec{H}$ and normal $\vec{B}$ dictate that

$$A_1 = A_2 \tag{10}$$

$$\frac{1}{\mu} \frac{\partial A_1}{\partial n} = \frac{1}{\mu_o} \frac{\partial A_2}{\partial n} \tag{11}$$

so (8) and (9) characterize the problem entirely. The real advantage to the above approach comes about in the intelligent choice of $\psi_i(\vec{r})$. The more intelligent this choice, the smaller will be the determination matrix and thus the set of eigenvalues governing the problem. This choice can be adopted by analytical insight or experimental data taken, for instance, at $t = 0$, $t = t_{final}/2$, and $t = t_{final}$ (in which case $N = 3$).

Solution proceeds by arbitrarily choosing "N" points inside and outside the body. The "N" points outside the body are then used to write "N" null field equations using (6c) and the "N" points inside are used with (7c) to yield "N" more. These "2N" equations result in a matrix as follows:

$$\begin{Bmatrix} -\int \psi_1 \frac{\partial G_1}{\partial n} & -\int \psi_2 \frac{\partial G_1}{\partial n} & \cdots & \int \psi_1 G_1 \\ \cdots & \cdots & \cdots & \cdots \\ \int \psi_N \frac{\partial G_2}{\partial n} & \cdots & -\int \psi_n \frac{\partial G_2}{\partial n} \end{Bmatrix} \begin{Bmatrix} C_1 \\ \vdots \\ C_N \\ D_1 \\ \vdots \\ D_N \end{Bmatrix} \equiv \underline{\underline{F}} \begin{bmatrix} \underline{C} \\ \underline{D} \end{bmatrix} = 0 \tag{12}$$

The eigenvalues of the system immediately drop out as those values of k for which the determinant of the matrix $\underline{\underline{F}}$ in (12) is zero. These must be found of several nonlinear root solving techniques (e.g., Newton Raphson, Secant, etc.). Once the zero determinant values of ($\underline{\underline{F}}$) are known, a new matrix $\underline{\underline{F}}$ can be defined

$$\underline{\underline{F}}' = \underline{\underline{F}} + \underline{\lambda} \tag{13}$$

The eigenvectors $\underline{u}$ of $\underline{\underline{F}}'$, and thus of the original system, can be obtained via several numerical packages (e.g., QR algorithm, Jacobi iteration, etc.). The interfacial unknowns for all time is written in terms of the system eigenvectors $\underline{x}_1, \underline{x}_2, \cdots, \underline{x}_{2N}$ and the eigenvalues $\lambda_1, \lambda_2, \cdots, \lambda_{2N}$ as

$$\left\{ \begin{matrix} C_1 \\ \vdots \\ C_N \\ D_1 \\ \vdots \\ D_N \end{matrix} \right\} = \begin{bmatrix} \underline{C} \\ \underline{D} \end{bmatrix} = \sum_{i=1}^{2N} g_i e^{\lambda_i t} \underline{x}_i + \underline{x}_p(t) \tag{14}$$

where the g_i's are obtained from initial conditions. Typically, the field inside a conductor is known at $t = 0^+$ (identical to that before the transient); $\underline{x}_p(t)$ is the normal steady state solution. The interfacial unknowns are easily determined using "N" equations from (6a) and "N" null field equations (7c) to give a matrix equation for initial unknowns which is <u>not</u> homogeneous.

The Felix Cylinder Experiments

The methodology is now implemented for a 2-D, three region problem (Fig. 2). The Felix cylinder experiments involved three cylinders, one of which will be examined here. The cylinder is slit down its length. At t = 0, an external vertical field is allowed to collapse with time constant τ = 59.00 msec. We wish to predict the self-generated fields for all time. There is in addition an externally applied z-directed field. As will be shown, the length is long enough that for measurements in the center of the cylinder (at z = 0), the finite length, horizontal slits, and z-directed external field have no effect on the self-excited x-y field. The infinite cylinder with no slits will show an indiscernible difference in eddy current field at z = 0. Finite length effects must be considered when L < π/first eigenvalue "k" (this is roughly when L ≈ 3 * diameter).

The solution proceeds as follows. First, recognize that the following basis set satisfies all boundary constraints on A

$$A(r = a) = C \sin \theta \tag{15}$$

$$\frac{\partial A}{\partial r}(r = a) = D \sin \theta \tag{16}$$

$$A(r = b) = E \sin \theta \tag{17}$$

$$\frac{\partial A}{\partial r}(r = b) = F \sin \theta \tag{18}$$

Next evaluate 4 null field equations

$$0 = \int_0^{2\pi} \left\{D \sin \theta \, G_1 - C \sin \theta \frac{\partial G_1}{\partial r}\right\} a \, d\theta \; ; \; r > a \tag{19}$$

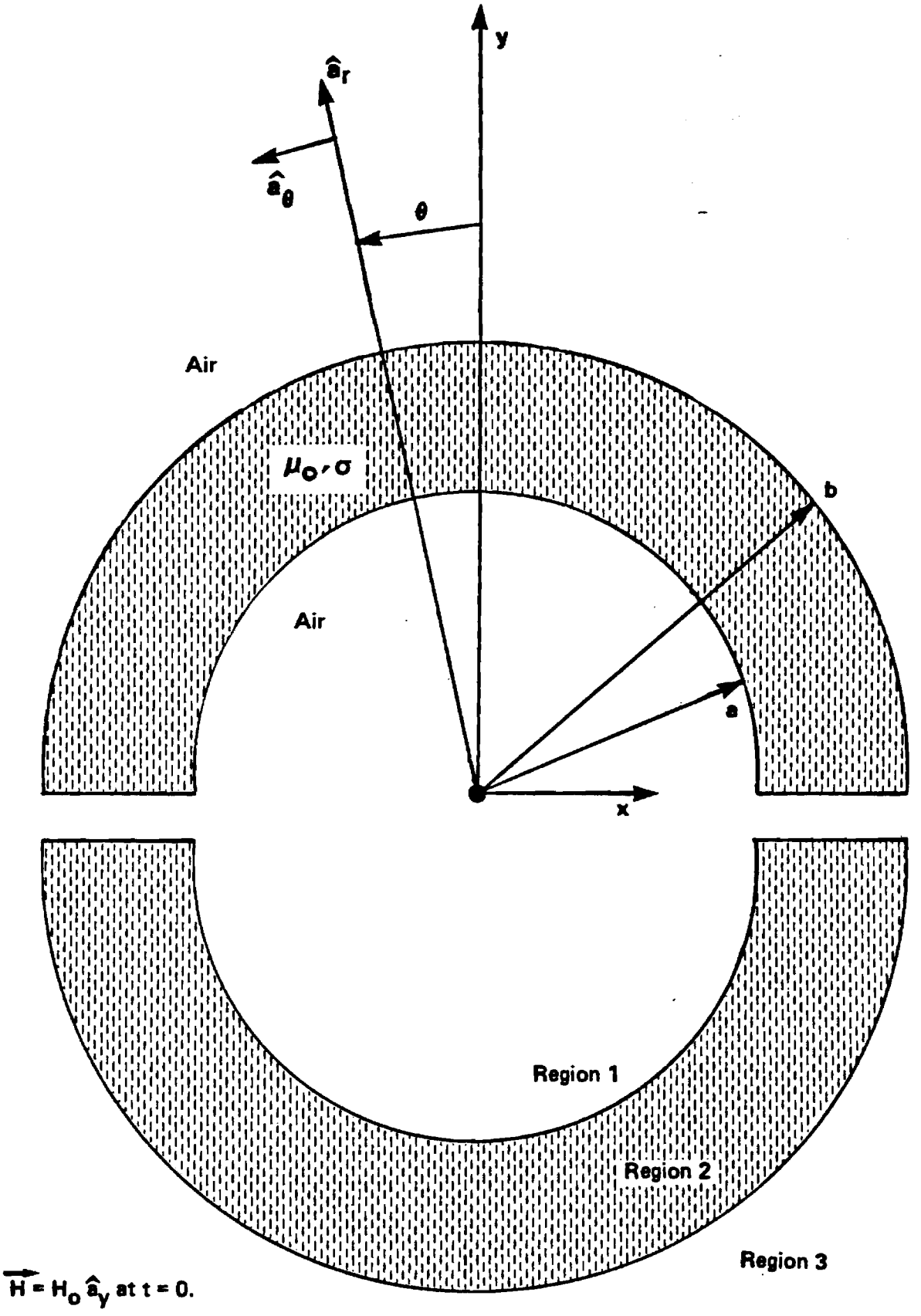

Figure 2. Felix Cylinder Experiment. Slit cylinder is immersed in a homogeneous field $\vec{H} = H_o \hat{a}_y$ at t = 0; a = 25.4mm, b = 50.8mm, length = 600mm, $\sigma = 2.538 \times 10^7$ mho/m; field collapses with time constant $\tau = 39.68$m sec.

$$0 = -\int_0^{2\pi} \left(D \sin\theta\, G_2 - C \sin\theta \frac{\partial G_2}{\partial r}\right) a\, d\theta$$

$$+ \int_0^{2\pi} \left(F \sin\theta\, G_2 - E \sin\theta \frac{\partial G_2}{\partial r}\right) b\, d\theta \; ; \; r < a \tag{20}$$

$$0 = -\int_0^{2\pi} \left(D \sin\theta\, G_2 - C \sin\theta \frac{\partial G_2}{\partial r}\right) a\, d\theta$$

$$+ \int_0^{2\pi} \left(F \sin\theta\, G_2 - E \sin\theta \frac{\partial G_2}{\partial r}\right) b\, d\theta \; ; \; r > b \tag{21}$$

$$0 = -\int_0^{2\pi} \left(F \sin\theta\, G_3 - E \sin\theta \frac{\partial G_3}{\partial r}\right) b\, d\theta \; ; \; r < b \tag{22}$$

where

$$G_1(r,r') = G_2(r,r') = -\frac{\ln|\bar{r}-\bar{r}'|}{2\pi}$$

$$G_2(r,r') = -\frac{j}{4} H_o^{(2)}(k(r-r'))$$

$$k = \frac{\lambda}{\mu\sigma}$$

Note, it is necessary to avoid putting null field points along the $\theta = 0$ or $\theta = 180°$ axes or the origin where integration of $\sin\theta$ terms identically yields zero. Otherwise no restraints are made. The system of equations (19)-(22) are written as the matrix

$$\begin{bmatrix} \star & \star & 0 & 0 \\ \star & \star & \star & \star \\ \star & \star & \star & \star \\ 0 & 0 & \star & \star \end{bmatrix} \begin{bmatrix} C \\ D \\ E \\ F \end{bmatrix} = 0 \tag{23}$$

The determinant of (23) is then evaluated for various values of k to determine zeros or eigenvalues. For the short cylinder dimension, as in Figure 2, the first three zeros were found to be 50.2830, 144.1659, 258.9145; a plot of the

determinant of (23) versus k is shown in Fig. 3 (along with the exact prediction which follows). The higher order eigenvalues are well removed from the base temporal decay; these higher order eigenvalues are reflective of the short temporal diffusion of the field across the thickness of the cylinder, a fact made more clear by looking at longer, thinner cylinders. For a medium sized cylinder with a = 57.14 mm, b = 69.85 mm, length = 600 mm, the eigenvalues k were found to be 51.4501, 257.9221, and 500.1842. A still larger cylinder with a = 131.7 mm, b = 136.5 mm, length = 1200 mm, gave eigenvalues k = 56.074, 659.2865, 1311.4041. Notice the increased separation between eigenvalues in each case reflective of the shorter relative diffusion time of the field through the cylinder walls.

As will be shown shortly, to predict the response to any external field drive, it suffices to determine the response to an external field H_o which drops instantaneously to zero; the final field being determined via convolution. Since the response field is dominated entirely by the first eigenvalue ($e^{\lambda_1 t}$), we need only predict C, D, E, and F at $t = 0^+$. At $t = 0^+$, only the field internal to the cylinder ($r < a$) is known to be equal to the value $H_o \hat{a}_y$ (or $A_z = H_o r \sin\theta$), the field at any other position being uncertain. The constants C, D, E, F follow by solving three null field equations in regions 2 and 3, and one inhomogeneous integral equation for region 1.

$$H_o r \sin\theta = \int_0^{2\pi} \left(D \sin\theta\, G_1 - C \sin\theta \frac{\partial G_1}{\partial r}\right) a\, d\theta \; ; \; r < a \tag{24}$$

$$0 = -\int_0^{2\pi} \left(D \sin\theta\, G_2 - C \sin\theta \frac{\partial G_2}{\partial r}\right) a\, d\theta$$

$$+ \int_0^{2\pi} \left(F \sin\theta\, G_2 - E \sin\theta \frac{\partial G_2}{\partial r}\right) b\, d\theta \; ; \; r < a \tag{25}$$

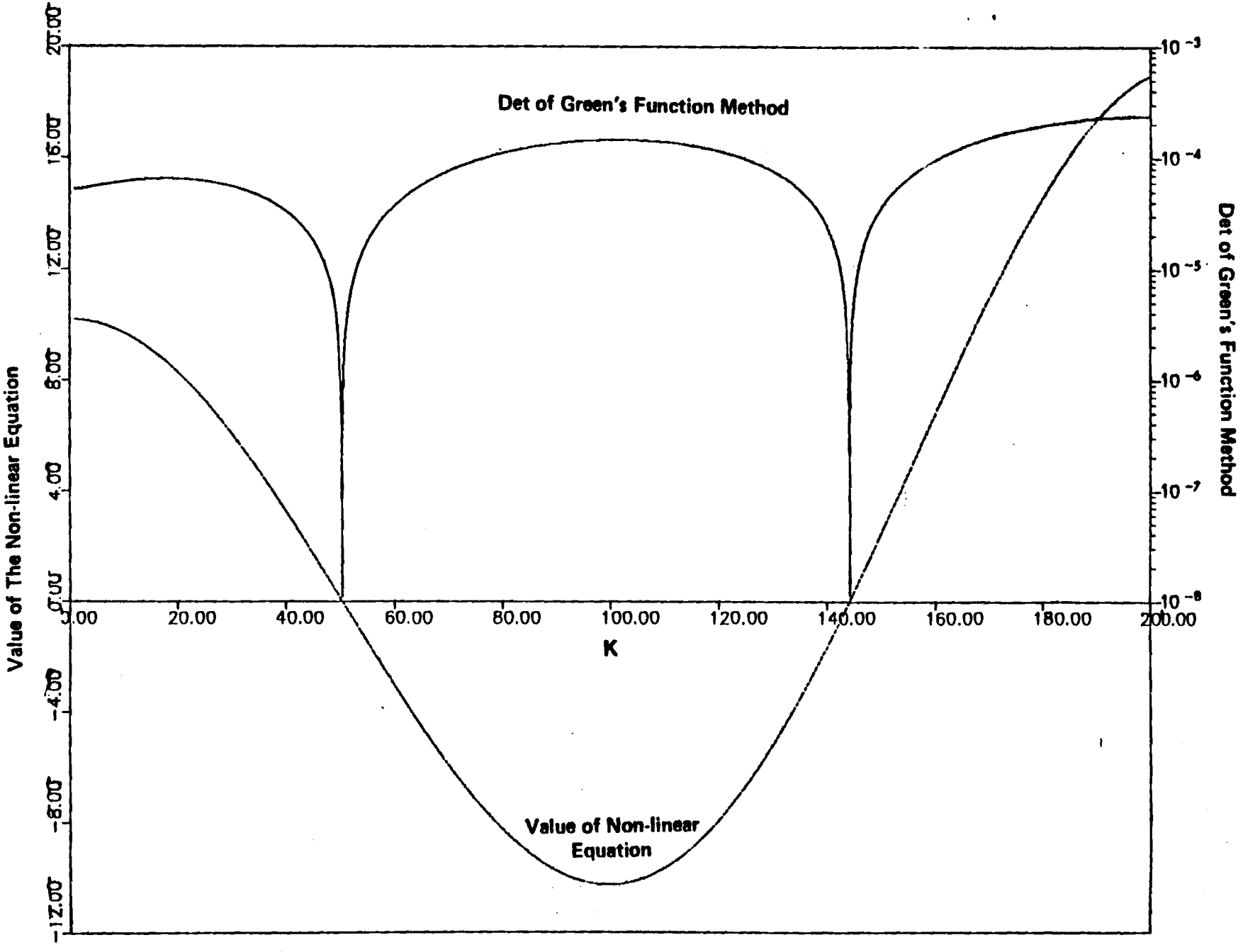

Fig. 3 Eigenvalues from Exact and Null-field Integral Calculations
Zeros of K are the Eigenvalues

$$0 = -\int_0^{2\pi} \left(D \sin\theta\, G_2 - C \sin\theta \frac{\partial G_2}{\partial r}\right) a\, d\theta$$

$$+ \int_0^{2\pi} \left(F \sin\theta\, G_2 - E \sin\theta \frac{\partial G_2}{\partial r}\right) b\, d\theta \; ; \; r > b \tag{26}$$

$$0 = -\int_0^{2\pi} \left(F \sin\theta\, G_3 - E \sin\theta \frac{\partial G_3}{\partial r}\right) b\, d\theta \; ; \; r < b \tag{27}$$

Once the constants are determined, the standard integral equations ((6a) and (7a)) yield the solution everywhere. This procedure has been implemented on a Cyber CDC; the results agree with those predicted by an exact solution to 5 decimal places (.001% error). These results are shown in the next section, where the exact solution is derived for comparison.

Analytical Formulation of the Eddy Current (Step Response) Field

In the exact analytical formulation possible in this test case, one begins by performing a separation of variables on $\nabla^2 A + k^2 A = 0$. The result for regions 1, 2, and 3 is

$$A_1 = Cr \sin\theta\, e^{-\frac{k^2}{\mu\sigma} t} \tag{28}$$

$$A_2 = \left[AJ_1(kr) + BY_1(kr)\right] \sin\theta\, e^{-\frac{k^2}{\mu\sigma} t} \tag{29}$$

$$A_3 = \frac{D}{r} \sin\theta\, e^{-\frac{k^2}{\mu\sigma} t} \tag{30}$$

Enforcing the boundary conditions on A_2 and its normal derivative at $r = a$ and $r = b$ leads to an eigenvalue equation

$$[2J_1(kb) + kb(J_o(kb) - J_2(kb))][2Y_1(ka) - ka(Y_o(ka) - Y_2(ka))]$$
$$= [2J_1(ka) - ka(J_o/ka) - J_2(ka)][2Y_1(kb) + kb(Y_o(kb) - Y_2(kb))] \quad (31)$$

The numerical plot of (31) is shown in Fig. 3 to yield the same eigenvalues as those predicted by the integral technique.

By requiring the field internal to the cylinder to be H_o at $t = 0^+$ as above, we determine the constants A, B, C, D to be respectively (normalized to H_o)

Small Cylinder

A = 0.05899

B = 0.009081

C = 1

D = 0.001524

Medium Cylinder

A = 0.04878

B = 0.1281

C = 1

D = 0.004045

Large Cylinder

A = 0.2491

B = -0.3827

C = 1

D = 0.01798

These are again within 0.001% of the results found from the integral technique.

Total Transient Solution

So far we have found only the self-field due to the cylinder in response to step change in external field.

$$Hy = H_o - H_o u_{-1}(+) \tag{32}$$

The actual source field is

$$Hy = H_o - H_o u_{-1}(+) + H_o e^{-\alpha t} u_{-1}(+) \tag{33}$$

where

α = 39.68 msec.

The total response field is realized through a convolution of $(-dH_y/dt)$ with $e^{-\lambda t}$, i.e.,

$$\begin{aligned} H_{response} &= \int_0^t \left(-\frac{d}{dt}(H_y)_{t=\tau}\right) e^{-(t-\tau)} d\tau \\ &= \int_0^t \alpha H_o e^{-\alpha\tau} e^{-\frac{k^2}{\mu\sigma}(t-\tau)} d\tau \\ &= \frac{\alpha e^{-\frac{k^2}{\mu\sigma}t}}{\frac{k^2}{\mu\sigma} - \alpha} \left(e^{(\frac{k^2}{\mu\sigma} - \alpha)t} - 1\right) \end{aligned} \tag{34}$$

The total field is found as the response field (34) plus the source field $H_o e^{-\alpha t}\hat{a}_y$. Recalling that $H_r = \frac{1}{r}\frac{\partial A_z}{\partial \theta}$ and $H_\theta = -\frac{\partial A_z}{\partial r}$, it is a simple matter to construct the following solution table (Table I) for the total field. A plot of the response field and total field in region 2 (or 3) at r = b of the small cylinder is shown in Figs. 4 and 5 (H_r and H_θ).

The reader should note that the cylinder current density $\underline{J} = -\nabla^2 \underline{A}$ does not change its spatial character with time unless secondary and tertiary eigenvalues are significant in the problem. The current distribution through-

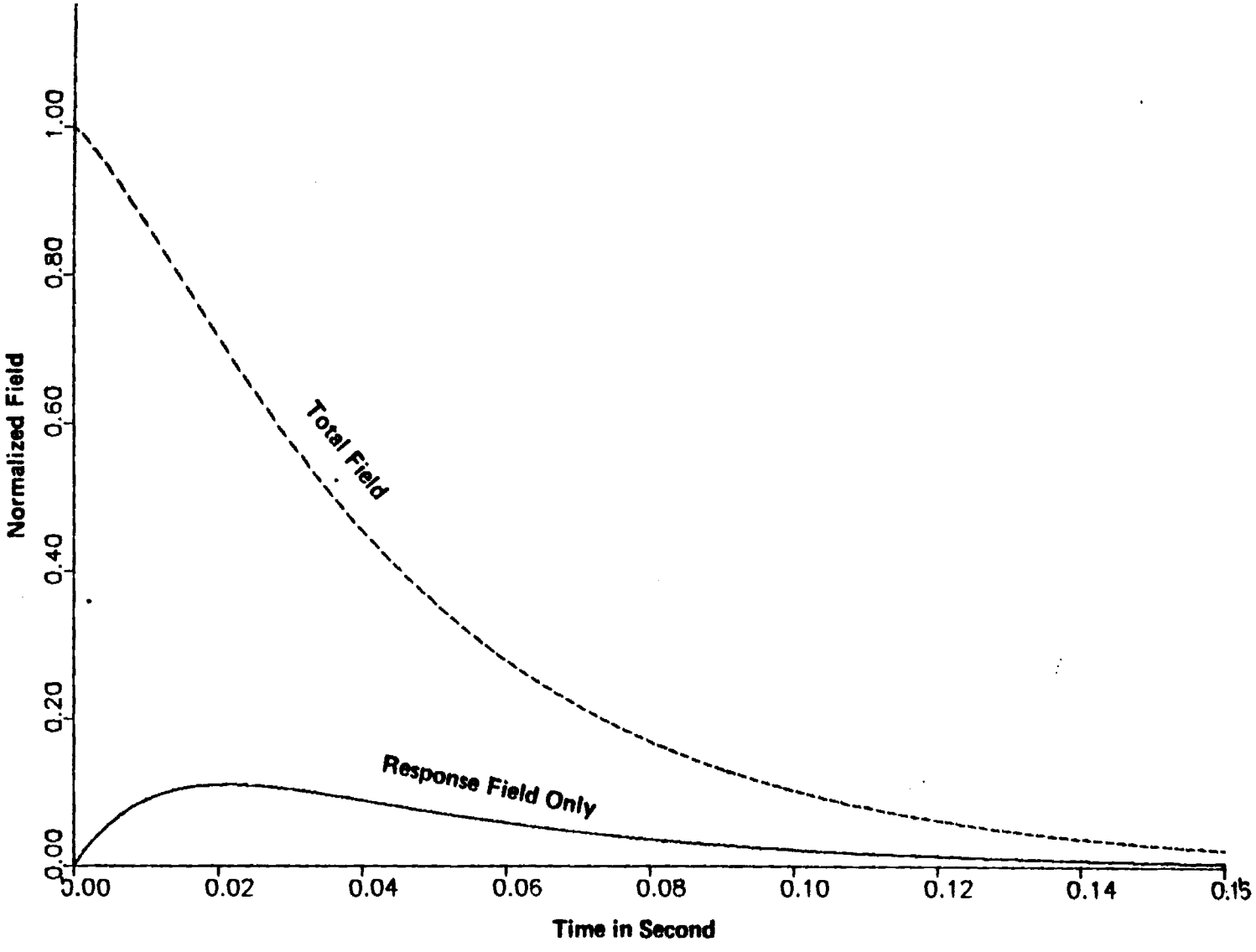

Fig. 4 R Component of Region(2) at Outer Radius

Outer Diameter 0.1016 meter, Thickness 0.0254 meter

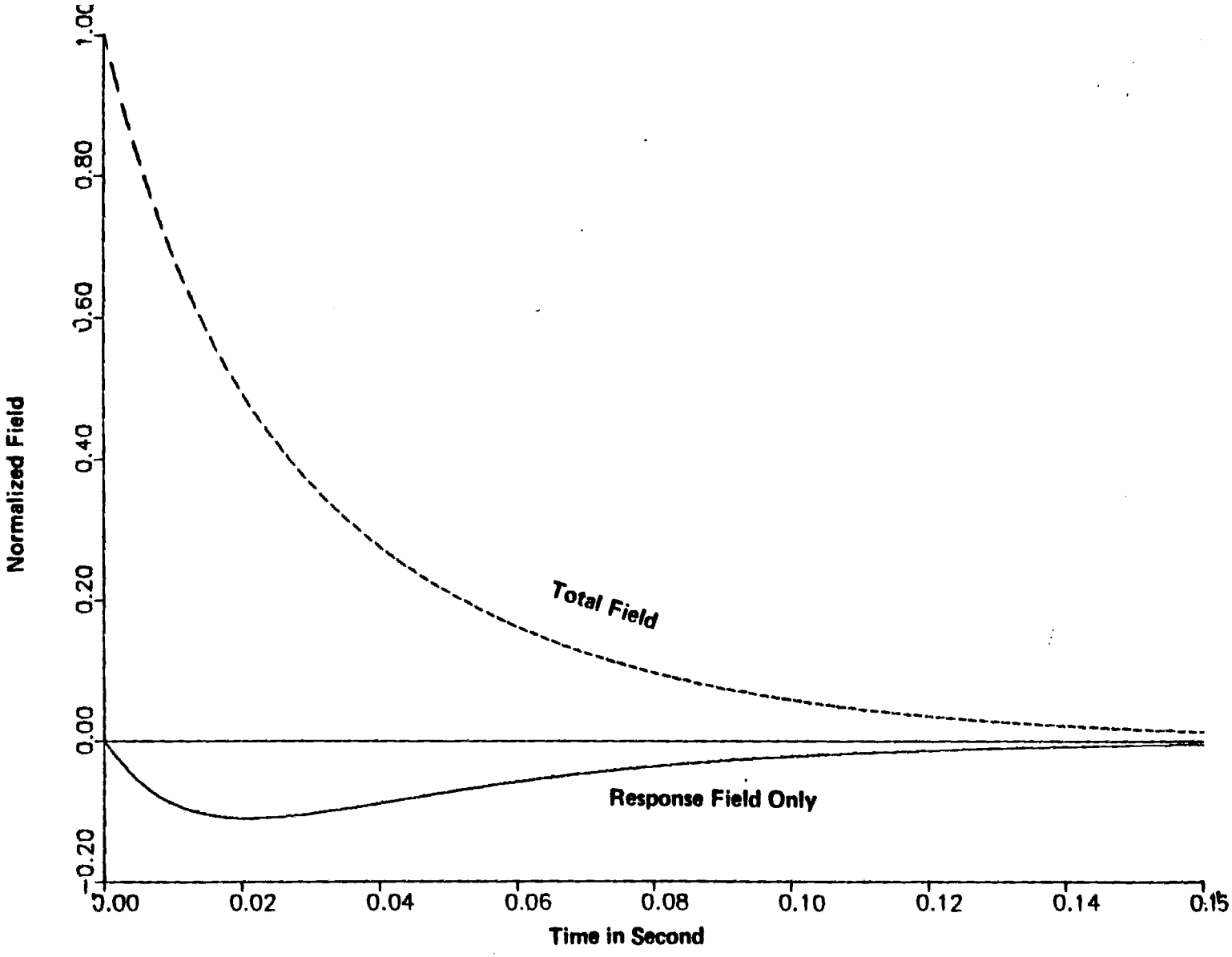

Fig. 5 Theta Component of Region(2) at Outer Radius

Outer Diameter 0.1016 meter, Thickness 0.0254 meter

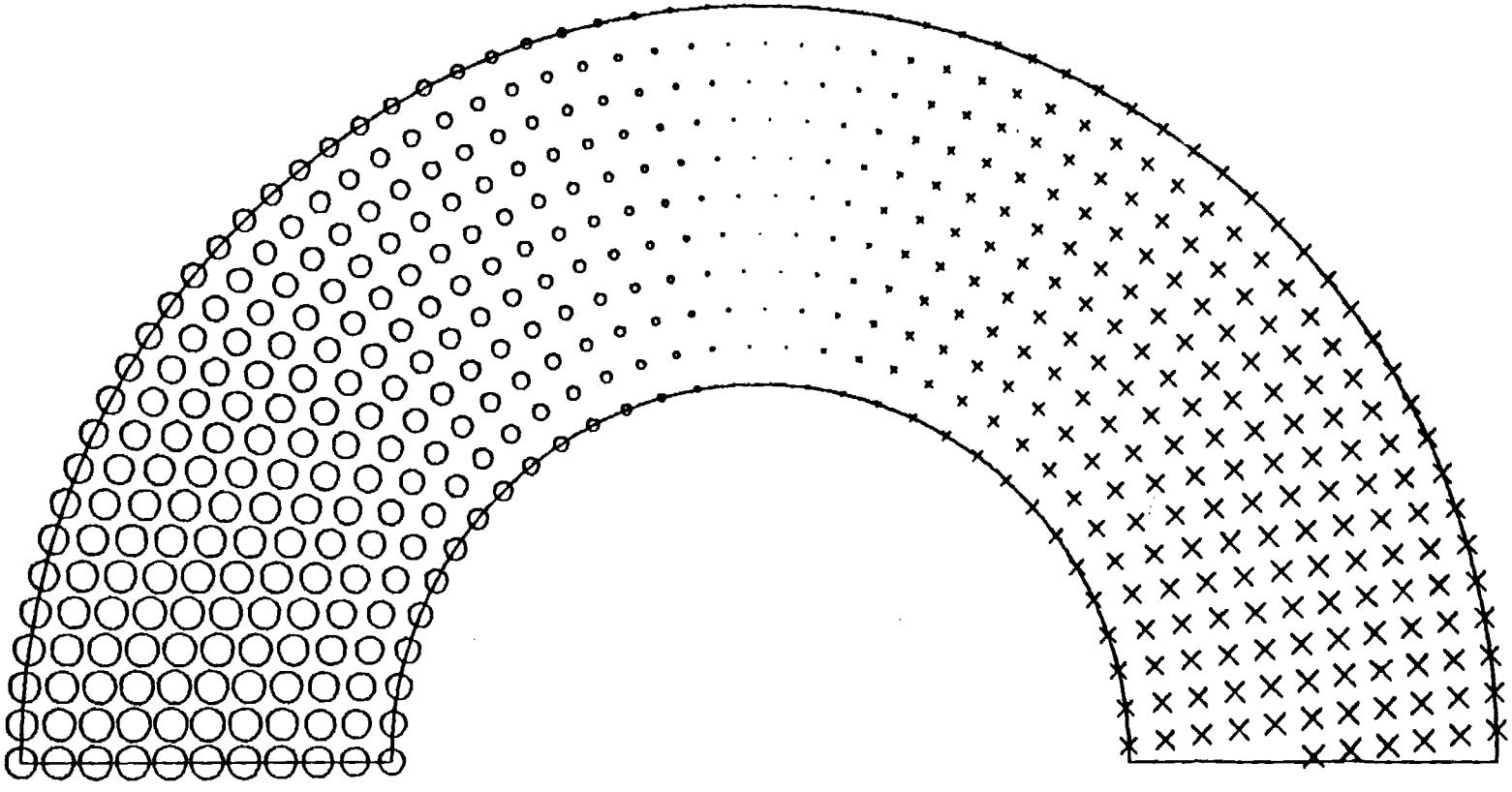

Fig. 6 Distribution of Current in the Annular Region

Magnitude of Current Density is Represented by the Size of X—O

out the cylindrical annulus is depicted in Fig. 6 by x's and o's whose size is indicative of the current density strength. Fig. 7 gives a more analytical picture of the current density radial distribution for θ = 0°, 22.5°, 45°, 67.5°, and 90°.

Finite Length Effects

A first refinement taken to account for finite length effects is obtained by reconsidering the governing equation, $\nabla^2 A - \mu\sigma \frac{\partial A}{\partial t} = 0$. As before, we first separate into space and time, letting

$$A_z = U(\vec{r})e^{-\lambda t} = R(r)Z(z)\Theta(\theta)e^{-\lambda t}$$

Then with $k'^2 = \mu\sigma\lambda$, it follows that

$$\frac{1}{r}\frac{d}{dr}\left(r\frac{dR}{dr}\right) + \left[\left(k'^2 - \ell^2\right) - \frac{m^2}{r^2}\right]R = 0 \qquad (35)$$

$$\frac{d^2\Theta}{d\theta^2} + m^2\Theta = 0 \qquad (36)$$

$$\frac{d^2Z}{dz^2} + \ell^2 Z = 0 \qquad (37)$$

For our problem meaningful solutions result when $m = 1$, $\ell = n\pi/L$ (i.e., $A \sim \sin\left(\frac{n\pi}{L}z\right)$ where L = total length). From (35) we find a new eigenvalue $k'^2 = k^2 + \ell^2 = k^2 + \left(\frac{n\pi}{L}\right)^2$ with a modified reciprocal time constant $\lambda = \frac{k^2 + (n\pi/L)^2}{\mu\sigma}$. Even for the short cylinder in Felix, the dominant eigenvalues with n = 1 have virtually no length modifications since k is so much larger than π/L.

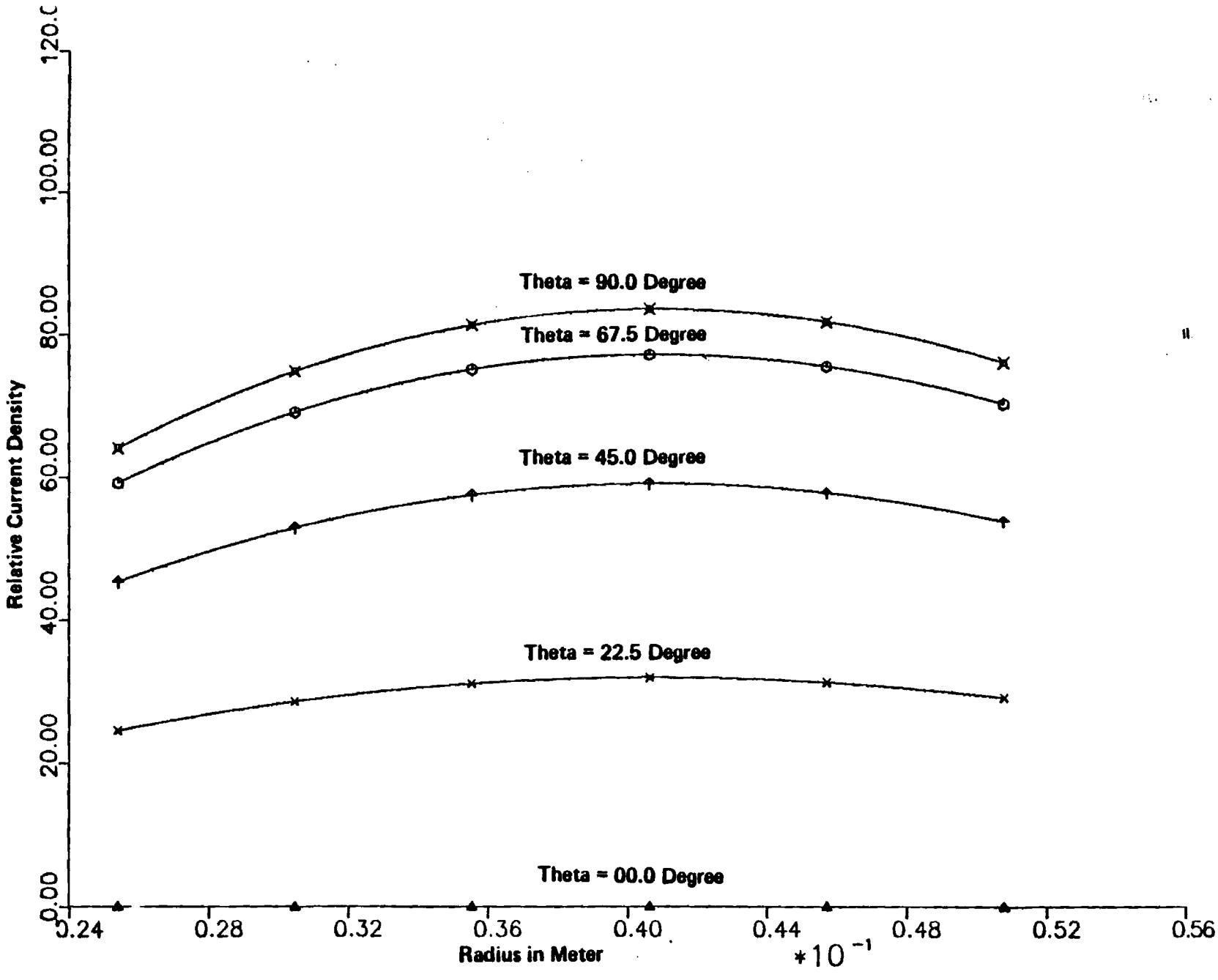

Fig. 7 **Distribution of Current**

Outer Diameter 0.1016 m, Thickness 0.0254 m

Discussion and Conclusions

The null field integral technique offers a rather simple method of predicting transient eddy current solutions using small determination matrices. The salient features of the technique revolve around the intelligent choice of interfacial basis functions. These basis functions can be inferred as perturbations from known solutions or from experimental tests. For example, one might conceivably construct a set of basis sets by looking at interfacial field data at $t = 0$, half way through the process, and near the end of a process.

An extension of the method to the short cylinder considering the 3-D nature of the field can be obtained by constructing the following basis sets for both A_z and A_θ

$$A_z, \quad \frac{\partial A_z}{\partial n} = \sin\theta \cos\frac{\pi}{L} z \tag{38}$$

$$A_\theta, \frac{\partial A_\theta}{\partial n} = \cos\theta \sin\frac{\pi}{L} z \tag{39}$$

where $z = 0$ is set at the midpoint (L/2) on the cylinder. Using these basis functions will necessitate the construction of an (8 x 8) determination matrix rather than the (4 x 4) used above. Of course, odd multiples of $\left(\frac{\pi}{L}\right)$ can be used, but these only yield higher order perturbations to the base system eigenvalues.

REFERENCES

[1] W. F. Praeg, et al., "Felix, An Experimental Facility to Study Electromagnetic Effects for First Wall, Blanket, and Shield Systems," Proc. 9th Symp. on Engineering Problems in Fusion Research, IEEE Pub. No. 81, Ch. 1715, pp. 1763-1766, 1981.

[2] L. R. Turner, et al., "Felix Construction Status and Experimental Program," Nucl. Technol./Fusion, Vol. 4, No. 2, Pt. 2, pp. 745-750, 1983.

[3] L. R. Turner, et al., "Results from the Felix Experiments on Electromagnetic Effects in Hollow Cylinders," Fifth Compumag Conference, Fort Collins, Colorado, pp. 356-359, 1985.

[4] S. Zhi-ming, et al., "The Finite Element Solution of Transient Axi Symmetrical Nonlinear Eddy Current Field Problems," Fifth Compumag Conference, Fort Collins, Colorado, pp. 241-244, 1985.

[5] B. Aldefeld, "A Numerical Solution of Transient Nonlinear Eddy Current Problems Including Moving Iron Parts," IEEE Trans. Magnetics, Vol. MAG-14, No. 5, pp. 371-373, 1978.

[6] A. Kameari and Y. Suzuki, "Eddy Current Analysis by the Finite Element Circuit Method," 7th Symposium, Knoxville, Tennessee, pp. 1386-1392.

[7] S. Tandon, A. Armor, and M. V. K. Chan, "Nonlinear Transient Finite Element Field Computation for Electrical Machines and Devices," IEEE Trans. Power App. Sys., Vol. PAS-102, pp. 1089-1096, May 1983.

Table 1. Total H field Response in the Cylinder

Component	Region	H
H_r	(1)	$H_o \cos\theta \left(e^{-\alpha t} + T(t)\right)$
	(2)	$H_o \cos\theta\, e^{-\alpha t} + \frac{H_o}{r}\left[AJ_1(kr) + BY_1(kr)\right]\cos\theta\, T(t)$
	(3)	$H_o \cos\theta\, e^{-\alpha t} + \frac{H_o D}{r^2}\cos\theta\, T(t)$
H_θ	(1)	$-H_o \sin\theta \left[e^{-\alpha t} + T(t)\right]$
	(2)	$-H_o \sin\theta \left(e^{-\alpha t} - \left[\frac{kA}{2}\left(J_o(kr) - J_2(kr)\right)\right.\right.$ $\left.\left. + \frac{kB}{2}\left(Y_2(kr)_o - Y_2(kr)\right)T(+)\right]\right)$
	(3)	$-H_o \sin\theta \left[e^{-\alpha t} - \frac{D}{r^2}T(t)\right]$

where $T(t) = \alpha \dfrac{e^{-\frac{k^2}{\mu\sigma}t}}{\left(\frac{k^2}{\mu\sigma} - \alpha\right)}\left(e^{\left(\frac{k^2}{\mu\sigma} - \alpha\right)t} - 1\right)$

ACKNOWLEDGEMENTS

This work was supported by the Department of Energy under the auspices of the Argonne National Laboratory. The authors wish to give special thanks to Dr. Rich Mattas for his support and encouragement.

E-21-638

Performance Schedule
Argonne National Laboratory E21-638

The following represents a performance profile for the above named contract.

I. 8-15-85 to 1/15/86 ; Analyze the 2-D transient fields of the FELIX cylinder using the eigenvalue technique.

II. 11-1-86 to 7-15-86 ; Analyze the 3-D case study of the same cylinder experiments; Break down the 3-D fields in terms of the u-v second order vector potential method. Perform an over-specification of the fields by adding both interfacial and null field points to specify the modal weighting constants.

III. 5-1-86 to 7-31-86 ; Add additional eigenvalues per mode to enhance accuracy if necessary.

IV. 6-1-86 to 8-31-86 ; Compare the analytical predictions to the measured FELIX data for as many cases as possible.

V. 7-15-86 to 8-31-86 ; Write up the results as a final report.

PREDICTION OF 3-D MAGNETIC FIELD TRANSIENTS IN THE SHORT CYLINDER FELIX EXPERIMENT

The goal of this phase of work for Argonne is to predict the three-dimensional induced fields within the short cylinder. Specifically, the experiment of key focus will be the short cylinder exposed to a decaying transverse magnetic field. The integral equation approach will be used to predict the induced currents and commensurate field. The u-v technique fostered by C. Emson, W. Trowbridge, and J. Simkin at the last Compumag Conference will be incorporated into the integral approach to eliminate Green's Dyadics from the formulation. One begins assuming $\overline{A} = \nabla \times \overline{W}$ where

$$\overline{W} = \hat{e}u + \hat{e} \times \nabla v \tag{1}$$

In the conductor Emson, et al. show that

$$\nabla \times \nabla \times \overline{A} - k^2\overline{A} = 0 \tag{2}$$

is replaced with

$$\nabla^2 u + k^2 u = 0 \tag{3}$$

and

$$\nabla^2 v + k^2 v = 0 \ . \tag{4}$$

Outside the conducting cylinder, it follows that with $\overline{H} = -\nabla\psi$, or

$$\nabla^2 \psi = 0 \tag{5}$$

There are, therefore, three null field integral equations in the problem,

$$0 = \iint \left(\frac{\partial u}{\partial n} G_1 - u \frac{\partial G_1}{\partial n}\right) ds \tag{6}$$

$$0 = \iint \left(\frac{\partial v}{\partial n} G_1 - v \frac{\partial G_1}{\partial n}\right) ds \tag{7}$$

$$0 = -\iint \left(\frac{\partial \psi}{\partial n} G_2 - \psi \frac{\partial G_2}{\partial n}\right) ds \tag{8}$$

At either the inner or outer radius of the cylinder, u, v, ψ, and their normal derivatives can be represented in terms of some basis functions ϕ which look like

$$\phi = \begin{matrix} \sin\theta \\ \cos\theta \end{matrix} \quad \begin{matrix} \sin \frac{\pi}{L} Z \\ \cos \frac{\pi}{L} Z \end{matrix} , \tag{9}$$

the choice of sin/cos differing for the variables u, v, ψ.

Choosing two null field points both within and outside the cylinder gives us six equations with 12 unknowns (u, v, ψ with normal derivatives both at the inner and outer radius; we assume a linear fit at $Z = \pm L$ (cylinder length 2L)). We obtain six additional equations from the boundary conditions $\hat{n} \times \|\bar{H}\| = 0$ and $\hat{n} \cdot \|\bar{B}\| = 0$. Thus the system is completely represented in terms of a 6 x 6 determination matrix, the eigenvalues of which are dictated by the zeros of the determinant.

The complete field is predicted after determining these eigenvalues via the eigenvalue modal approach (recent paper to IEEE, Davey, Hsiu, and Turner). A valid objection might be raised as to the validity of the basis function choice. In reality we expect fields whose spatial harmonic decomposition will contain $\sin \frac{n\pi}{L} Z$ | $\cos \frac{n\pi}{L} Z$ with n odd. These terms will be much smaller than the fundamental components. Their omission will hopefully alter

slightly the eigenmode being sought. The long cylinder results which give some background limits for us to work from, suggest that this is a reasonable assumption.

3-D TRANSIENT EDDY CURRENT CALCULATIONS FOR THE FELIX CYLINDER EXPERIMENTS

by

Kent R. Davey
School of Electrical Engineering
Georgia Institute of Technology
Atlanta, Georgia 30332-0250

July 1986

ABSTRACT

The three-dimensional eddy current transient field problem is formulated first using the U-V method. This method breaks the vector Helmholtz equation into two scalar Helmholtz equations. Null field integral equations and the appropriate boundary conditions germaine to the problem are used to set up an identification matrix which is independent of null field point locations. Embedded in the identification matrix are the unknown eigenvalues of the problem representing its impulse response in time. These eigenvalues are found by equating the determinant of the identification matrix to zero. The eigenvalues, which can be equated with temporal response, are found to be intimately linked to the initial forcing function which triggers the transient in question. When this initial forcing function is Fourier decomposed into its respective spatial harmonics, it is possible to associate with each Fourier component a unique eigenvalue by this technique. The true transient solution comes through a convolution of the impulse response so obtained with the particular external field decay governing the problem at hand. The technique is applied to the Felix medium cylinder and compared to data. A pseudoanalytic confirmation of the eigenvalues so obtained is formulated to validate the procedure.

INTRODUCTION

Approaches to transient eddy current problems to date tend to fall in to one of two categories [1-4]:

1. Time Domain developed by a forward difference procedure albeit explicit or implicit. Spatial discretizations are pursued in much the same way as present time harmonic problems.
2. Time domain developed via the characteristic eigenvalues/eigenvectors of the system. The spatial domain is characterisitcally pursued via either finite difference or finite element techniques.

The first approach is computationally intensive involving the solution of the entire spatial domain recursively throughout the time period of interest. The second approach is theoretically more efficient, but is fraught with many other problems. If one chooses to approach the problem using large scale spatial discretizations, as is characteristic of most finite element approaches, this necessitates large identification matrices and thus a host of eigenvalues, most of which are spurious and subdominant. Since most real world problems characteristically have a handfull of dominant eigenvalues, it is natural to capitalize on a technique which extracts those dominant eigenvalues as its principle feature. It is with the intent of capitalizing on the positive features of the eigenvalue approach, while minimizing the size of matrices and thus the number of eigenvalues, that the present research was undertaken. A general theory involving the use of null field integral equations determining 3-D eigenvalues is developed. The theory is applied to the Argonne Felix cylinder experiments [5-7]. The general formulation preceding the null field integral technique involves the use of a second order vector potential, a method discussed by [8-10] bus as far as the authors are aware

of, never implemented here to date. After the null field integral technique predicts the eigenvalues associated with the problem, the total transient field solution is realized through a convolution of the impulse response with a particular external field decay generating the transient.

A general overview of the process is as follows:

1. Start with the eigenvalue formulation of the eddy current problem.
2. Break the vector Helmholtz equation into scalar Helmholtz equations using the U-V method, i.e., the second order vector potential developed in [8-10].
3. Use the null field equations and the boundary conditions to set up the identification matrix which is independent of null field point locations.
4. Back out the transient solution through the impulse response from eigenvalues as Fourier sum based on the initial field shape. (Note each transient solution depends on the shape of the driving field, i.e., each harmonic has a different decay time depending on the shape of the initial field.)
5. Derive the true transient solution as a convolution of the impulse response derived in step 4 with the particular external field decay for the problem at hand.

Steps 1 through 5 were applied to the medium Felix cylinder and the results are compared with experimental data. In addition, we compare eigenvalues obtained with the integral technique to those predicted with a pseudo-analytic analysis of the cylinder.

THE SECOND ORDER VECTOR POTENTIAL FORMULATION - THE U-V METHOD

The vector Helmholtz equation for the magnetic vector potential is

$$\nabla^2\bar{A} - \mu\sigma \frac{\partial \bar{A}}{\partial t} = 0 \ . \tag{1}$$

Assume that $\bar{A} = \vec{A}e^{-\lambda t}$. The parameter "$\lambda$" is a key parameter, an eigenvalue of the problem representing the characteristic temporal decay time of the field. It is, of course, a function of the forcing function (shape) giving rise to the transient. It is this eigenvalue λ (actually a set of them) that we seek. Defining $k^2 = \mu\sigma\lambda$, (1) is written as

$$\nabla^2\vec{A} + k^2\vec{A} = 0 \tag{2}$$

where $\vec{B} = \nabla \times \vec{A}$. We begin by defining a second vector potential

$$\vec{A} = \nabla \times \vec{W} \tag{3}$$

where

$$\vec{W} = \hat{e}u + \hat{e} \times \nabla v \tag{4}$$

and $\hat{e}$ is a fixed unit vector $(\hat{a}_r, \hat{a}_z, \hat{a}_\theta, \ldots)$. Inserting (3) into (2) gives

$$-\nabla \times \left[\nabla \times \nabla \times \vec{W} - k^2\vec{W}\right] = 0 \tag{5}$$

or

$$\nabla \times \left[\nabla^2\vec{W} + k^2\vec{W} - \nabla(\nabla \cdot \vec{W})\right] = 0 \tag{6}$$

or finally

$$\nabla^2\vec{W} + k^2\vec{W} = 0 \ . \tag{7}$$

It is important to emphasize that no gauge on $\vec{W}$ has been applied. In fact, as P. Hammond [8] points out, it is inconsistent to attempt to impose one since it forces u and v to have certain spatial dependencies assumed a priori.

The cylinder transient field of interest in this paper suggests the assignment of $\hat{a}_z$ for $\hat{e}$. It follows then that

$$\vec{W} = \hat{a}_z u + \hat{a}_z \times \nabla v = \hat{a}_z u + \hat{a}_\theta \frac{\partial v}{\partial r} + \hat{a}_r \left(-\frac{1}{r}\frac{\partial v}{\partial \theta}\right) . \tag{8}$$

The expansion of $\nabla^2\vec{W}$ in cylindrical coordinates gives

$$\begin{aligned}\nabla^2\vec{W} = &\left[\frac{\partial}{\partial r}\left(\frac{1}{r}\frac{\partial}{\partial r}\left(-\frac{\partial v}{\partial \theta}\right)\right) - \frac{1}{r^3}\frac{\partial^3 v}{\partial \theta^3} - \frac{2}{r^2}\frac{\partial^2 v}{\partial r\,\partial \theta} - \frac{1}{r}\frac{\partial^3 v}{\partial z^2 \partial \theta}\right]\hat{a}_r \\ &+ \left[\frac{\partial}{\partial r}\left(\frac{1}{r}\frac{\partial}{\partial r}\left(r\frac{\partial v}{\partial r}\right)\right) + \frac{1}{r^2}\frac{\partial^2}{\partial \theta^2}\frac{\partial v}{\partial r} + \frac{\partial^2}{\partial z^2}\frac{\partial v}{\partial r} - \frac{2}{r^3}\frac{\partial^2 v}{\partial \theta^2}\right]\hat{a}_\theta \\ &+ \left[\frac{1}{r}\frac{\partial}{\partial r}\left(r\frac{\partial u}{\partial r}\right) + \frac{1}{r^2}\frac{\partial^2 u}{\partial \theta^2} + \frac{\partial^2 u}{\partial z^2}\right]\hat{a}_z .\end{aligned} \tag{9}$$

The r component of (9) is just $\left(-\frac{1}{r}\frac{\partial}{\partial \theta}\nabla^2 v\right)$. The θ component of (9) is $\frac{\partial}{\partial r}(\nabla^2 v)$. The z component of (9) is $\nabla^2 u$. Thus, from (7) it is clear that the total problem is solved by insuring that both u and v satisfy the Helmholtz equation

$$\nabla^2 v + k^2 v = 0 \tag{10}$$

$$\nabla^2 u + k^2 u = 0 \tag{11}$$

From the fact that $\vec{B} = \nabla \times \nabla \times \vec{W}$ and $\vec{J} = \frac{1}{\mu}\nabla \times \vec{B}$, it is possible to relate these quantities $\vec{A}$, $\vec{B}$, and $\vec{J}$ to u and v. Table I summarizes these relationships.

TABLE I

RELATION OF A, B, AND J TO u AND v

$\vec{A}$	Equivalent Expression in u and v
A_r	$\frac{1}{r}\frac{\partial u}{\partial \theta} - \frac{\partial^2 v}{\partial r \partial z}$
A_θ	$-\left[\frac{\partial u}{\partial r} + \frac{1}{r}\frac{\partial^2 v}{\partial \theta \partial z}\right]$
A_z	$\nabla^2 v - \frac{\partial^2 v}{\partial z^2}$
$\vec{B}$	
B_r	$\frac{\partial^2 u}{\partial r \partial z} - \frac{k^2}{r}\frac{\partial v}{\partial \theta}$
B_θ	$\frac{1}{r}\frac{\partial^2 u}{\partial \theta \partial z} + k^2 \frac{\partial v}{\partial r}$
B_z	$\frac{\partial^2 u}{\partial z^2} + k^2 u$
$\vec{J}$	
J_r	$k^2\left[\frac{1}{r}\frac{\partial u}{\partial \theta} - \frac{\partial^2 v}{\partial r \partial z}\right]$
J_θ	$-k^2\left[\frac{1}{r}\frac{\partial^2 v}{\partial \theta \partial z} + \frac{\partial u}{\partial z}\right]$
J_z	$k^2\left[\frac{\partial^2 v}{\partial r^2} + \frac{1}{r}\frac{\partial v}{\partial r} + \frac{1}{r^2}\frac{\partial^2 v}{\partial \theta^2}\right]$

BASIS FUNCTIONS AND THE NULL FIELD INTEGRAL TECHNIQUE

Figure 1 depicts the geometry of the problem. The cylindrical shell (inner radius "a", outer radius "b", length "ℓ") is stressed by a y directed field. At time t = 0, this external field collapses to zero with a time constant τ (5 to 40 msec). As suggested by Figure 2, it is appropriate to think about this as a three region problem (note all three regions come in contact at $Z = \pm \ell/2$). In regions 1 and 3, we let $\vec{H} = -\nabla\psi$ and solve

$$\nabla^2\psi = 0 \ . \tag{12}$$

In region 2, we solve

$$\nabla^2 u + k^2 u = 0 \tag{13}$$

$$\nabla^2 v + k^2 v = 0 \ . \tag{14}$$

The integral solution of (12)-(14) is respectively

$$\begin{matrix} \psi(r) \ ; \ r \in V_{Air} \\ \frac{\psi(r)}{2} \ ; \ r \text{ surface} \\ 0 \quad ; \ r \notin V_{Air} \end{matrix} = \oint_S \left[\frac{\partial\psi(r')}{\partial n} G(r,r') - \psi(r') \frac{\partial G(r,r')}{\partial n}\right] ds \tag{15}$$

where $G(r,r') = \dfrac{1}{4\pi|\bar{r} - \bar{r}'|}$;

$$\begin{matrix} u(r) \ ; \ r \in V_{conductor} \\ \frac{u(r)}{2} \ ; \ r \text{ surface} \\ 0 \quad ; \ r \notin V_{conductor} \end{matrix} = \oint_S \left[\frac{\partial u(r')}{\partial n} G_c(r,r') - u(r') \frac{\partial G_c}{\partial n}(r,r')\right] ds \tag{16}$$

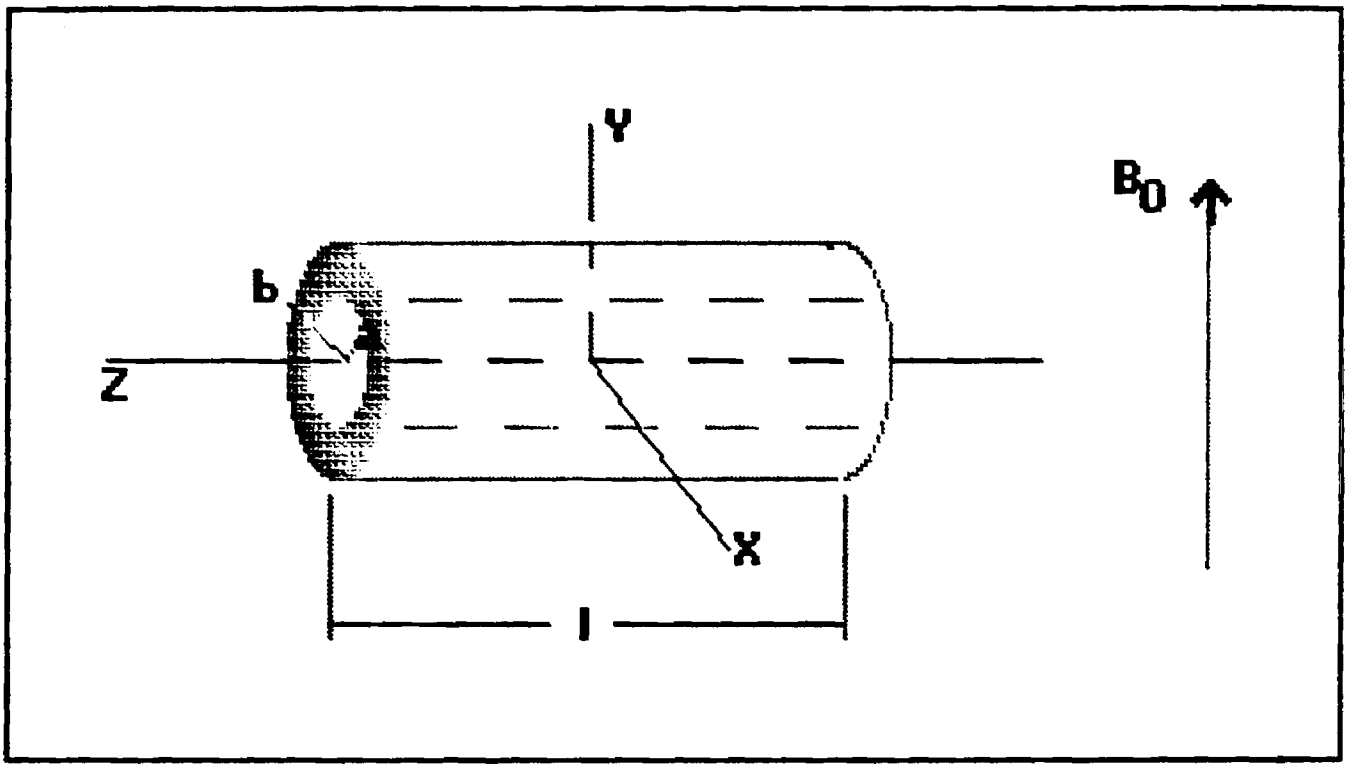

FIG.1 FELIX CYLINDER STRESSED BY A VERTICAL B FIELD;INNER RADIUS a,OUTER RADIUS b.

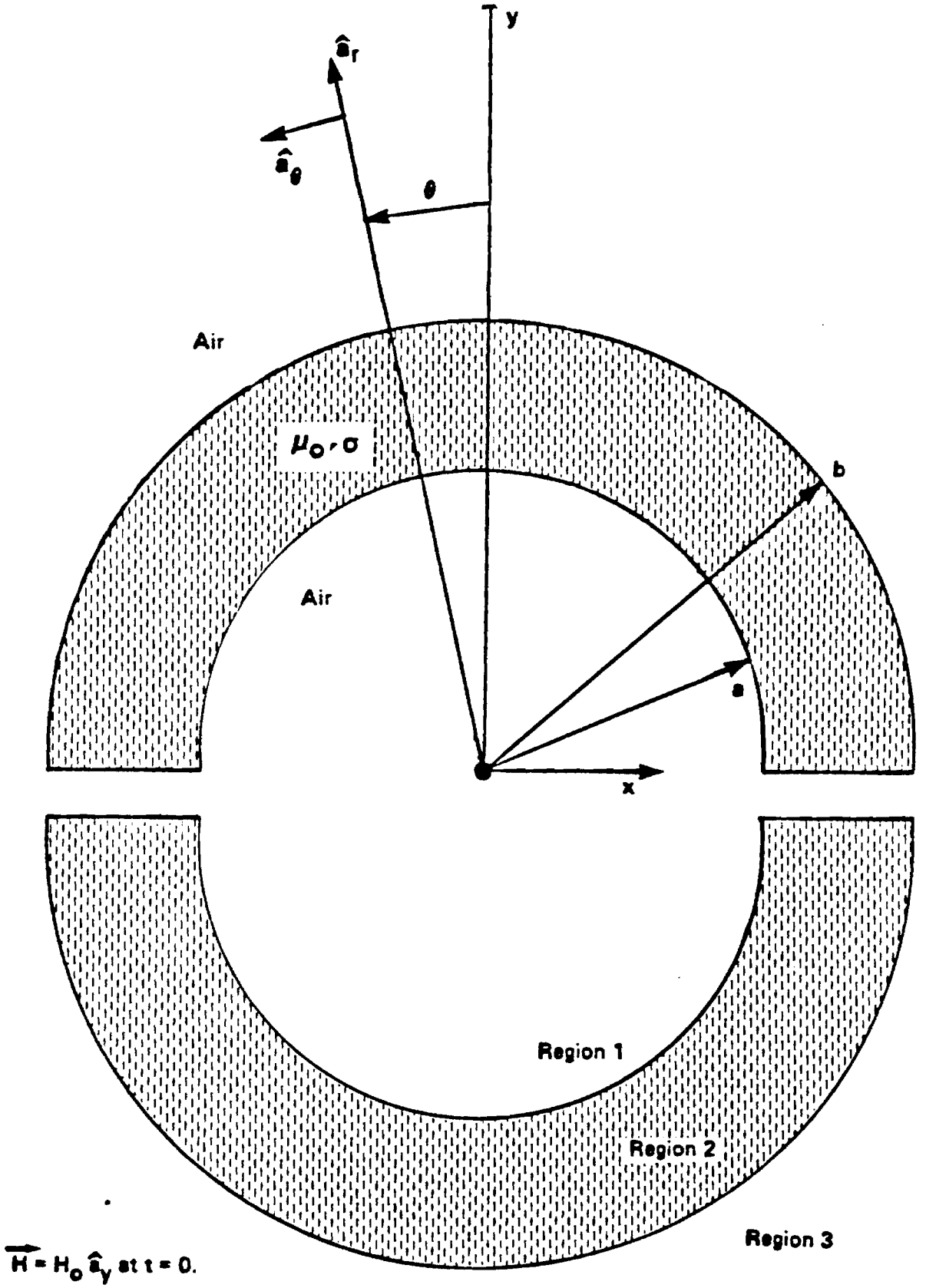

Figure 2. Felix Cylinder Experiment. Slit cylinder is immersed in a homogeneous field $\vec{H} = H_o \hat{a}_y$ at t = 0; a = 57.1 mm, b = 69.8 mm, length = 300 mm, $\sigma = 2.538 \times 10^7$ mho/m; field collapses with time constant τ = 39.68 m sec.

$$\begin{cases} v(r) \;;\; r \in V_{conductor} \\ \frac{v(r)}{2} \;;\; r \text{ surface} \\ 0 \;;\; r \notin V_{conductor} \end{cases} = \oint_S \left[\frac{\partial v(r')}{\partial n} G_c(r,r') - v(r') \frac{\partial G_c}{\partial n}(r,r')\right] ds \qquad (17)$$

where

$$G_c(r,r') = \frac{e^{jk|\bar{r}-\bar{r}'|}}{4\pi|\bar{r} - \bar{r}'|} .$$

We choose to solve (15)-(17) using (15c), (16c), and (17c). The approach is as follows:

1. Assign appropriate basis functions to the interfacial fields ψ, u, v, and their normal derivatives.
2. Pick arbitrary null field points outside the volumes of interest.
3. Impose the boundary conditions that tangential H and normal B be continuous across each interface.
4. Set up a matrix, the identification matrix, using the equations from (15c)-(17c).
5. Determine the eigenvalues k for which the determinant of the identification matrix is zero. Note: these eigenvalues are the "fingerprints" of the object and would correspond to resonances were this a scattering problem!
6. Reconstruct the transient response in terms of these eigenvalues.

It is surprising how easy step 1 is for most problems! For the problem at hand, we know a priori that no θ directed current exists at $\theta = \pm \pi/2$. By symmetry, it is also obvious that J_z is zero at $\theta = 0, \pi$. Furthermore, $J_r = 0$ at $r = a$ and $r = b$. Both J_θ and J_z can be expressed as a combination of sinusoidal functions as follows:

$$J_\theta = \Sigma\, C_{\theta n} \sin \frac{n\pi}{\ell} z \cos\theta \tag{18}$$

$$J_z = \Sigma\, C_{zn} \cos \frac{n\pi}{\ell} z \sin\theta \tag{19}$$

Table II summarizes the appropriate basis functions for ψ, u, and v consistent with (18), (19), and Table I.

We have 12 unknowns (A,B,C,D,E,F,G,H,I,J,K,L), 6 boundary conditions (Table II), and 6 integral equations ((15c), (16c), (17c)) written both at r = a and r = b. [Note, the integral equations involve integration around the ends. The fields at the ends must be a combination of Bessel functions (J_1, and Y_1); the weighting of the J and Y Bessel functions is chosen so as to yield the assumed fields Table II at r = b and r = a. Unless the cylinder is very short or very fat, these end effects are small.] Thus we have a 6 x 6 identification matrix. The zeros of this matrix's determinant were calculated for modal surfaces n = 1,3,5,7,9, and 11. The results are shown in Table III.

PSEUDO-ANALYTICAL FORMULATION

By way of arriving at alternative analytical result, we sought a solution assuming the fields repeated every "2ℓ" lengths in z space. Solutions to (12)-(14) are

$$\psi(r,\theta,z) = \begin{cases} AI_1\left(\frac{n\pi}{\ell} r\right)\cos\theta\cos\left(\frac{n\pi}{\ell} z\right) ; \text{ region 1} \\ BK_1\left(\frac{n\pi}{\ell} r\right)\cos\theta\cos\left(\frac{n\pi}{\ell} z\right) ; \text{ region 3} \end{cases} \tag{20, 21}$$

$$u(r,\theta,z) = \left[C_1 J_1(\beta r) + C_2 Y_1(\beta r)\right]\cos\theta\sin\left(\frac{n\pi}{\ell} z\right) ; \text{ region 2} \tag{22}$$

$$v(r,\theta,z) = \left[D_1 J_1(\beta r) + D_2 Y_1(\beta r)\right]\sin\theta\cos\left(\frac{n\pi}{\ell} z\right) ; \text{ region 2} \tag{23}$$

TABLE II

REPRESENTATION OF ψ, u, and v AND BOUNDARY CONDITION REQUIREMENTS

Scalar Variable	Functional Representation r = a	r = b
ψ	$A\cos\left(\frac{n\pi}{\ell} z\right)\cos\theta$	$B\cos\left(\frac{n\pi}{\ell} z\right)\cos\theta$
$\frac{\partial\psi}{\partial r}$	$C\cos\left(\frac{n\pi}{\ell} z\right)\cos\theta$	$D\cos\left(\frac{n\pi}{\ell} z\right)\cos\theta$
u	$E\sin\left(\frac{n\pi}{\ell} z\right)\cos\theta$	$F\sin\left(\frac{n\pi}{\ell} z\right)\cos\theta$
$\frac{\partial u}{\partial r}$	$G\sin\left(\frac{n\pi}{\ell} z\right)\cos\theta$	$H\sin\left(\frac{n\pi}{\ell} z\right)\cos\theta$
v	$I\cos\left(\frac{n\pi}{\ell} z\right)\sin\theta$	$J\cos\left(\frac{n\pi}{\ell} z\right)\sin\theta$
$\frac{\partial v}{\partial r}$	$K\cos\left(\frac{n\pi}{\ell} z\right)\sin\theta$	$L\cos\left(\frac{n\pi}{\ell} z\right)\sin\theta$

Impose 6 Boundary Conditions ; $\hat{n} \cdot |\vec{B}| = 0$, $\hat{n} \times |\vec{H}| = 0$

$$A = \frac{E\ell}{n\pi}\left(k^2 - \left(\frac{n\pi}{\ell}\right)^2\right)$$

$$K = \frac{E\ell}{an\pi}$$

$$C = \frac{k^2}{a} I - G\left(\frac{n\pi}{\ell}\right)$$

$$B = \frac{F\ell}{n\pi}\left(k^2 - \left(\frac{n\pi}{\ell}\right)^2\right)$$

$$L = \frac{F\ell}{bn\pi}$$

$$D = \frac{k^2}{b} J - H\frac{n\pi}{\ell}$$

TABLE III

CALCULATION OF EIGENVALUES

Modal Value n	Integral Value	Pseudoanalytical Value
1	52.0	51.99
3	61.0	61.42
5	74.0	74.48
7	87.0	87.13
9	99.0	99.02
11	110.0	110.32

where

$$\beta^2 = k^2 - \left(\frac{n\pi}{\ell}\right)^2 .$$

Boundary conditions require that $\nabla \times \vec{A}\Big|_{\text{conductor}} = -\nabla\psi\Big|_{\text{Air}}$ on the interface. These conditions and their commensurate requirements and A, B, C_1, C_2, D_1, and D_2 are summarized in Table IV. The six equations in six unknowns can be solved exactly as with the integral technique for the unknown eigenvalues. The results are listed in Table III for comparison with the integral technique formalism; a discrepancy of less than 1% was observed.

One important case develops when $k^2 = (n\pi/\ell)^2$. The solutions corresponding to (20)-(23) collapse to

$$\psi(r,\theta,z) = \begin{cases} AI_1\left(\frac{n\pi}{\ell} r\right)\cos\theta\cos\frac{n\pi}{\ell} z \text{ ; region 1} \\ BK_1\left(\frac{n\pi}{\ell} r\right)\cos\theta\cos\frac{n\pi}{\ell} z \text{ ; region 3} \end{cases} \tag{24}$$

(25)

$$u(r,\theta,z) = \left(\frac{C_1}{r} + C_2 r\right)\cos\theta\sin\left(\frac{n\pi}{\ell} z\right) \text{ ; region 2} \tag{26}$$

$$v(r,\theta,z) = \left(\frac{D_1}{r} + D_2 r\right)\sin\theta\cos\left(\frac{n\pi}{\ell} z\right) \text{ ; region 2} \tag{27}$$

If we attempt to match boundary conditions (Table IV, $\frac{\partial^2 u}{\partial z^2} + k^2 u = -\frac{\partial \psi}{\partial z}$), there results

$$AI_1\left(\frac{n\pi}{\ell} a\right) = 0 \tag{28}$$

$$BK_1\left(\frac{n\pi}{\ell} b\right) = 0 . \tag{29}$$

This yields the trivial result that A = B = 0.

TABLE IV

ANALYTIC BOUNDARY CONDITIONS/CONSTRAINTS

Boundary Conditions

$$r \text{ component } ; \frac{\partial^2 u}{\partial r \partial z} - \frac{k^2}{r}\frac{\partial v}{\partial \theta} = -\frac{\partial \psi}{\partial r}\Big|_{\substack{r=a \\ r=b}}$$

$$\theta \text{ component } ; \frac{1}{r}\frac{\partial^2 u}{\partial \theta \partial z} + k^2\frac{\partial v}{\partial r} = -\frac{1}{r}\frac{\partial \psi}{\partial \theta}\Big|_{\substack{r=a \\ r=b}}$$

$$z \text{ component } ; \frac{\partial^2 u}{\partial z^2} + k^2 u = -\frac{\partial \psi}{\partial z}\Big|_{\substack{r=a \\ r=b}}$$

Commensurate Constraints

$r = a$

$$\frac{n\pi}{\ell}\left[C_1 J_1'(\beta a) + C_2 Y_1'(\beta a)\right] - \frac{k^2}{a}\left[D_1 J_1(\beta a) + D_2 Y_1(\beta a)\right] = -A I_1'\left(\frac{n\pi}{\ell}a\right)$$

$$-\frac{1}{a}\left[C_1 J_1(\beta a) + C_2 Y_1(\beta a)\right]\left(\frac{n\pi}{\ell}\right) + k^2\left[D_1 J_1'(\beta a) + D_2 Y_1'(\beta a)\right] = \frac{A}{a} I_1\left(\frac{n\pi}{\ell}a\right)$$

$$-\left(\frac{n\pi}{\ell}\right)^2\left[C_1 J_1(\beta a) + C_2 Y_1(\beta a)\right] + k^2\left[C_1 J_1(\beta a) + C_2 Y_1(\beta a)\right] = \frac{n\pi}{\ell} A I_1\left(\frac{n\pi}{\ell}a\right)$$

$r = b$

$$\frac{n\pi}{\ell}\left[C_1 J_1'(\beta b) + C_2 Y_1'(\beta b)\right] - \frac{k^2}{b}\left[D_1 J_1(\beta b) + D_2 Y_1(\beta b)\right] = -B K_1'\left(\frac{n\pi}{\ell}b\right)$$

$$-\frac{1}{b}\left[C_1 J_1(\beta b) + C_2 Y_1(\beta b)\right]\left(\frac{n\pi}{\ell}\right) + k^2\left[D_1 J_1'(\beta b) + D_2 Y_1'(\beta b)\right] = \frac{B}{b} K_1\left(\frac{n\pi}{\ell}b\right)$$

$$-\left(\frac{n\pi}{\ell}\right)^2\left[C_1 J_1(\beta b) + C_2 Y_1(\beta b)\right] + k^2\left[C_1 J_1(\beta b) + C_2 Y_1(\beta b)\right] = \frac{n\pi}{\ell} B K_1\left(\frac{n\pi}{\ell}b\right)$$

These roots did pop out of both the integral and analytical formulations. They must be discarded. A signal (warning) to discard them is recognized by the fact that with $k = \frac{n\pi}{\ell}$, even the determinant of the non-null field identification matrix is zero; no information about the constants A-L can ever be inferred using these degenerate values for k.

TOTAL TRANSIENT RESPONSE

Which modal eigenvalue is used is dictated entirely by the initial field causing the transient. If the field at t = 0 were $\vec{H} = \hat{a}_y H_o \cos(\frac{3\pi}{\ell} z)$, we would use only the n = 3 eigenvalue and its associated temporal decay $(\frac{k^2}{\mu\sigma})$. (Actually there are higher order eigenvalues (k > 150) with each individual mode n which we did not bother to calculate since their temporal decay is so rapid.) In general, one must of course decompose the initial field into its spatial Fourier components (to a flat stimulus at t = 0 (H = H_o for all z)); we have

$$\vec{H} = \sum_{n=1,\text{odd}}^{\infty} (-1)^{\frac{n-1}{2}} \frac{4H_o}{n\pi} \cos(\frac{n\pi}{\ell} z) \quad . \tag{30}$$

Thus, the response to each component of the initial field is calculated separately (each with its own decay time) and weighted by the value "$\frac{4}{n\pi}$". Note the higher order modal surfaces decay rapidly. But since the higher order Fourier components contribute most significantly to the skirt regions of the field (near $z = \pm \ell/2$), one expects these regions to fall off more quickly due to the higher k values associated with the higher order modes.

The procedure for finding the transient field is as follows:

1. Set up five null field equations: (16c) (r < a and r > b); (17c) (r < a and r > b); (15c) (a < r <b only).

2. Set up one non-null field equation using (15a) ($r < a$). The region $r < a$ is the only place we know what H is at $t = 0^+$ (identical to $H_{external}$ at $t = 0^-$).

3. Solve the six equations (and boundary conditions) for the unknowns (A-L) for the modal component "n" of interest.

4. The field found using these values of (A-L) for the mode "n" and eigenvalue k define the cylinder response to a step change in the n^{th} component of external field

$$H_{y_n} = H_{o_n}\left(1 - u_{-1}(t)\right) . \tag{31}$$

The actual source field is

$$H_{y_n} = H_{o_n}\left\{1 - u_{-1}(t) + e^{-\alpha t}u(t)\right\} \tag{32}$$

where α is 5 to 40 msec for the FELIX experiments at Argonne. The total field response is realized through a convolution of $\left(\frac{-dH_{yn}}{dt}\right)$ with $e^{-\lambda t}$, i.e.,

$$H_{response} = \int_0^+ \left(-\frac{d}{dt}\,(H_y)_{t=\tau}\right)e^{-\lambda(t-\tau)}d\tau$$

$$= \frac{\alpha e^{-\frac{k^2}{\mu\sigma}t}}{\frac{k^2}{\mu\sigma} - \alpha}\left\{e^{\left(\frac{k^2}{\mu\sigma} - \alpha\right)t} - 1\right\} . \tag{33}$$

Thus (33) is the response (i.e., induced) field; the total field is (34) plus the external field $H_o e^{-\alpha t}\hat{a}_y$.

RESULTS

Figure 3 shows the predicted response fields via the integral u-v technique for the medium Felix cylinder along with the measured data. The reader should note that only modal numbers through n = 11 were considered; thus, the results should have at most a 10% error. Figure 4 shows a plot of the time the field peaks as a function of axial position. Figure 5 shows a plot of the peak field (normalized to reference value .02118 Tesla) versus axial position. As mentioned above, the cylinder end regions, being constructed from higher order "n" modes, decay more rapidly.

By way of assessing more completely the efficacy of this approach, the following additional calculations were performed and compared with the FELIX experimental results whenever possible (via a 2 exponential fit). In each case we plot the induced field versus time, the maximum induced field as a function of axial position, and the time that the induced field peaks as a function of axial position. The case studies are as follows:

1. Large FELIX cylinder, primary field time constant, τ = 39.68 msec (Figs. 6-8)
2. Medium (20 cm) FELIX cylinder, primary field time constant, τ = 6.87 msec (Figs. 9-11)
3. Medium (60 cm) FELIX cylinder, primary field time constant, τ = 39.68 msec (Figs. 12-14)
4. Small FELIX cylinder, primary field time constant, τ = 39.68 msec (Figs. 15-17)
5. Large FELIX cylinder, primary field time constant, τ = 6.87 msec (Figs. 18-20)

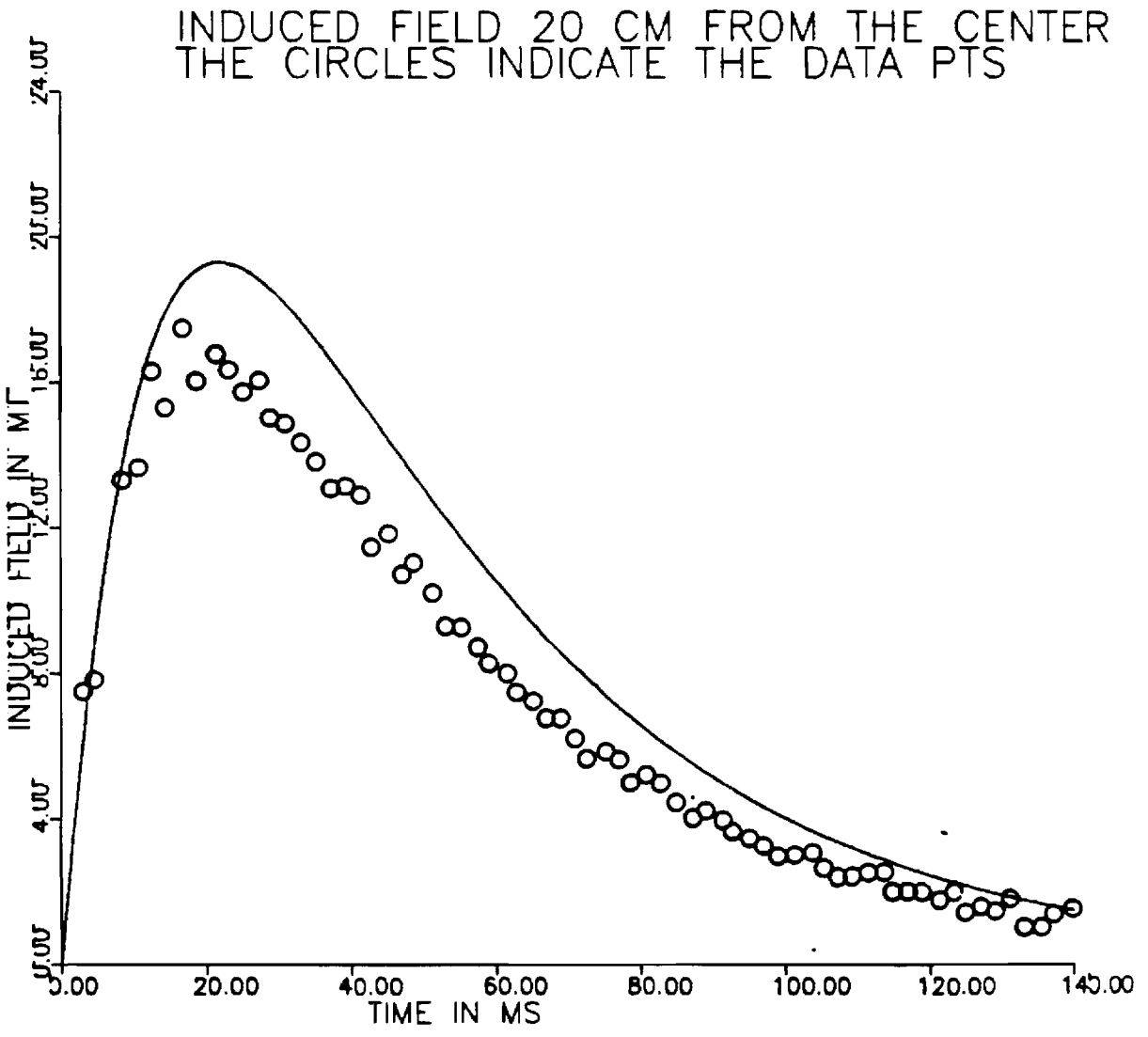

Figure 3. Predicted Induced Field Versus Time Along with Measure Data; The Main Field Decays with Characteristic Time 39.68 msec. ($a = .05715$ m, $b = .06985$ m, $\ell = .6$ m, $\sigma = 2.538 \times 10^7$ mho/m.)

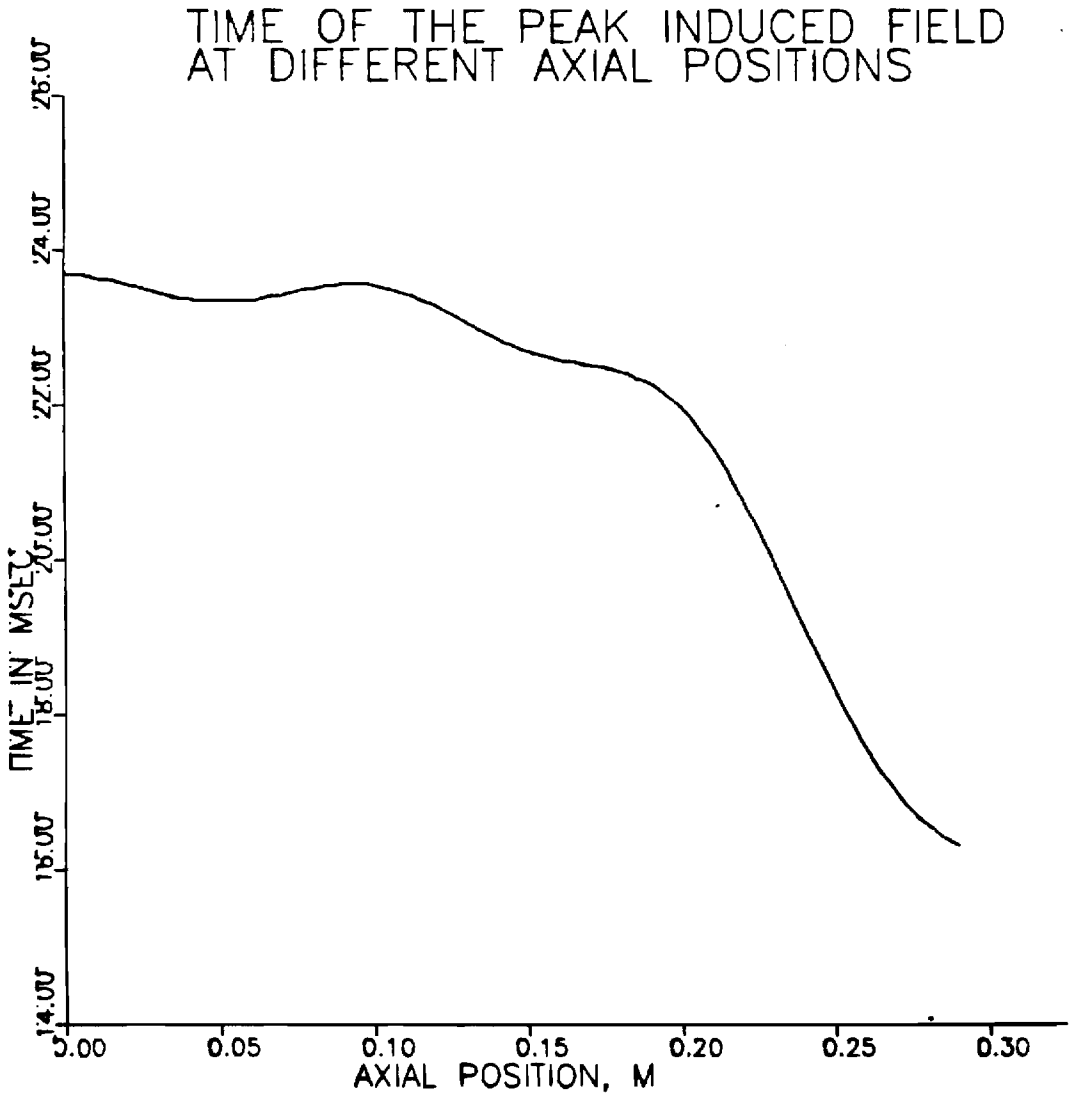

Figure 4. Prediction of Occurrence of Peak Field Time Versus Position in the Medium Cylinder.

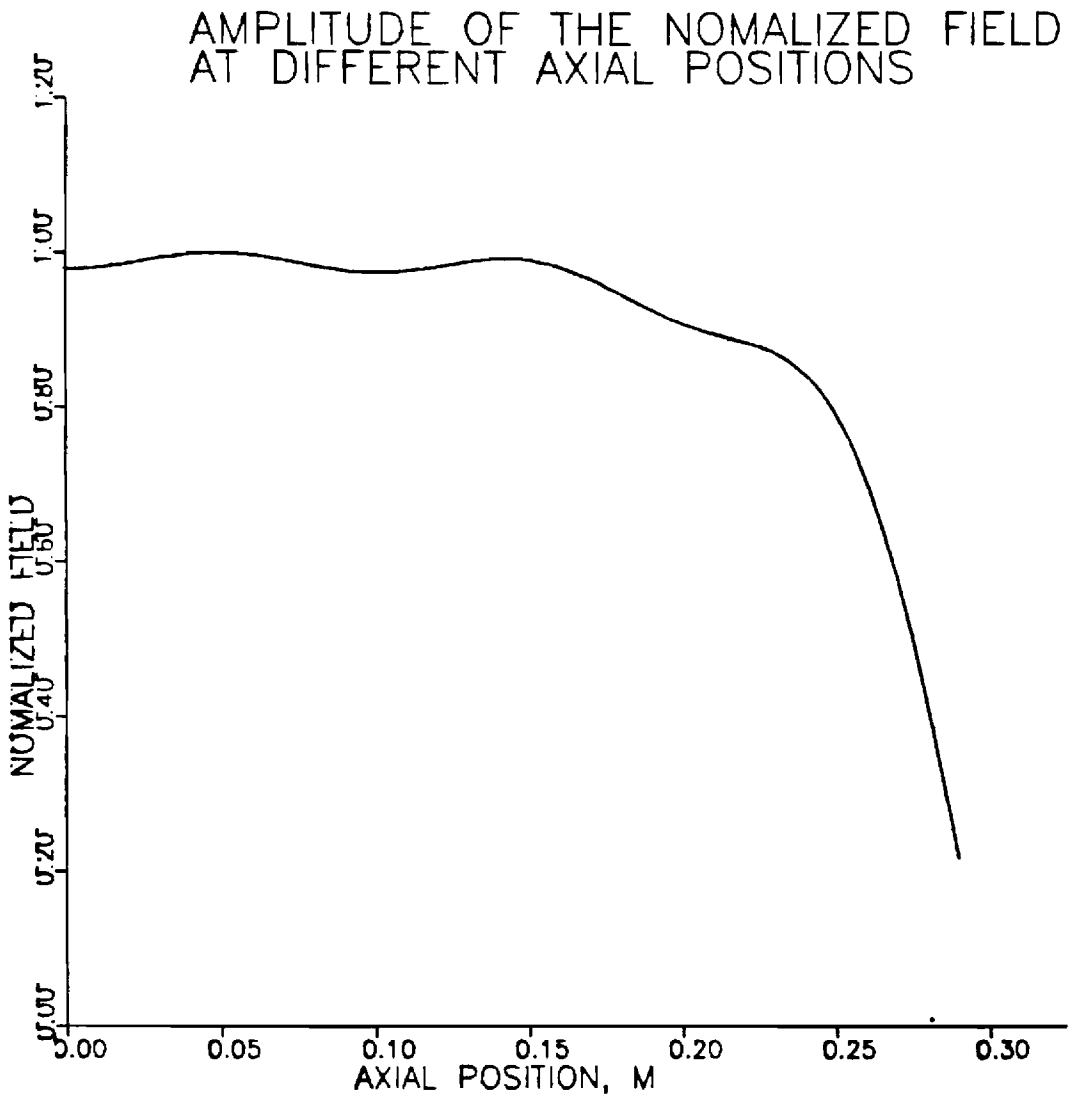

Figure 5. Prediction of Peak Amplitude Versus Axial Position in the Medium Cylinder.

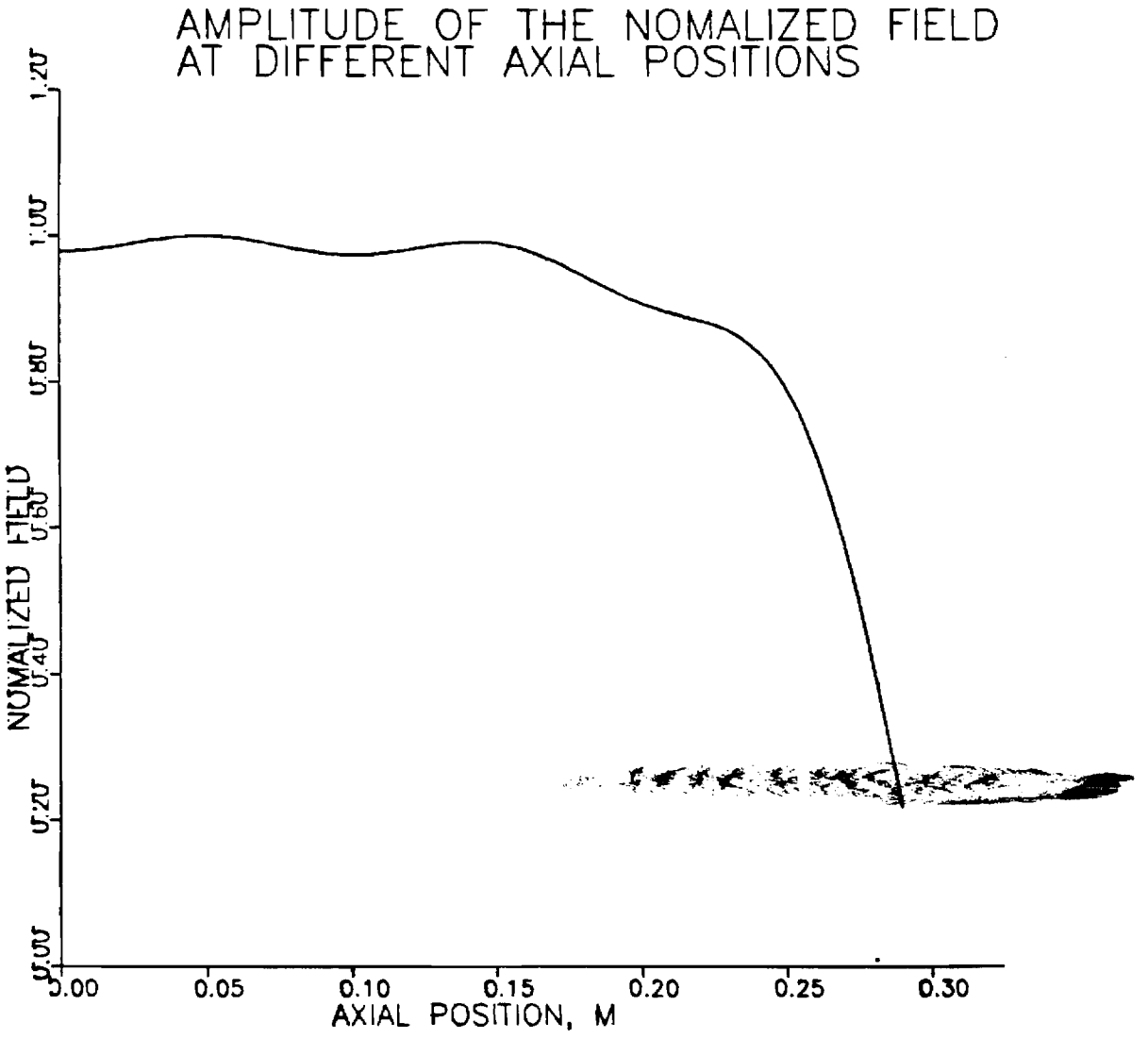

Figure 5. Prediction of Peak Amplitude Versus Axial Position in the Medium Cylinder.

6. Medium (40 cm) FELIX cylinder, primary field time constant, τ = 6.87 msec (Figs. 21-23)

7. Small FELIX cylinder, primary field time constant, τ = 6.87 msec (Figs. 24-26).

The dots or dashes on each curve are the experimental values.

As evident in the above plots, the results agree reasonably well, but there is room for improvement, especially as regards the large cylinder field predictions. As mentioned above, the results were obtained by treating the problem as a three region problem, employing 6 null field equations to derive the identification matrix. Borrowing on some techniques from the scattering research community [11], we suspected that a better approach would be to use equations (15b), (16b), and (17b) to yield 6 boundary equations as well as (16c) to give an additional null field equation. Thus, we formulate 7 equations for 6 unknowns. The matrix (now 7 x 6) must be multiplied by its transpose before searching for the eigenvalues as the determinant of this modified matrix. This numerical trick greatly stabilizes the problem. In fact, with this change, the problem can indeed be solved as a two region problem without artificial interfaces.

A second surprise resulted after this modification. In addition to the base resonances found for each mode as before, additional resonances (eigenvalues) appeared. For the 2-D problem we found 2 eigenvalues (k = 51 and k = 150). The second value is quite far removed and it so happens that the weighting constant multiplying the second eigenvalue (based on the initial conditions) is nearly zero.

The 3-D eigenvalues for mode 1 $\left(\cos \frac{\pi}{\ell} z\right)$ are k = 57, 107, 128, 151, 178. We seek the eigenvectors for each eigenvalue mode by mode exactly as explained above.

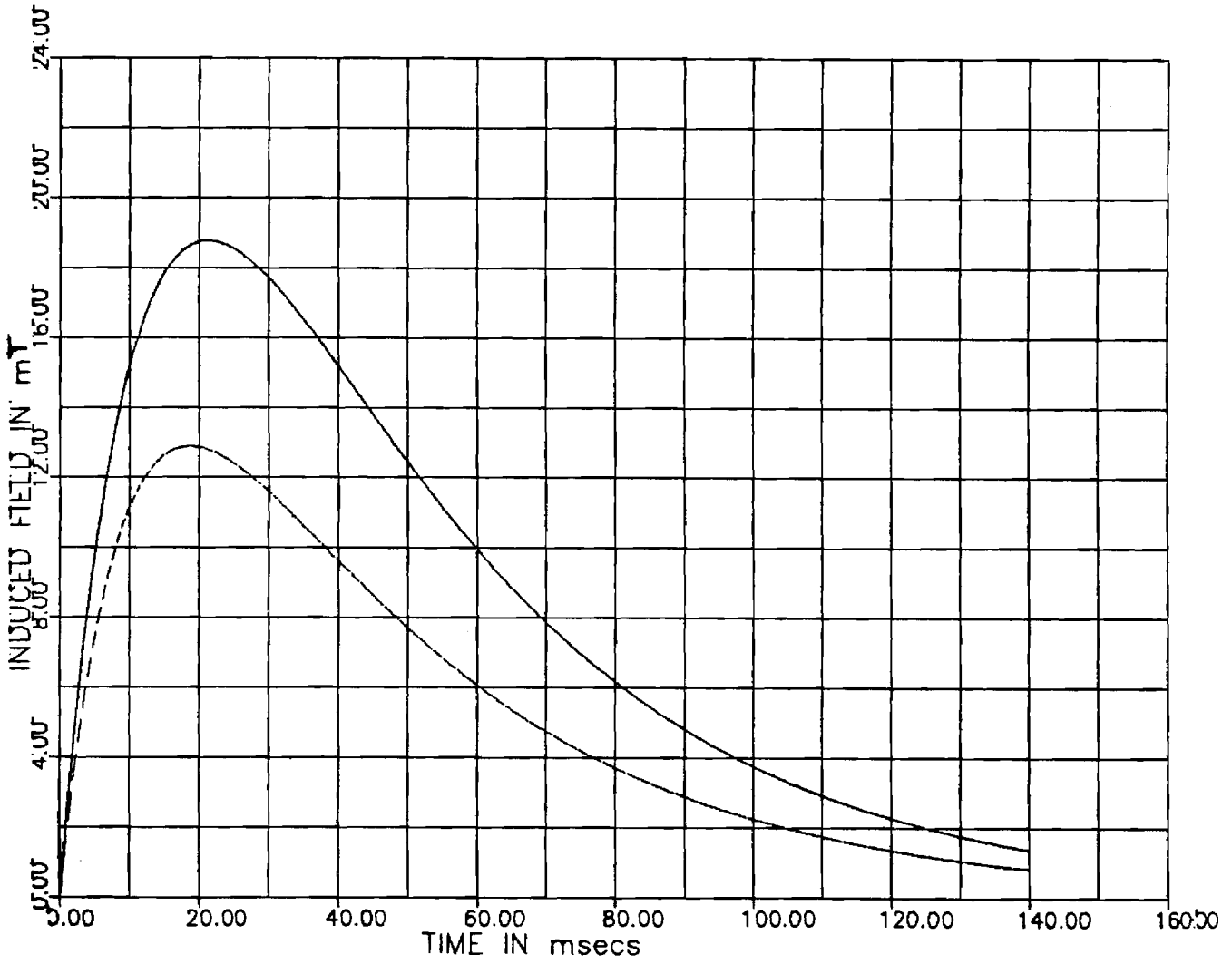

FIGURE 6. LARGE CYLINDER FIELDS, TIME CONSTANT = 39.68 msec

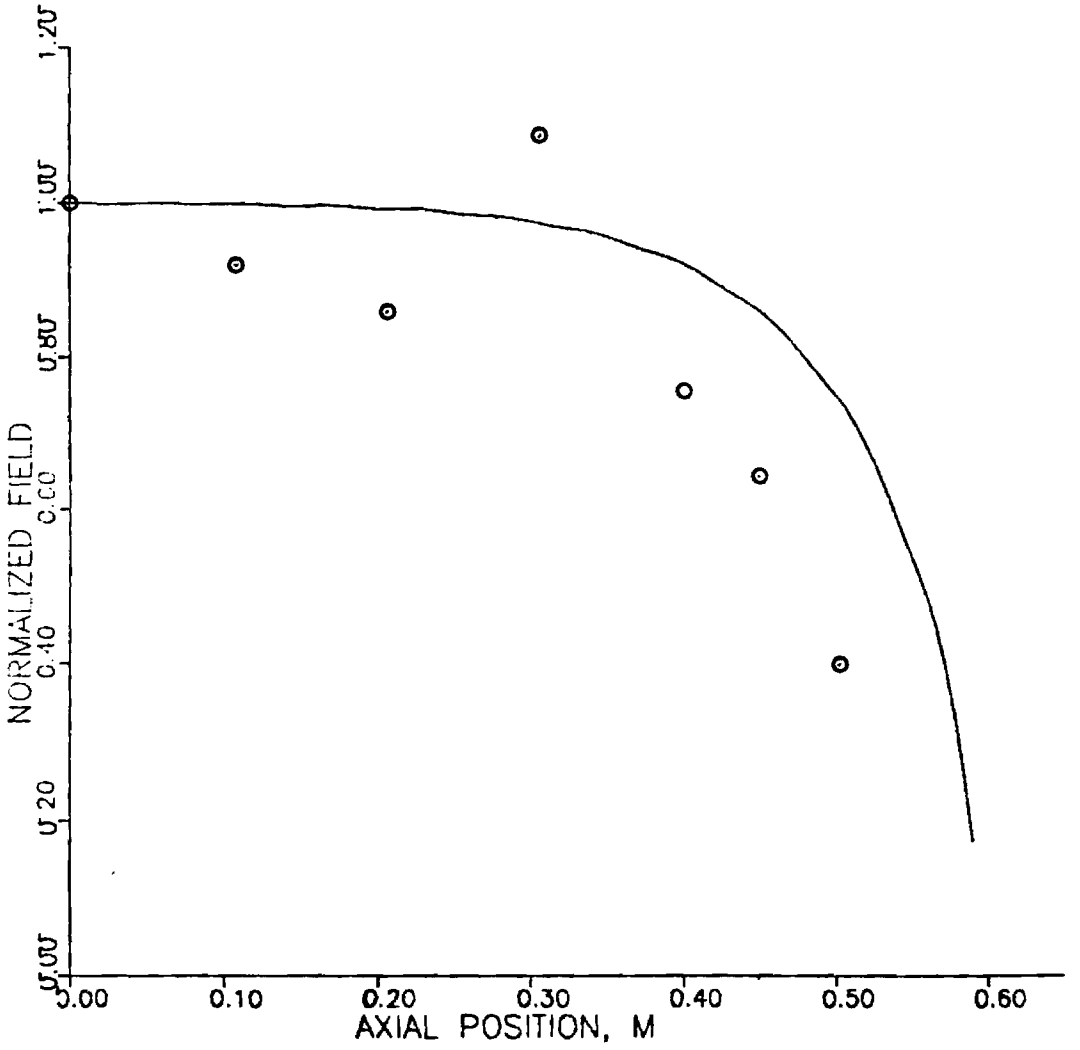

FIGURE 7. MAXIMUM INDUCED FIELD LARGE CYLINDER, TIME CONSTANT = 39.68 msec

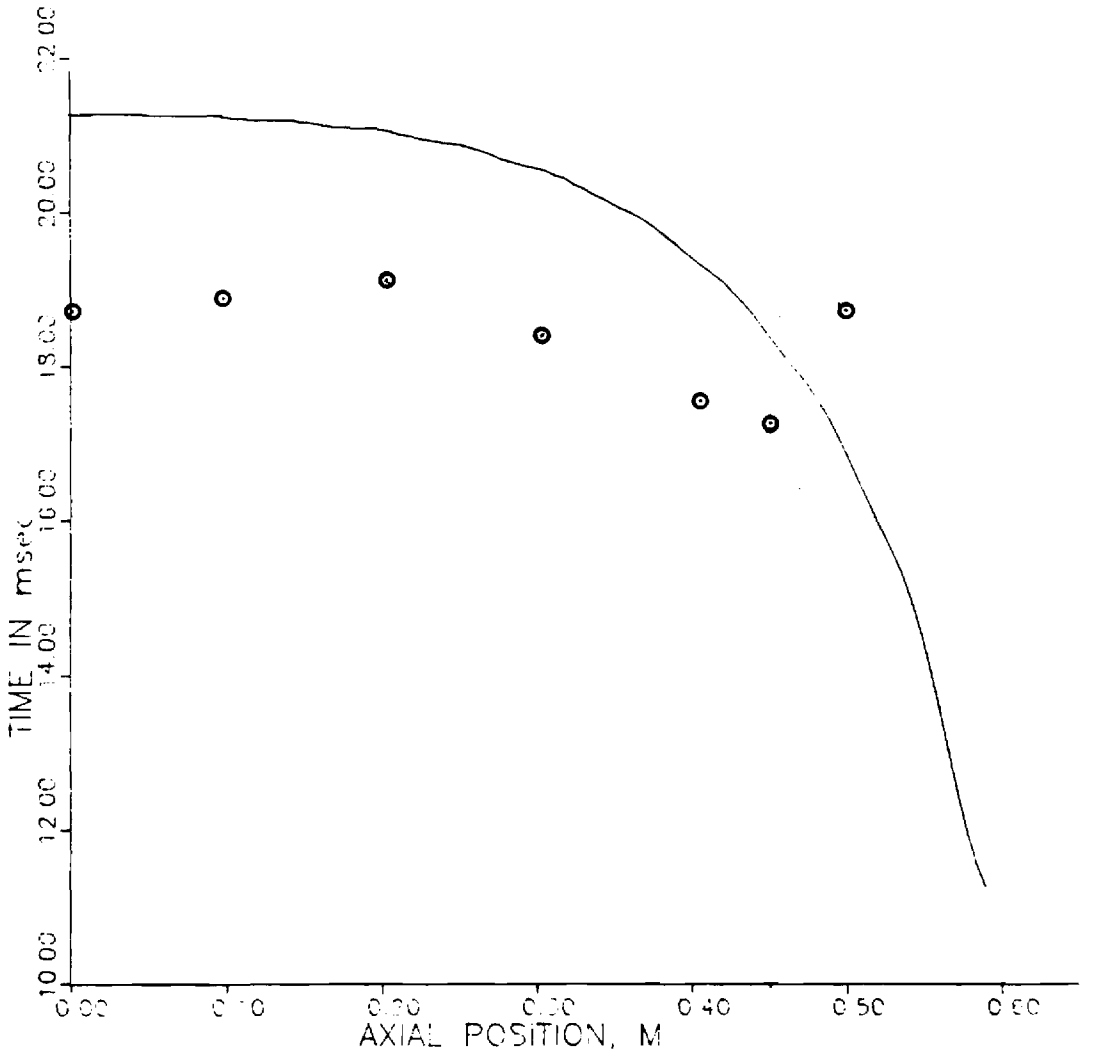

FIGURE 8. TIME OF THE PEAK INDUCED FIELD LARGE CYLINDER, TIME CONSTANT = 39.68 msec

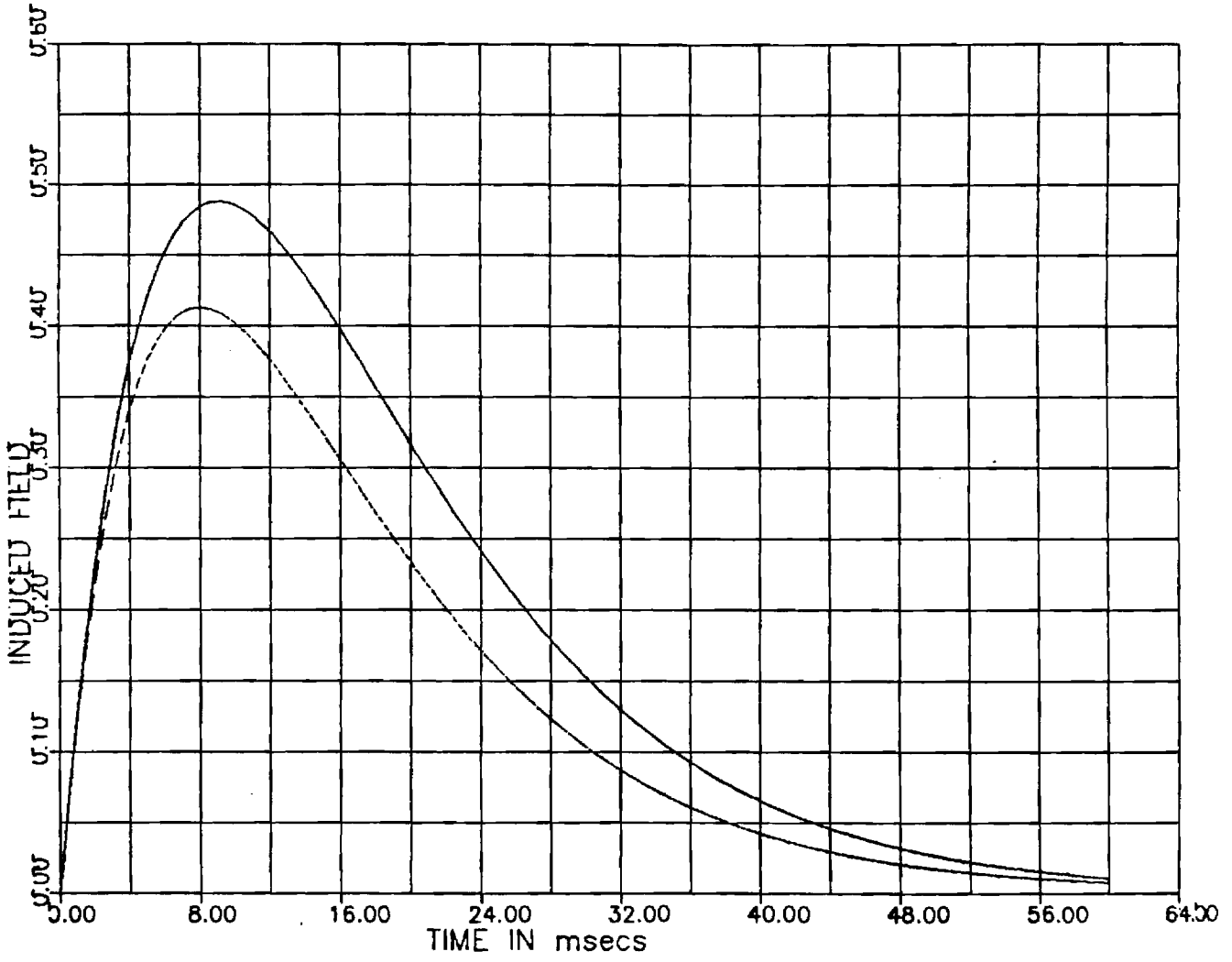

FIGURE 9. MEDIUM 20 cm CYLINDER, TIME CONSTANT = 6.87 msec WITH NORMALIZED INPUT FIELD

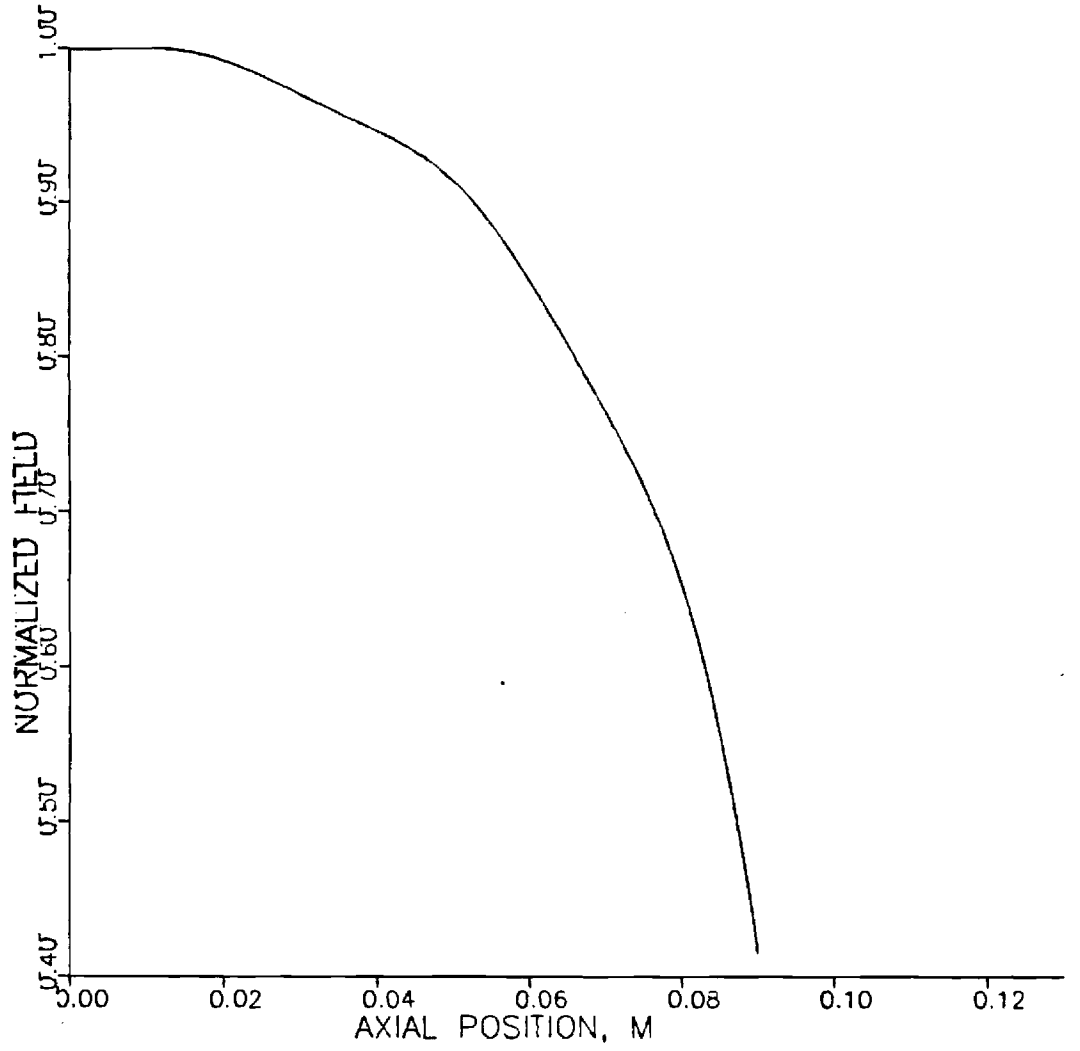

FIGURE 10. MAXIMUM INDUCED FIELD MEDIUM 20 cm CYLINDER, TIME CONSTANT = 6.87 msec

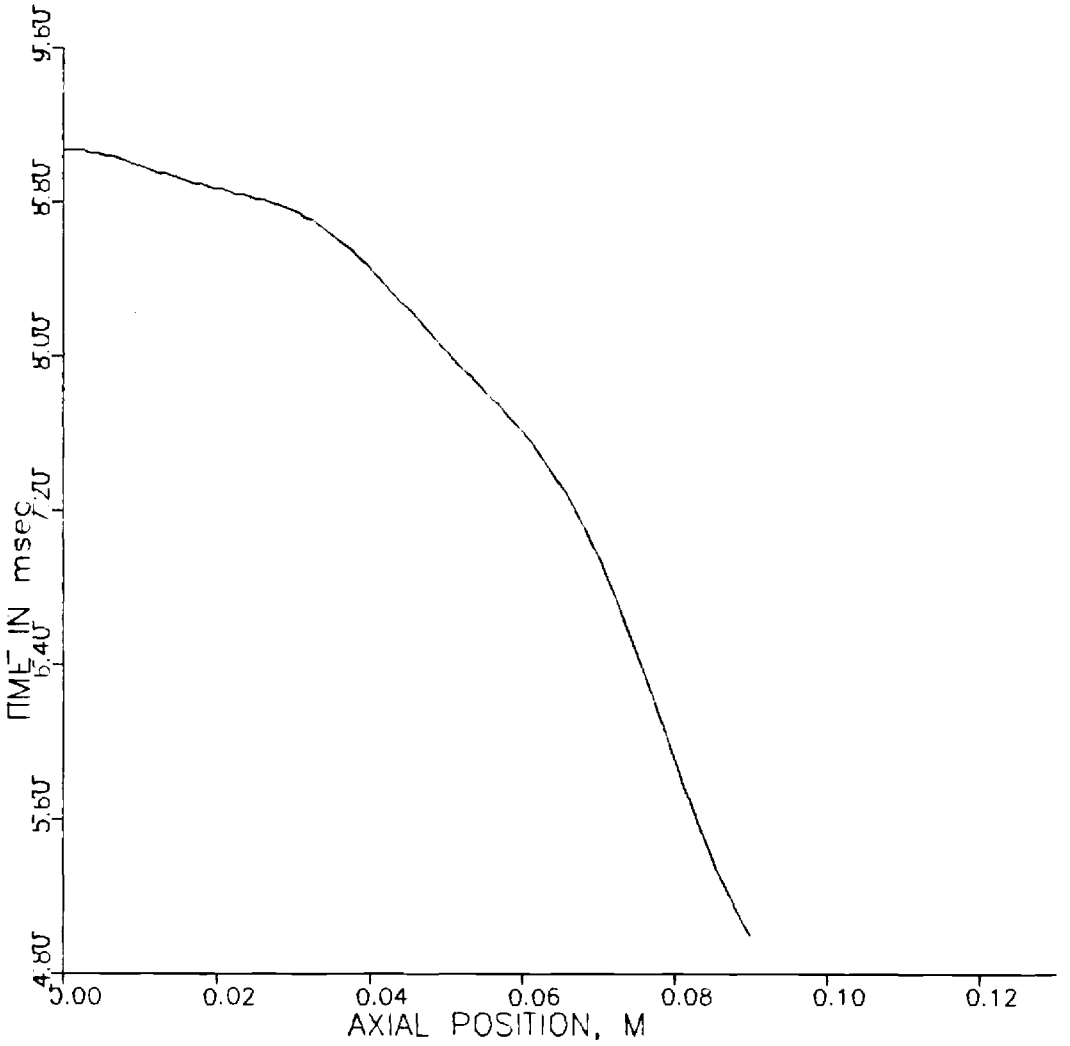

FIGURE 11. TIME OF THE PEAK INDUCED FIELD MEDIUM 20 cm CYLINDER TIME CONSTANT = 6.87 msec

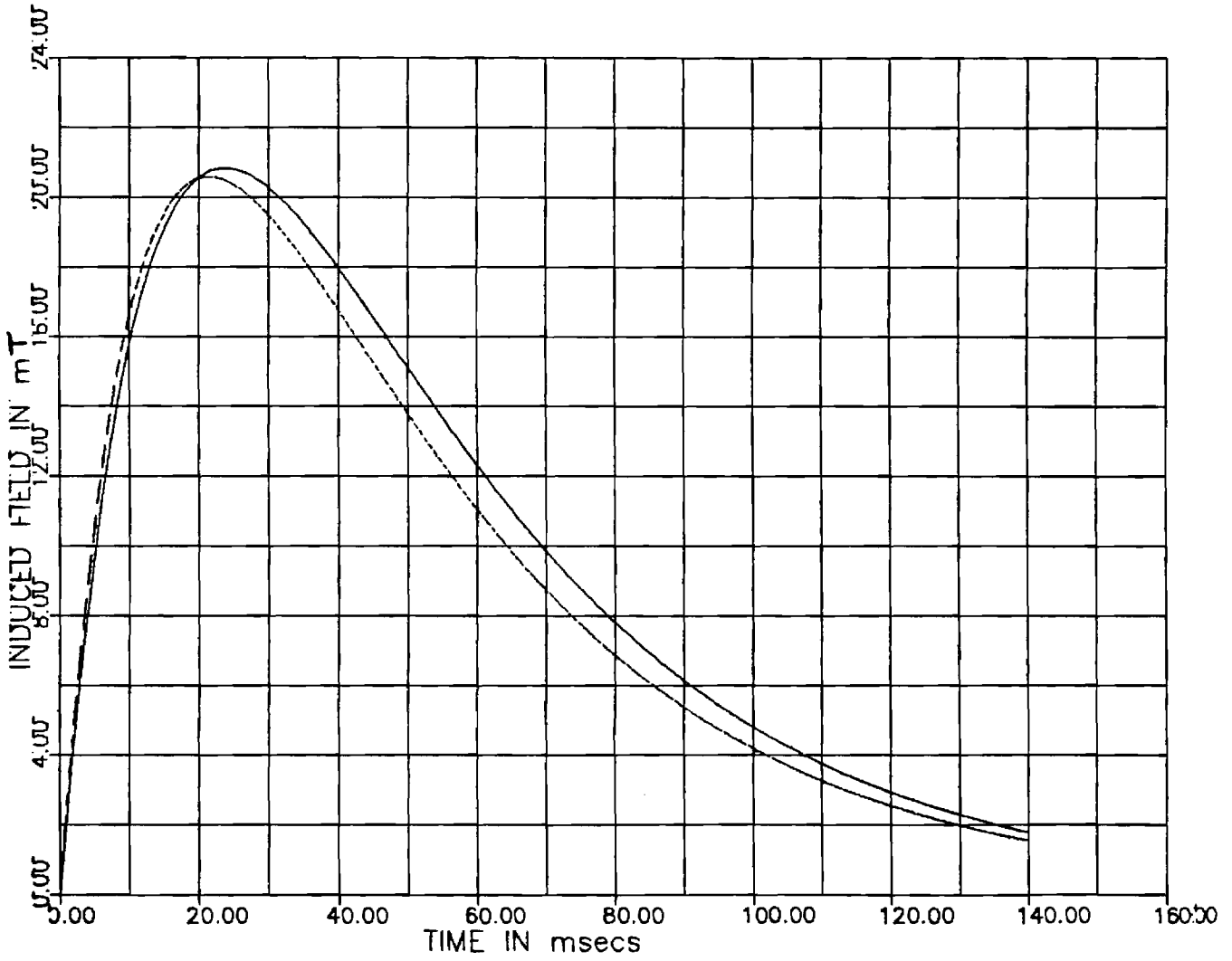

FIGURE 12. MEDIUM 60 cm CYLINDER, TIME CONSTANT = 39.68 msec

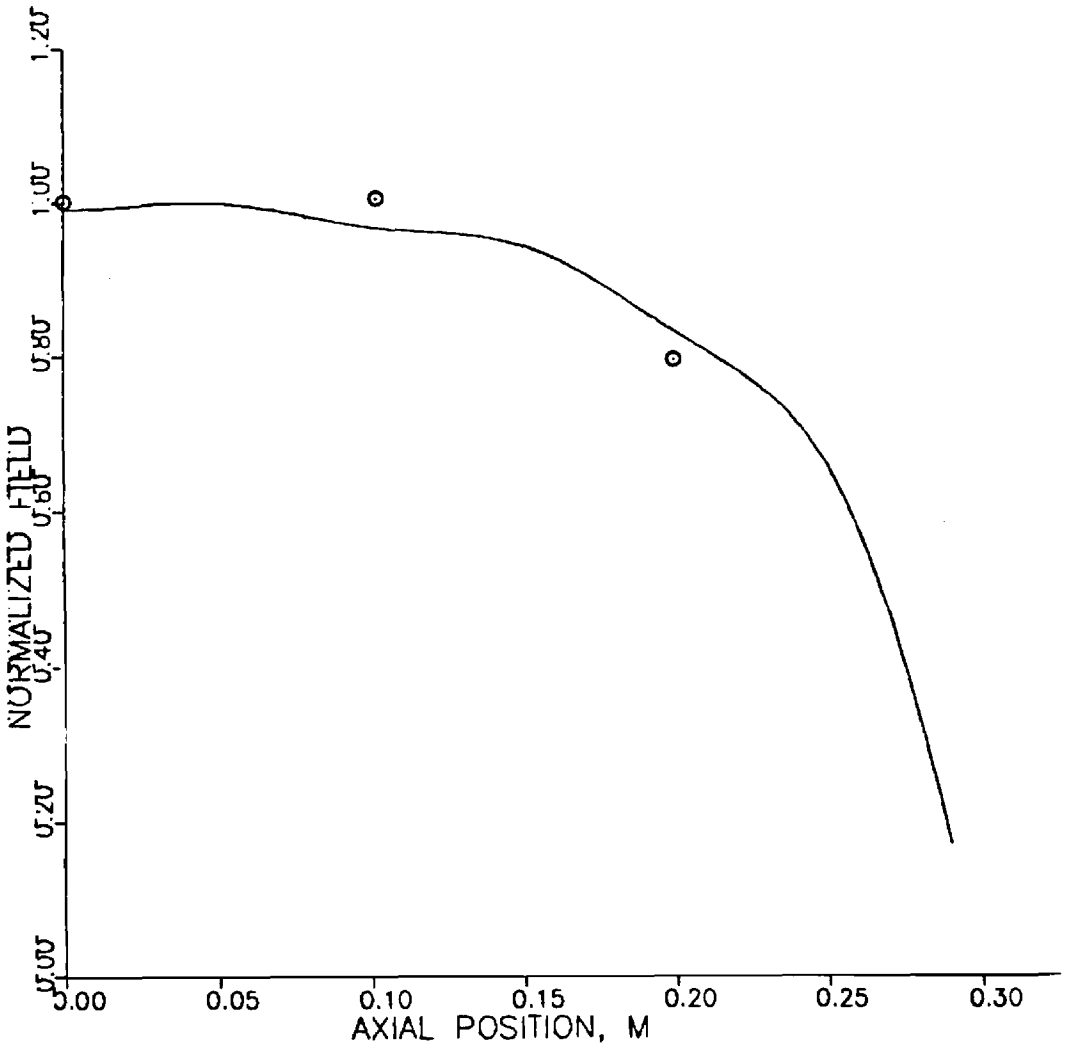

FIGURE 13. MAXIMUM INDUCED FIELD MEDIUM 60 cm CYLINDER, TIME CONSTANT = 39.68 msec

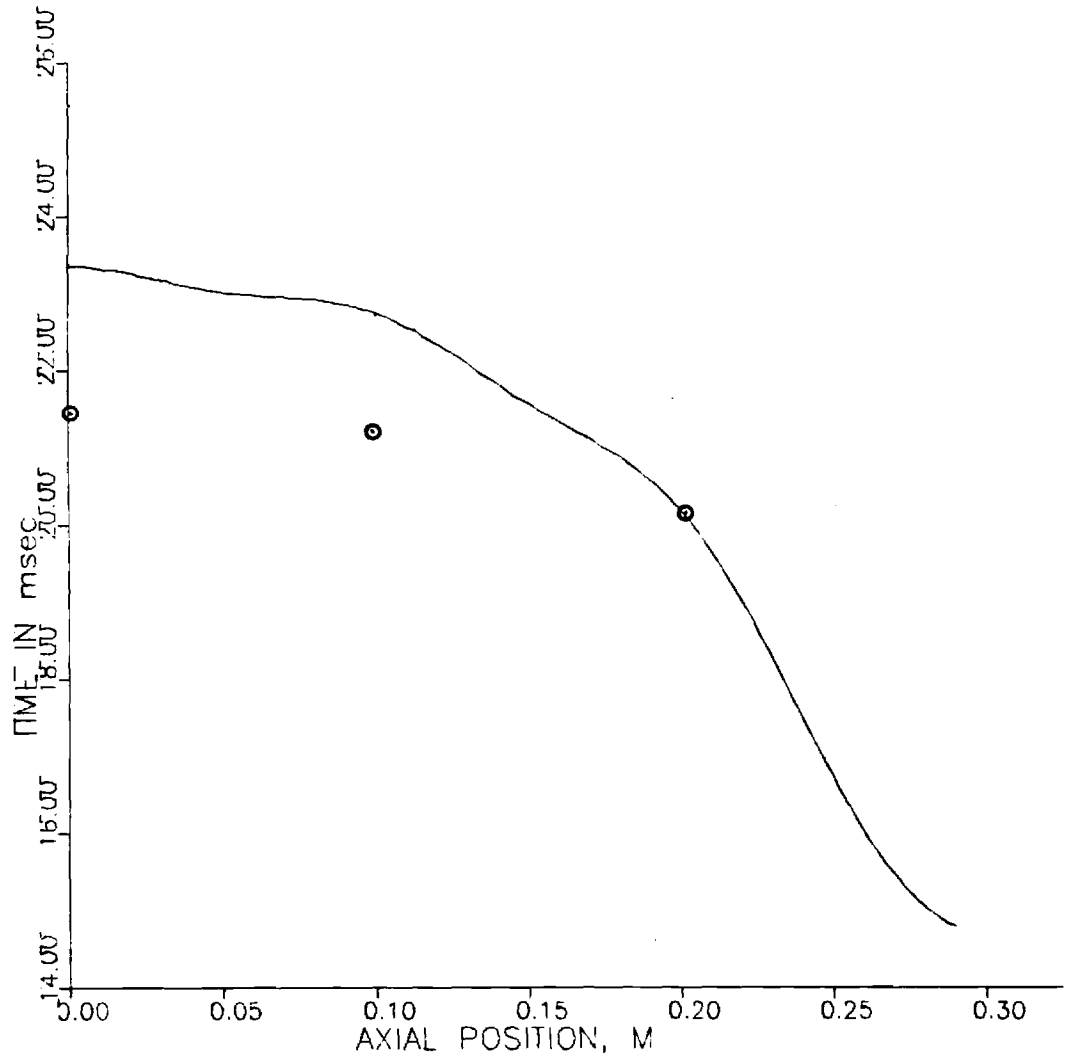

FIGURE 14. TIME OF THE PEAK INDUCED FIELD MEDIUM 60 cm CYLINDER TIME CONSTANT = 39.68 msec

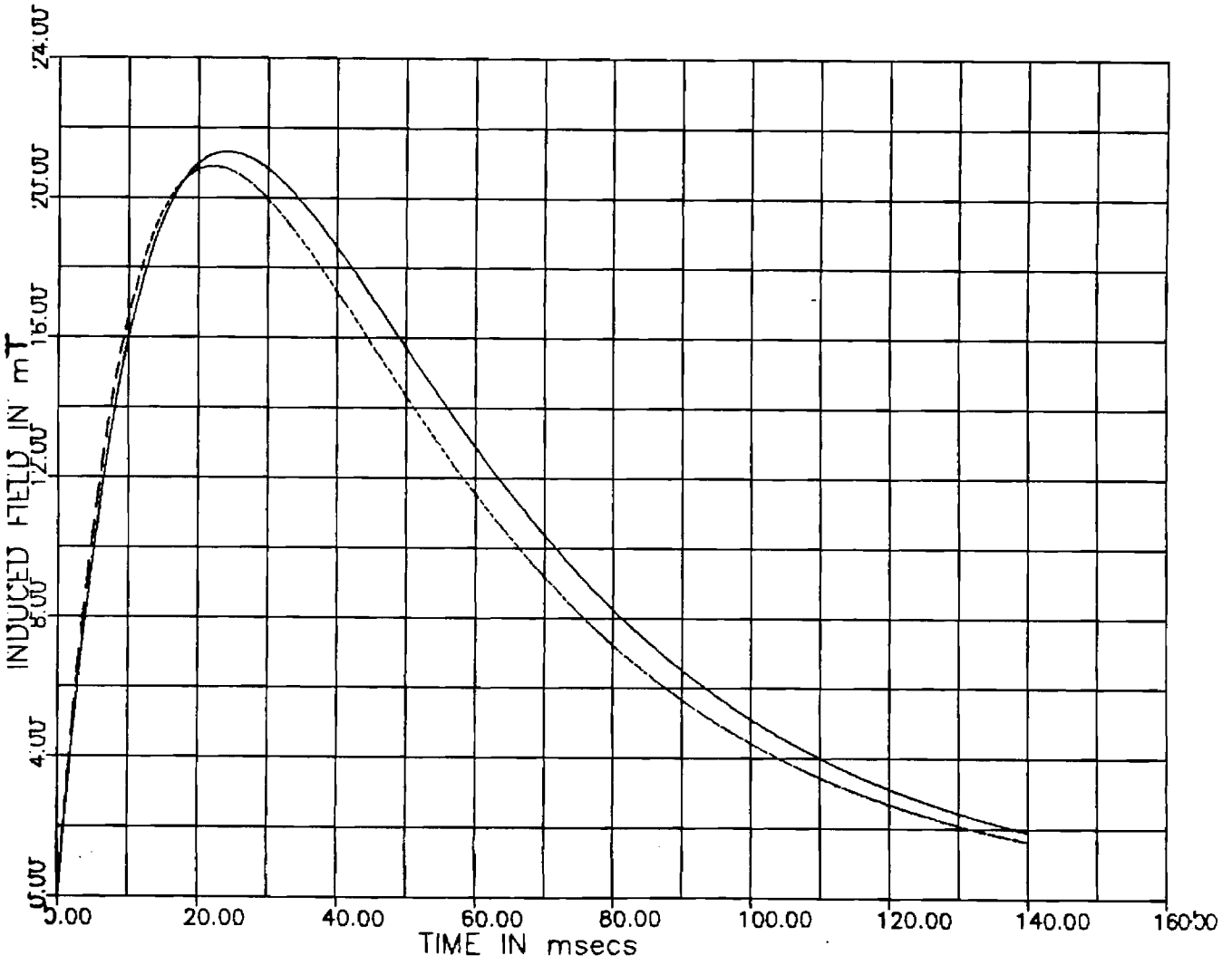

FIGURE 15. SMALL CYLINDER, TIME CONSTANT = 39.68 msec

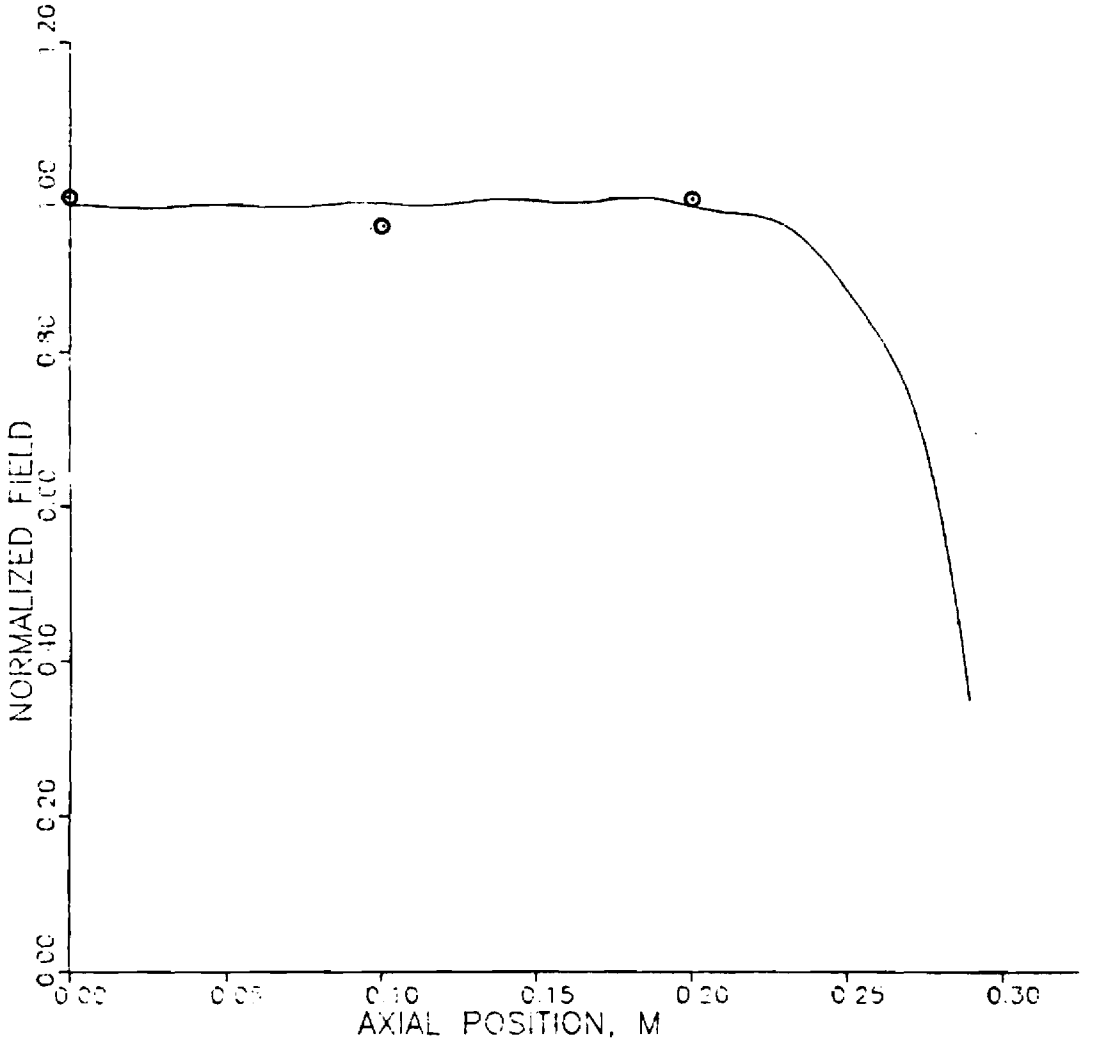

FIGURE 16. MAXIMUM INDUCED FIELD SMALL CYLINDER, TIME CONSTANT = 39.68 msec

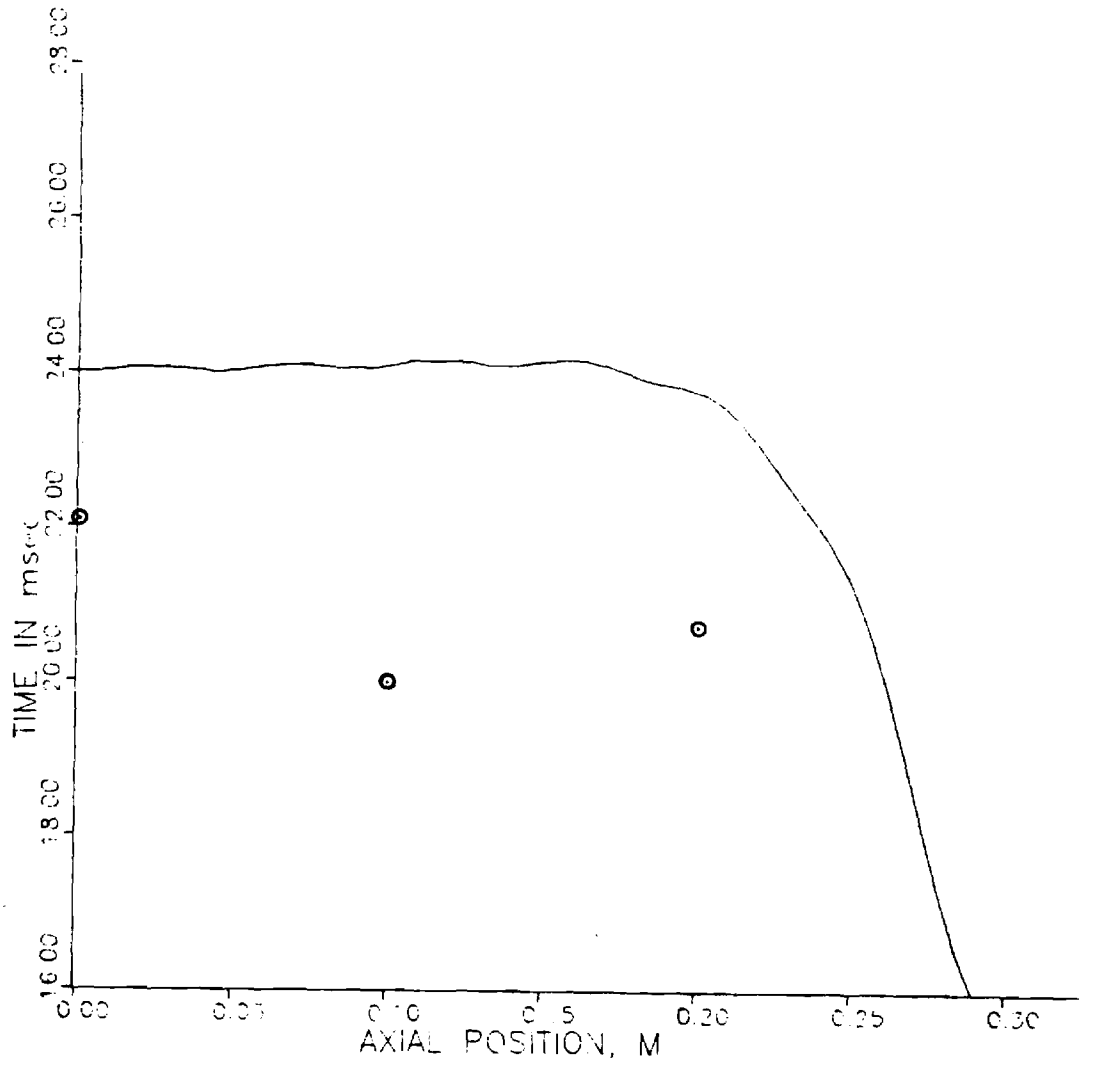

FIGURE 17. TIME OF THE PEAK INDUCED FIELD SMALL CYLINDER, TIME CONSTANT = 39.68 msec

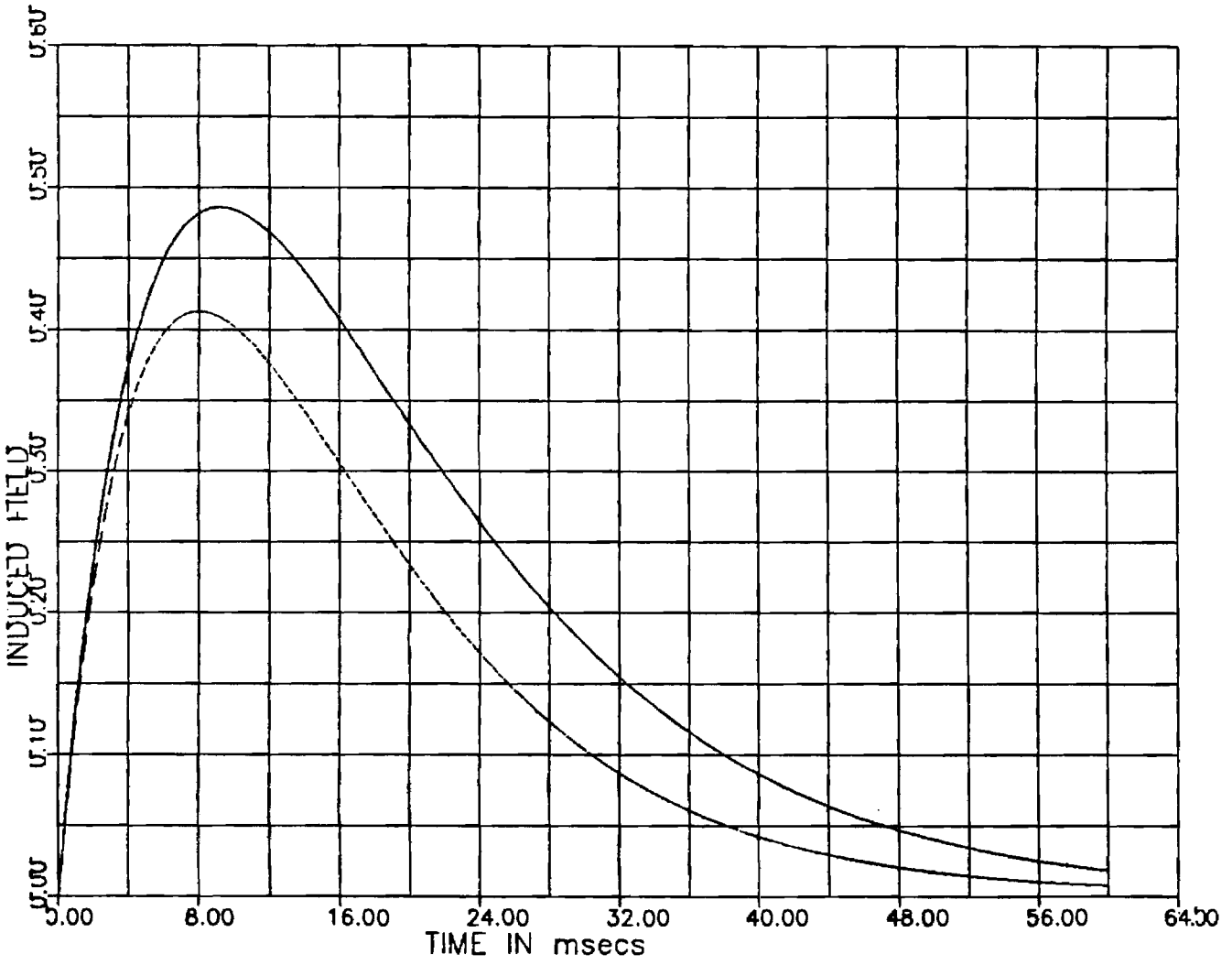

FIGURE 18. LARGE CYLINDER, TIME CONSTANT = 6.87 msec WITH NORMALIZED INPUT FIELD

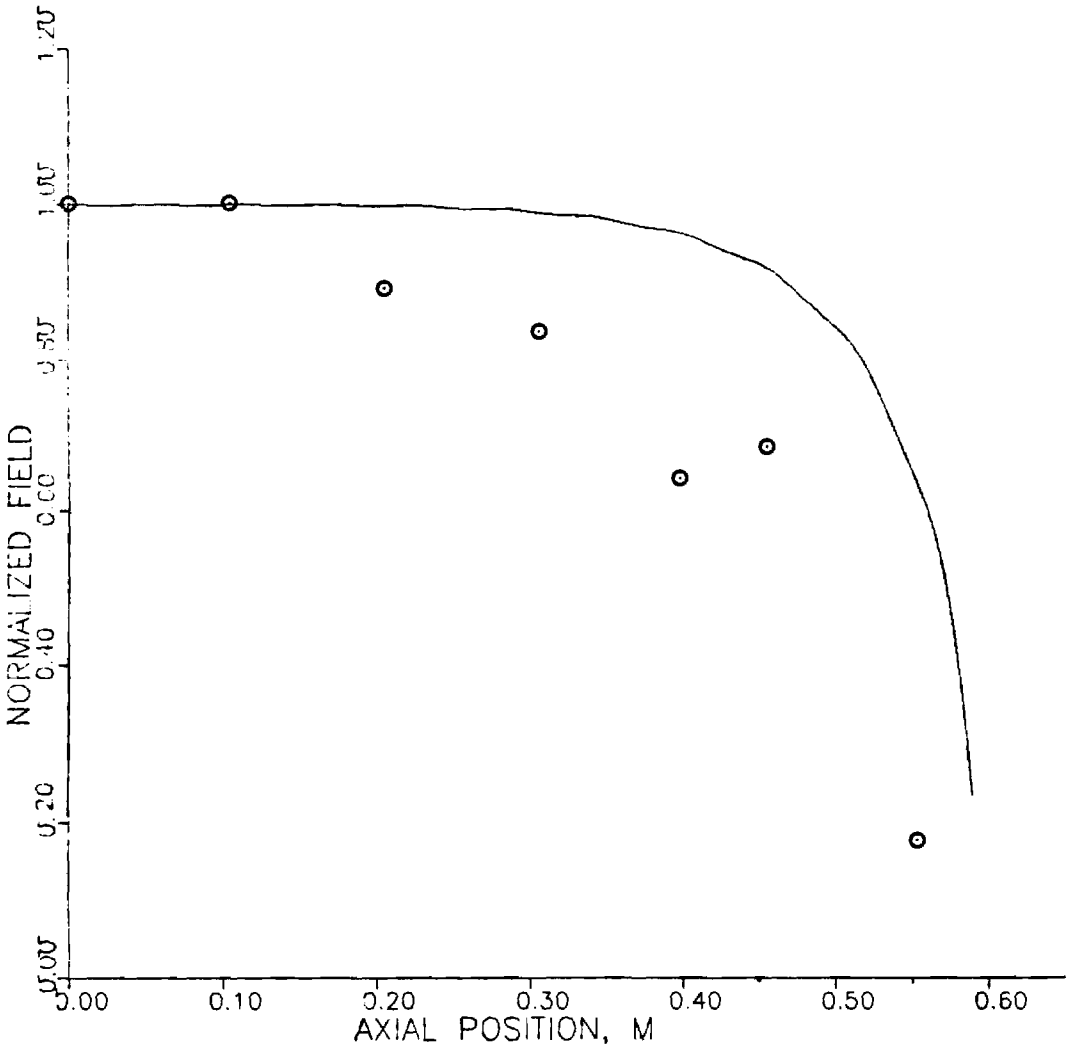

FIGURE 19. MAXIMUM INDUCED FIELD LARGE CYLINDER, TIME CONSTANT = 6.87 msec

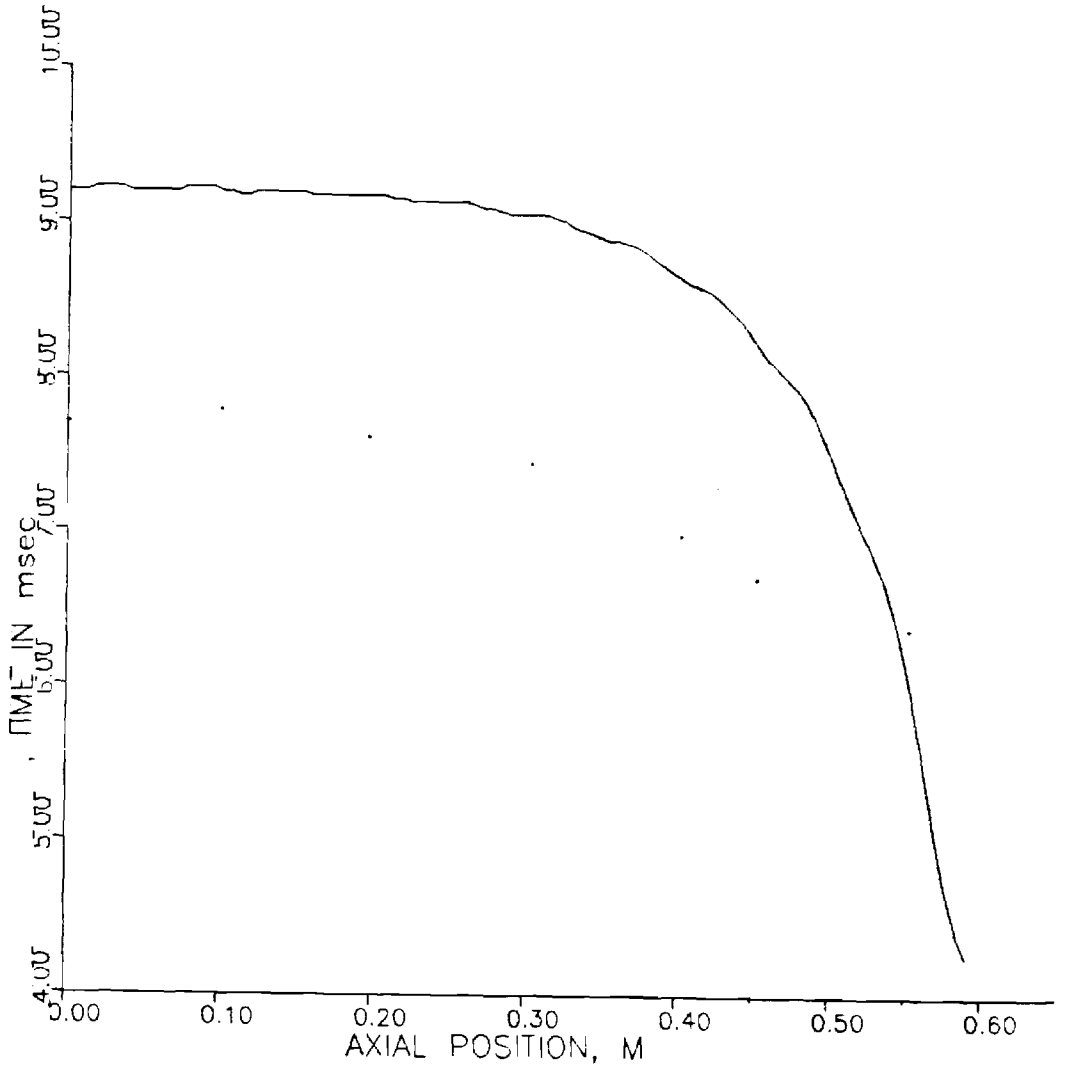

FIGURE 20. TIME OF THE PEAK INDUCED FIELD LARGE CYLINDER, TIME CONSTANT = 6.87 msec

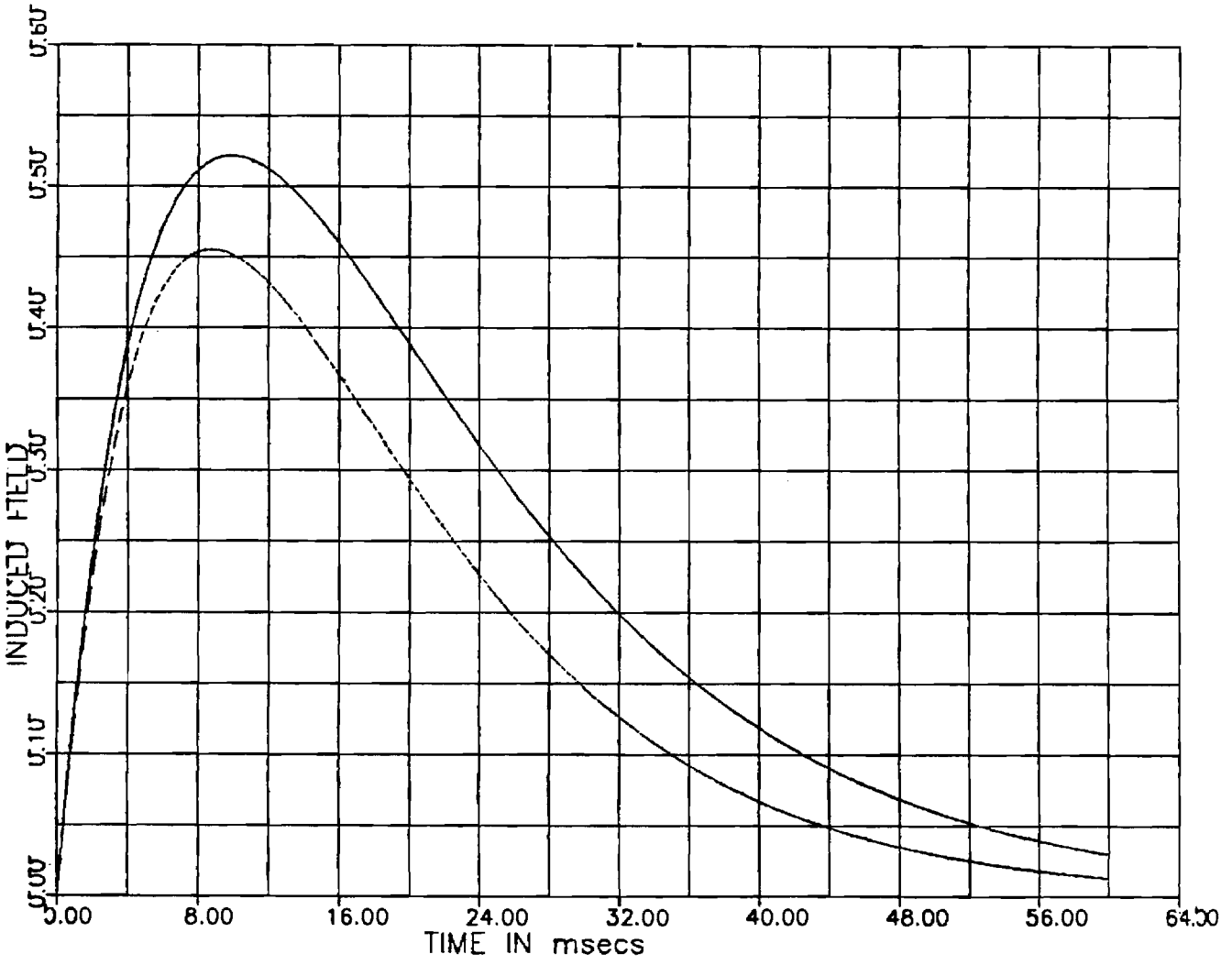

FIGURE 21. MEDIUM 40 cm CYLINDER, TIME CONSTANT = 6.87 msec WITH NORMALIZED INPUT FIELD

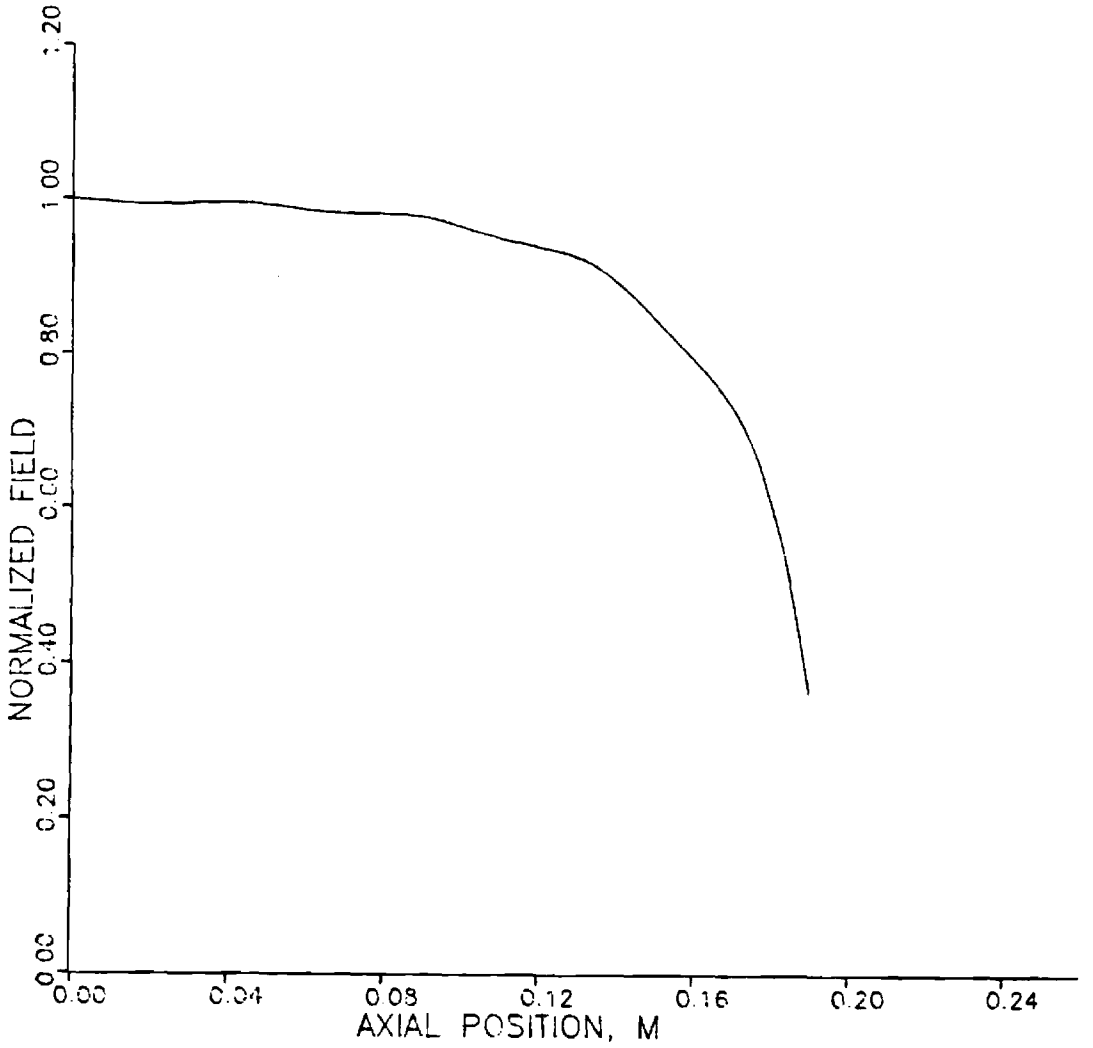

FIGURE 22. MAXIMUM INDUCED FIELD MEDIUM 40 cm CYLINDER, TIME CONSTANT = 6.87 msec

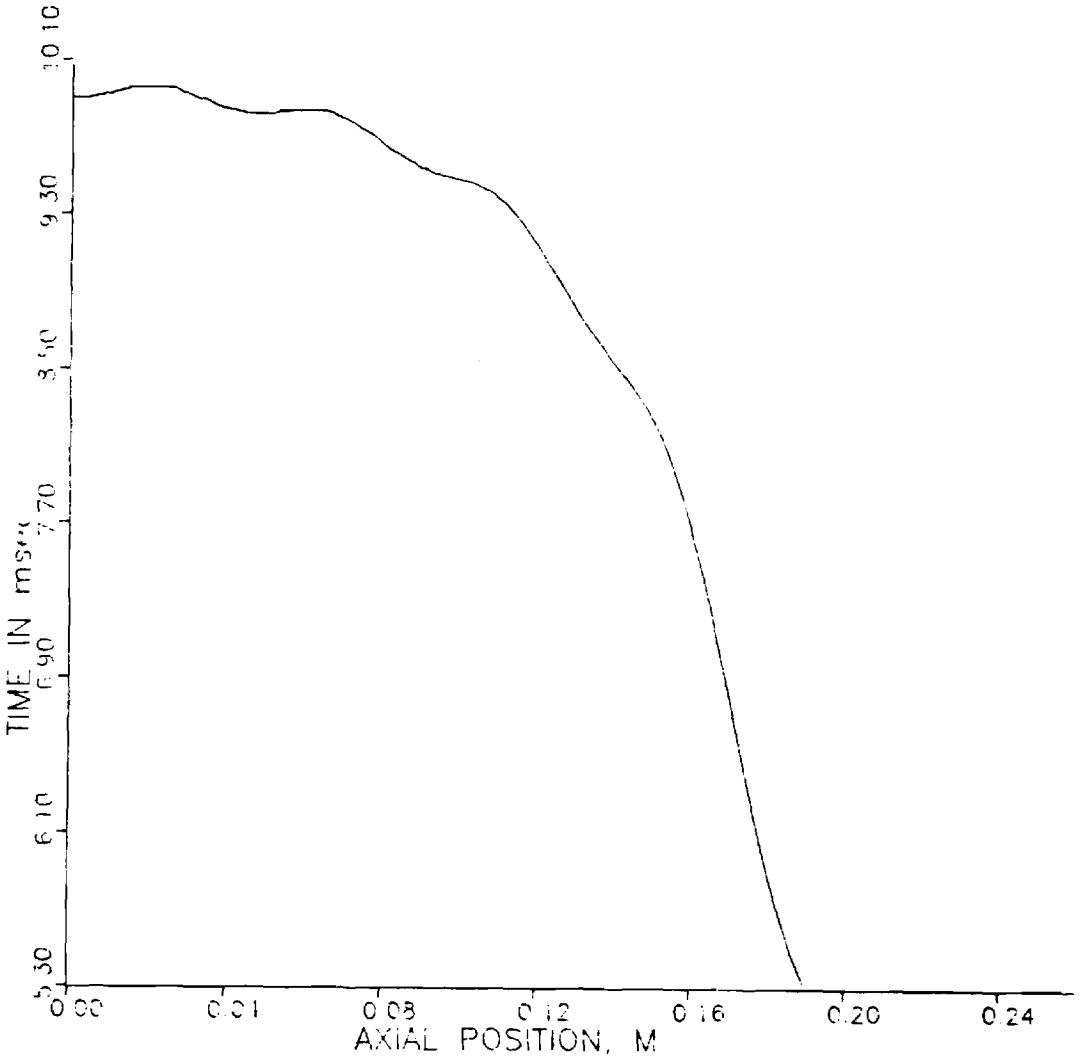

FIGURE 23. TIME OF THE PEAK INDUCED FIELD MEDIUM 40 cm CYLINDER, TIME CONSTANT = 6.87 msec

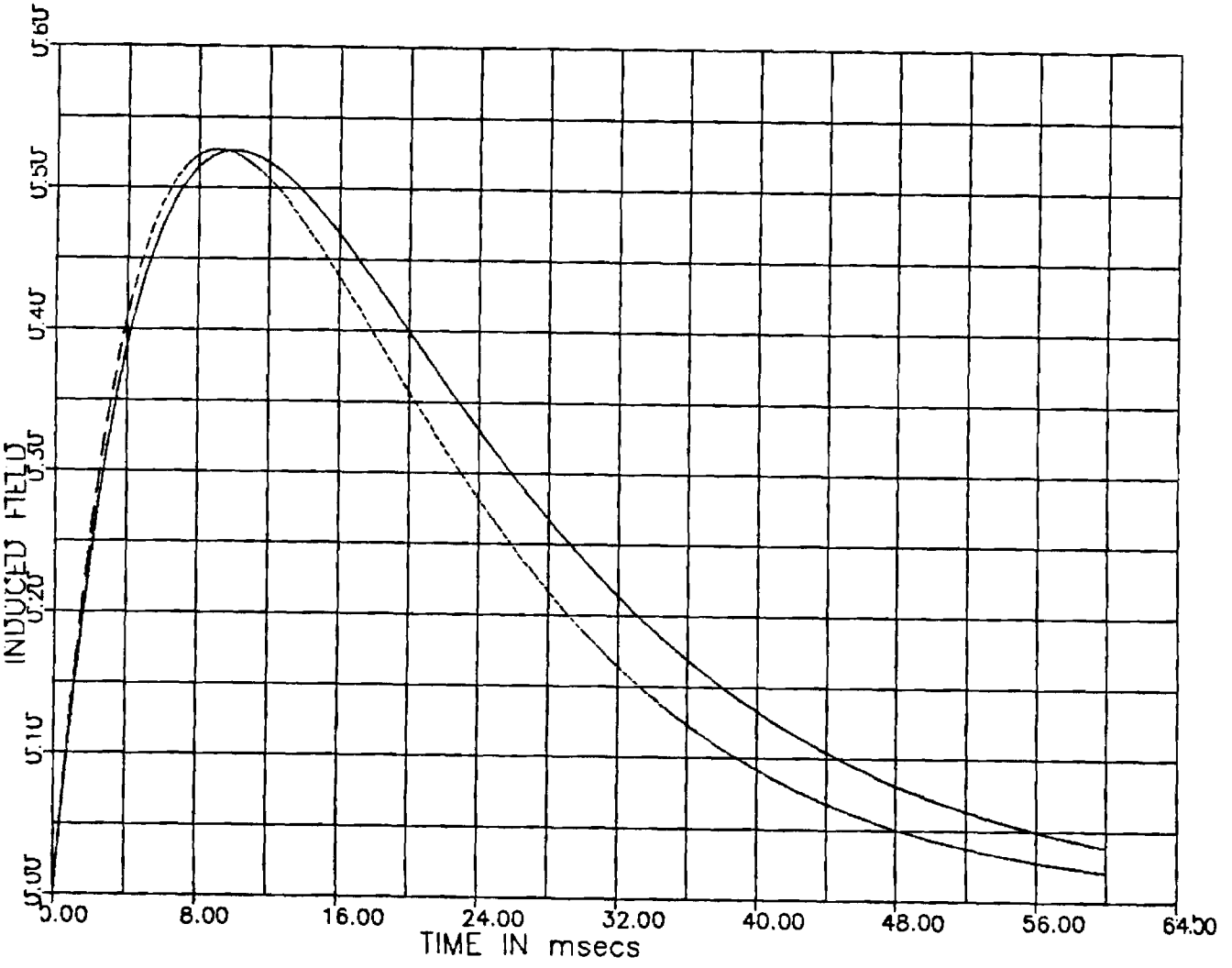

FIGURE 24. SMALL CYLINDER, TIME CONSTANT = 6.87 msec WITH NORMALIZED INPUT FIELD

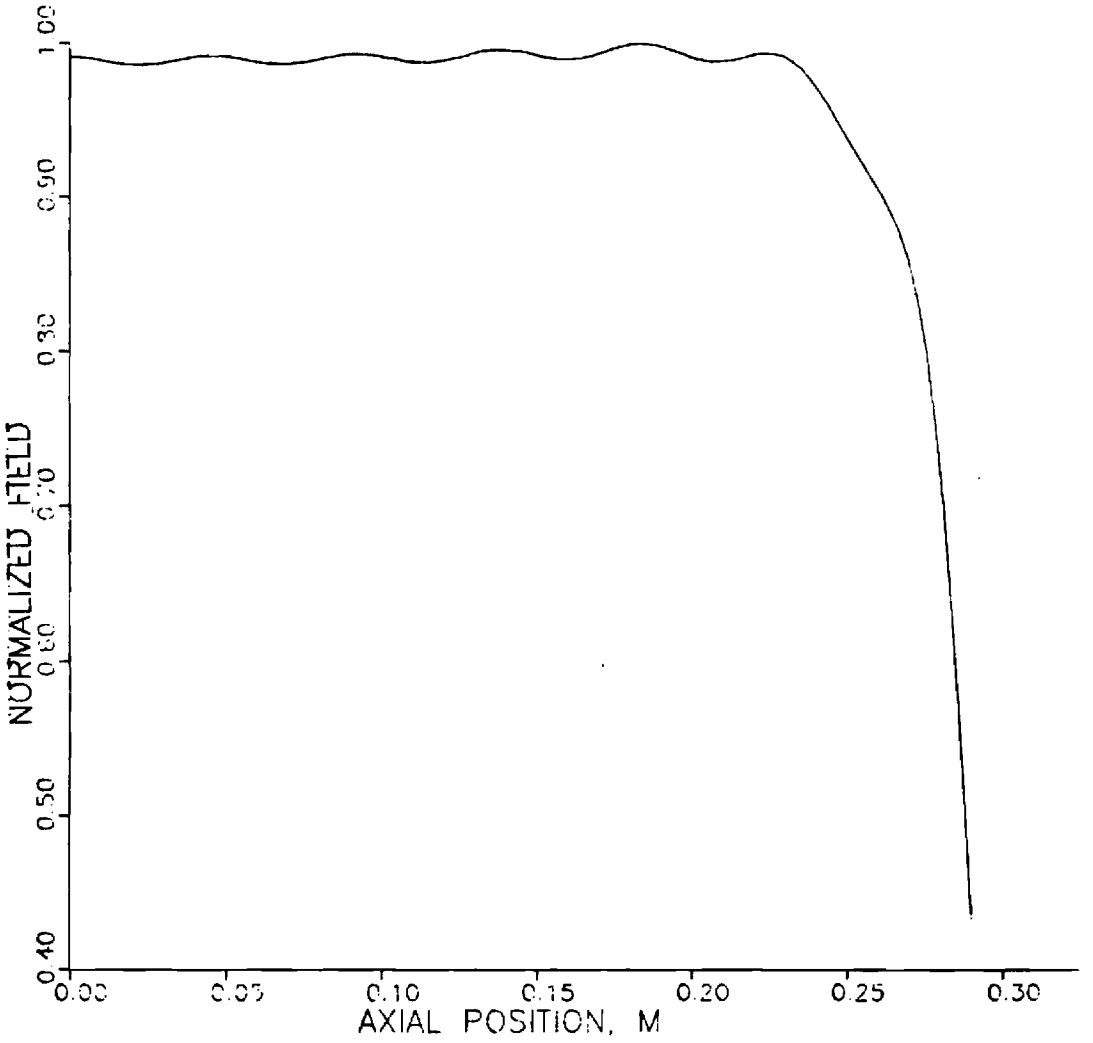

FIGURE 25. MAXIMUM INDUCED FIELD SMALL CYLINDER, TIME CONSTANT = 6.87 msec

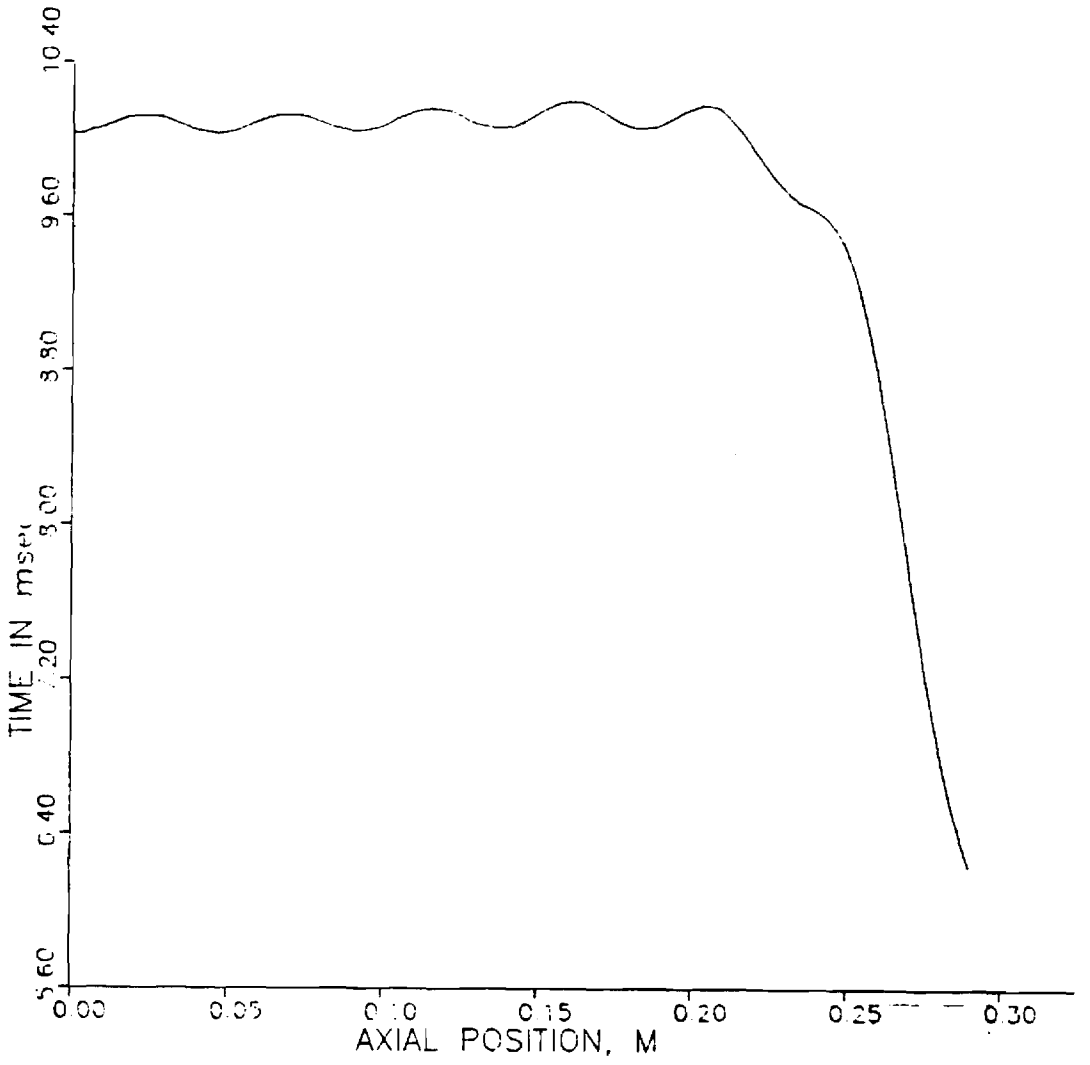

FIGURE 26. TIME OF THE PEAK INDUCED FIELD SMALL CYLINDER, TIME CONSTANT = 6.87 msec

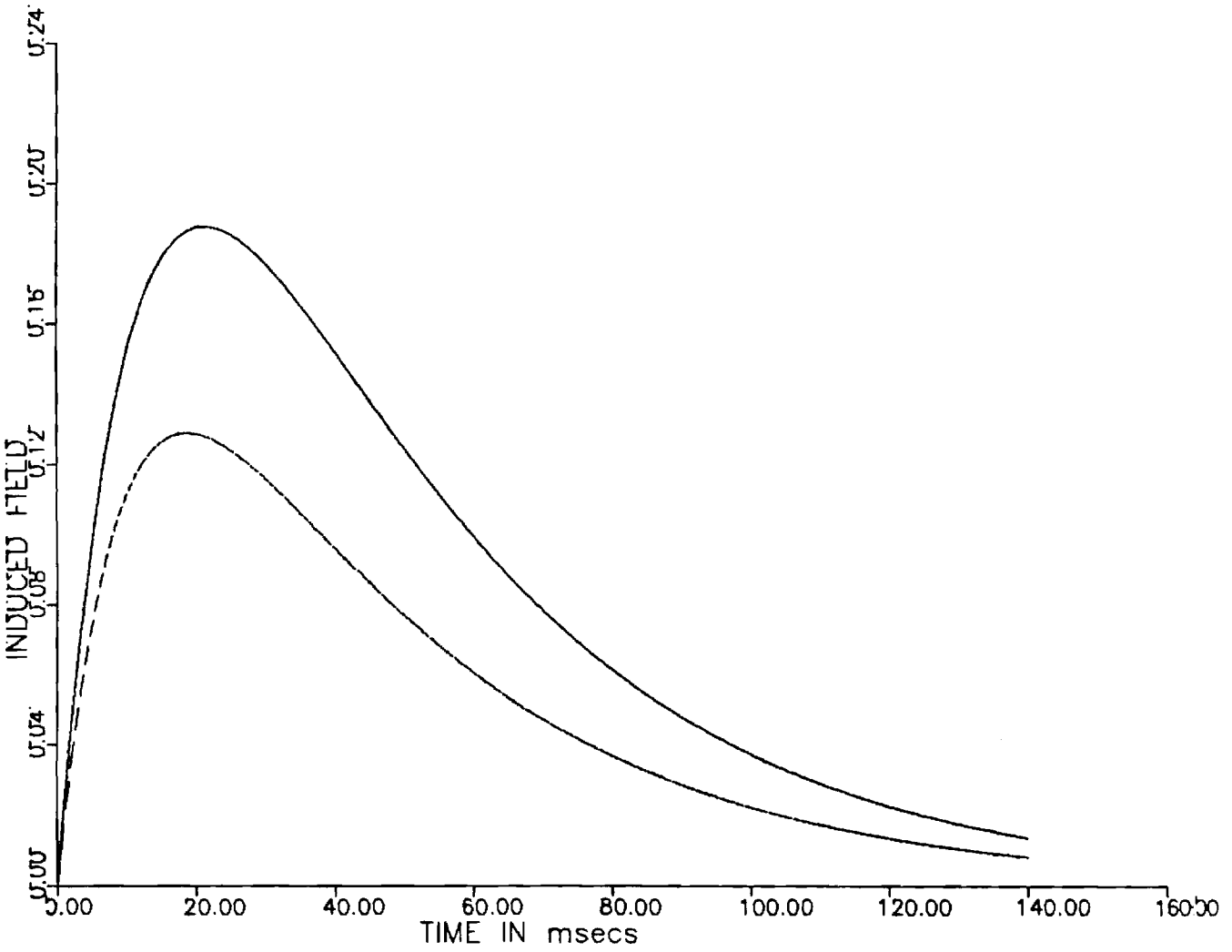

FIGURE 27. LARGE CYLINDER (ONE EIGENVALUE) WITH NORMALIZED INPUT FIELD, TIME CONSTANT = 39.68 msec

$$\underline{x} = \begin{vmatrix} A \\ B \\ C \\ D \\ E \\ F \end{vmatrix} = c_{11}\underline{x}_{11}e^{-\lambda_{11}t} + c_{21}\underline{x}_{21}e^{-\lambda_{21}t} + \cdots c_{n1}e^{-\lambda_{n1}t}$$

(for mode 1: $\cos(\frac{\pi}{\ell}z)$ or $\sin(\frac{\pi}{\ell}z)$)

$$+ c_{13}\underline{x}_{13}e^{-\lambda_{13}t} + c_{23}\underline{x}_{23}e^{-\lambda_{23}t} + \cdots c_{n3}e^{-\lambda_{n3}t}$$

(for mode 2: $\cos(\frac{3\pi}{\ell}z)$ or $\sin(\frac{3\pi}{\ell}z)$)

$$+ \text{higher order modes in z space} \qquad (34)$$

where the constants A-F are defined in Table II. Each eigenvector is weighted with a constant c chosen to satisfy the initial conditions. Constant "c_n" in Table II at $\theta = 0$, $z = 0$, must be equal to that part of the initial field which has a $\cos(\frac{n\pi}{\ell}z)$ dependence which happens to be $H_o \frac{4}{n\pi}(-1)^{n+1/2}$ for a uniform field - from the spatial Fourier decomposition. Likewise, the constant "A_n" at $\theta = 0$, $z = 0$, must equal the same field index $H_o \frac{4}{n\pi}(-1)^{n+1/2}$ times the radius. With 2 eigenvectors/mode, we can use these conditions to specify the weighting constants in (34).

By way of testing how important these additional eigenvalues/mode actually are, the additional eigenvalues for mode n = 1 were included (recall n = 1 has the lowest eigenvalues and strongest weighting). A dramatic improvement is evident in Figs. 27 and 28 for the large cylinder (τ = 39.6 msec) as an additional eigenvector is included. This improvement though not so striking is witnessed again in Figs. 29 and 30 for the large cylinder, τ = 6.87 msec. One would hope the trend might continue as 3 eigenvalues

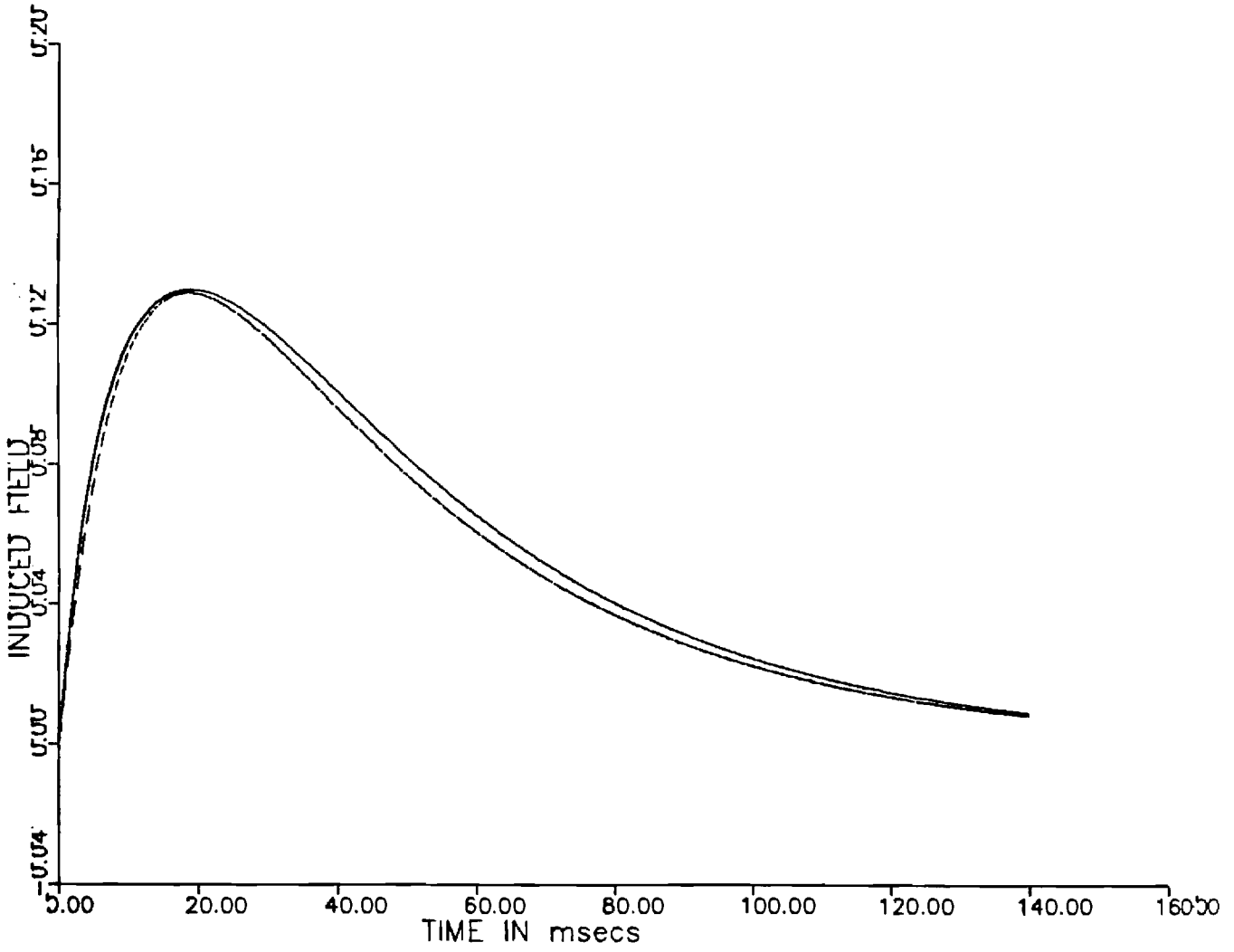

FIGURE 28. LARGE CYLINDER (TWO EIGENVALUES) WITH NORMALIZED INPUT FIELD, TIME CONSTANT = 39.68 msec

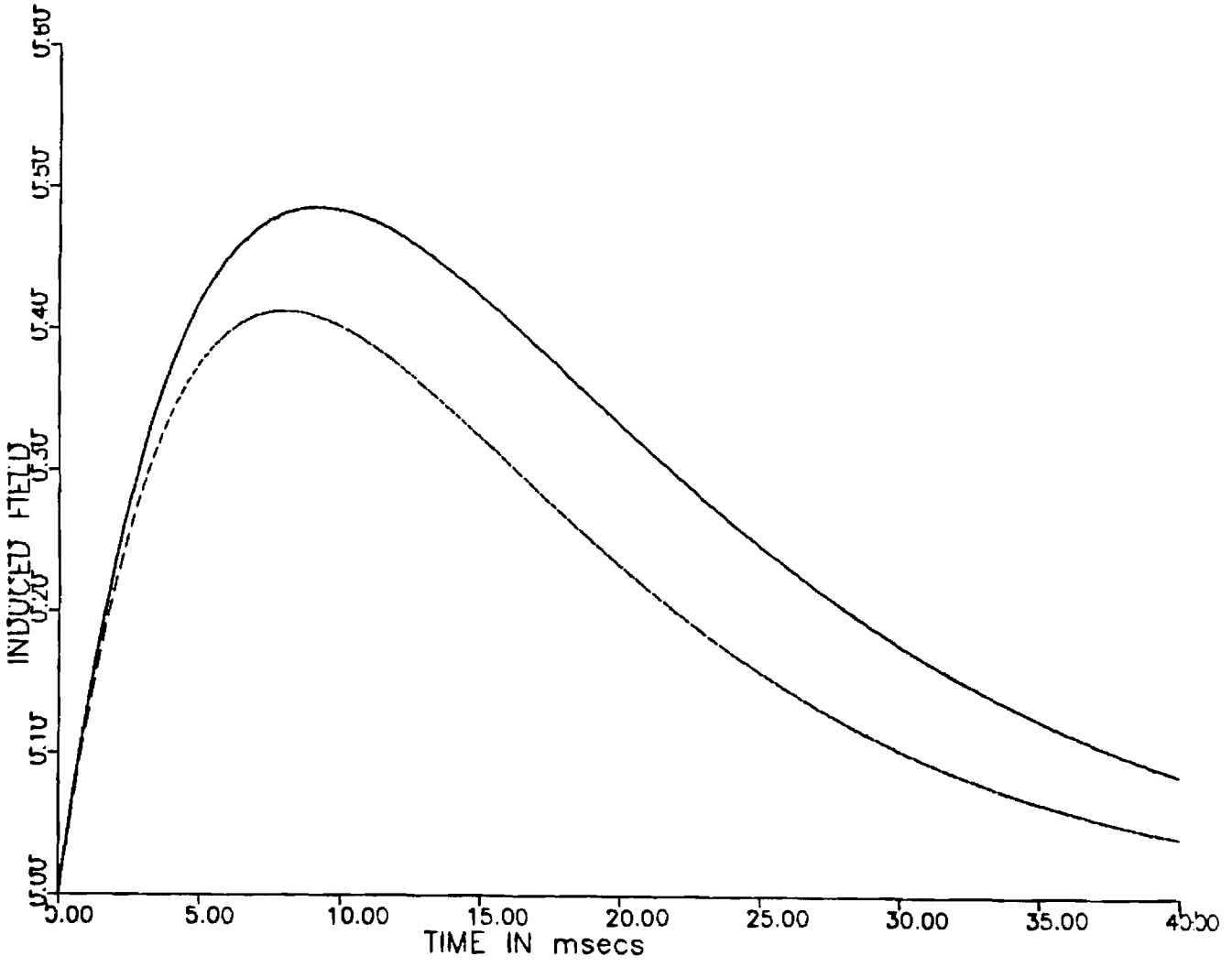

FIGURE 29. LARGE CYLINDER (ONE EIGENVALUE) WITH NORMALIZED INPUT FIELD, TIME CONSTANT = 6.87 msec

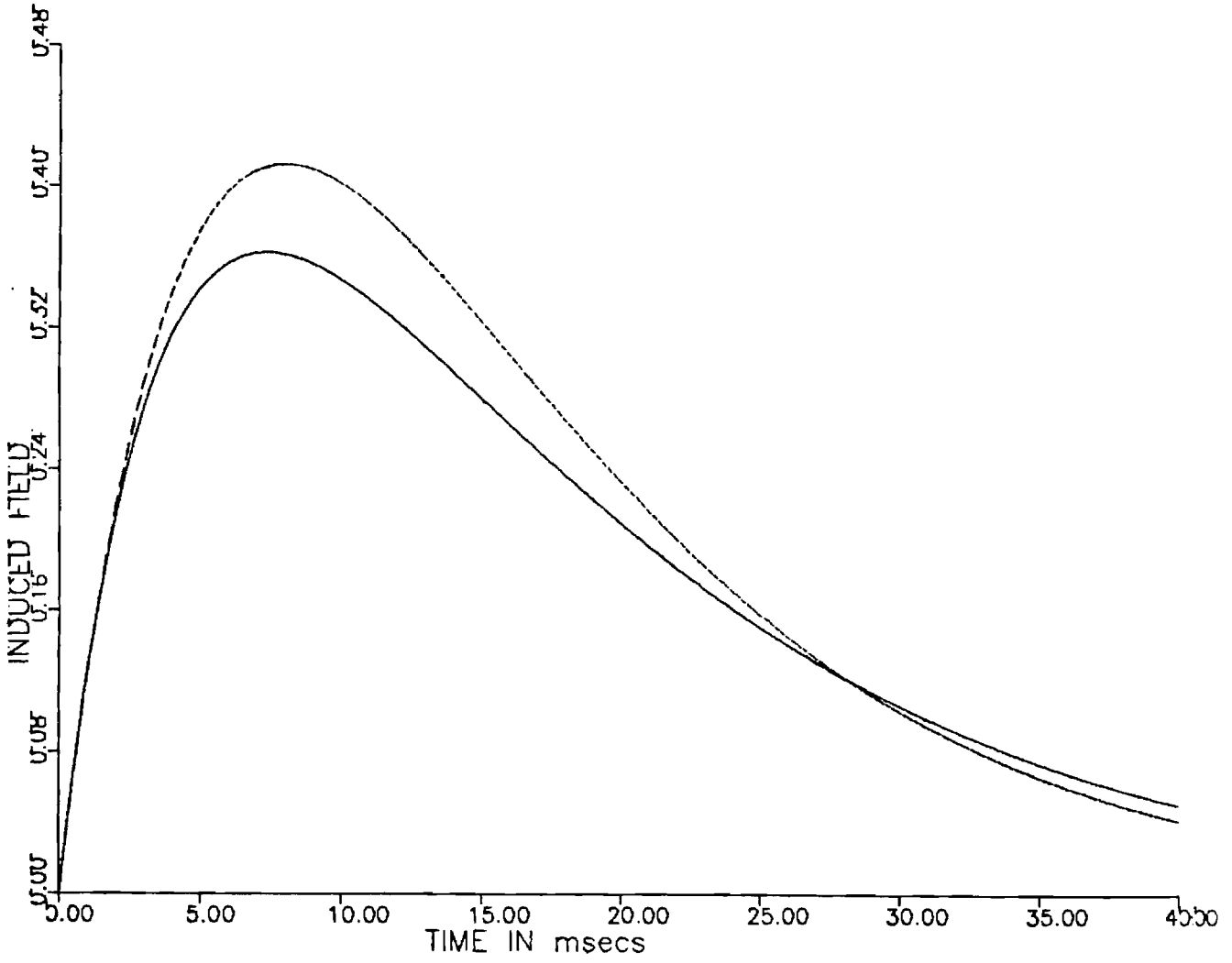

FIGURE 30. LARGE CYLINDER (TWO EIGENVALUES) WITH NORMALIZED INPUT FIELD, TIME CONSTANT = 6.87 msec

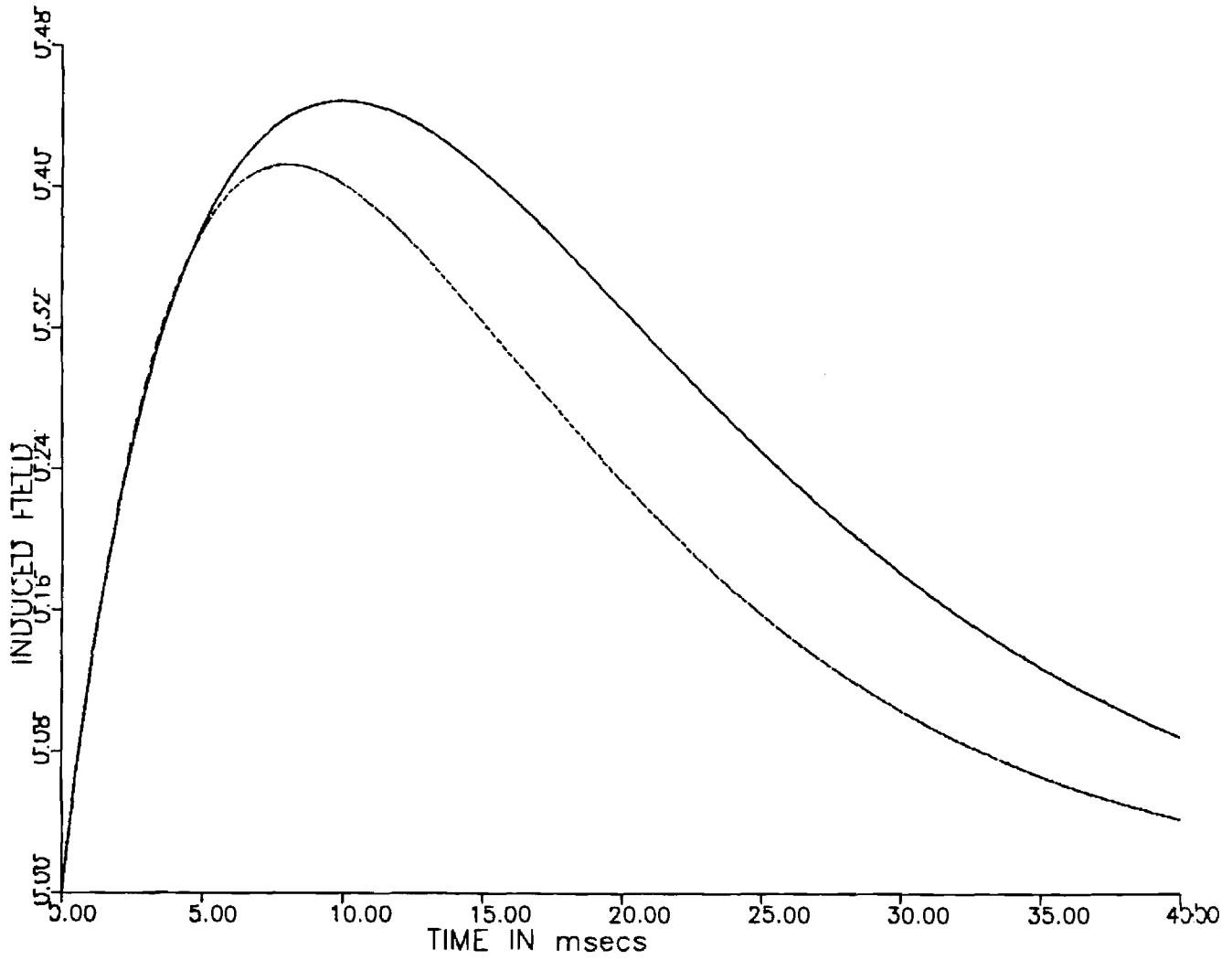

FIGURE 31. LARGE CYLINDER (THREE EIGENVALUES)WITH NORMALIZED INPUT FIELD, TIME CONSTANT = 6.87 msec

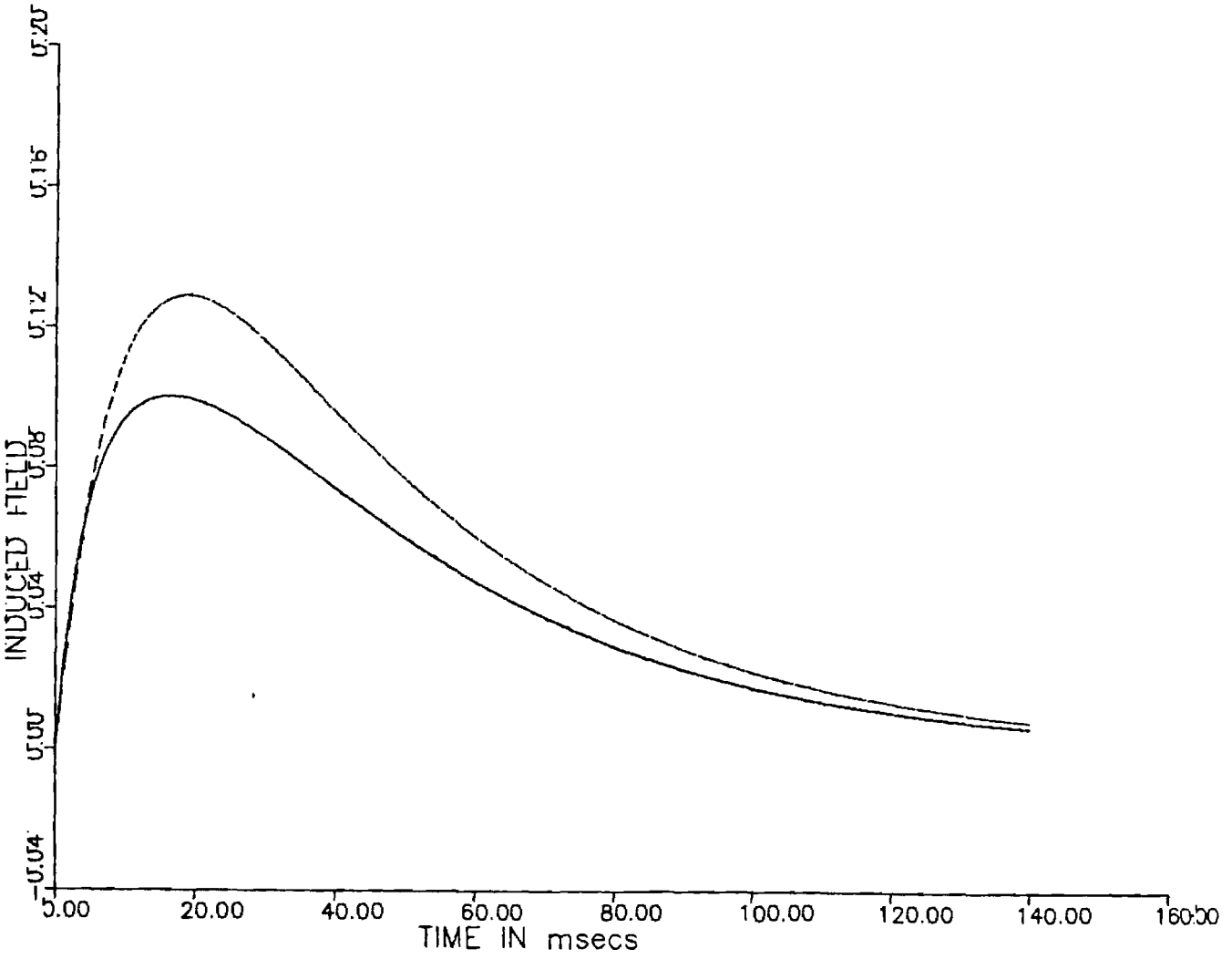

FIGURE 32. LARGE CYLINDER (FOUR EIGENVALUES) WITH NORMALIZED INPUT FIELD, TIME CONSTANT = 39.68 msec

(Fig. 31) and 4 eigenvalues (Fig. 32) per mode are included. It should be remembered that the third eigenvalue for mode 1 is of the same order of magnitude as the second eigenvalue for mode n = 3; thus, both must be incorporated before a consistent and improved result could be expected. The good agreement in Fig. 28 did not warrant the additional work.

As a check, we see that when reasonable agreement exists using one eigenvalue as is the case for the medium cylinder (Fig. 33, τ = 39.68 msec), adding an additional eigenvalue to the problem does not disturb the agreement (Fig. 34).

CONCLUSIONS

The contributions of this work are as follows:

1. Utilization of the u-v method to formulate a truly 3-D cylindrical problem in terms of scalar potentials without Dyadic Green's function.
2. Using the null field integral technique to calculate the characteristic eigenvalues of the cylinder.
3. Associating different eigenvalues with excitation field modal shape via Fourier decomposition.
4. Evaluation of the total 3-D field response using only 6 x 6 matrices via the use of smart basis functions.

Areas of future work include:

1. Selection of smart basis functions for generalized problems.
2. Assessment of the effects of the higher order eigenvalues for all modes "n".

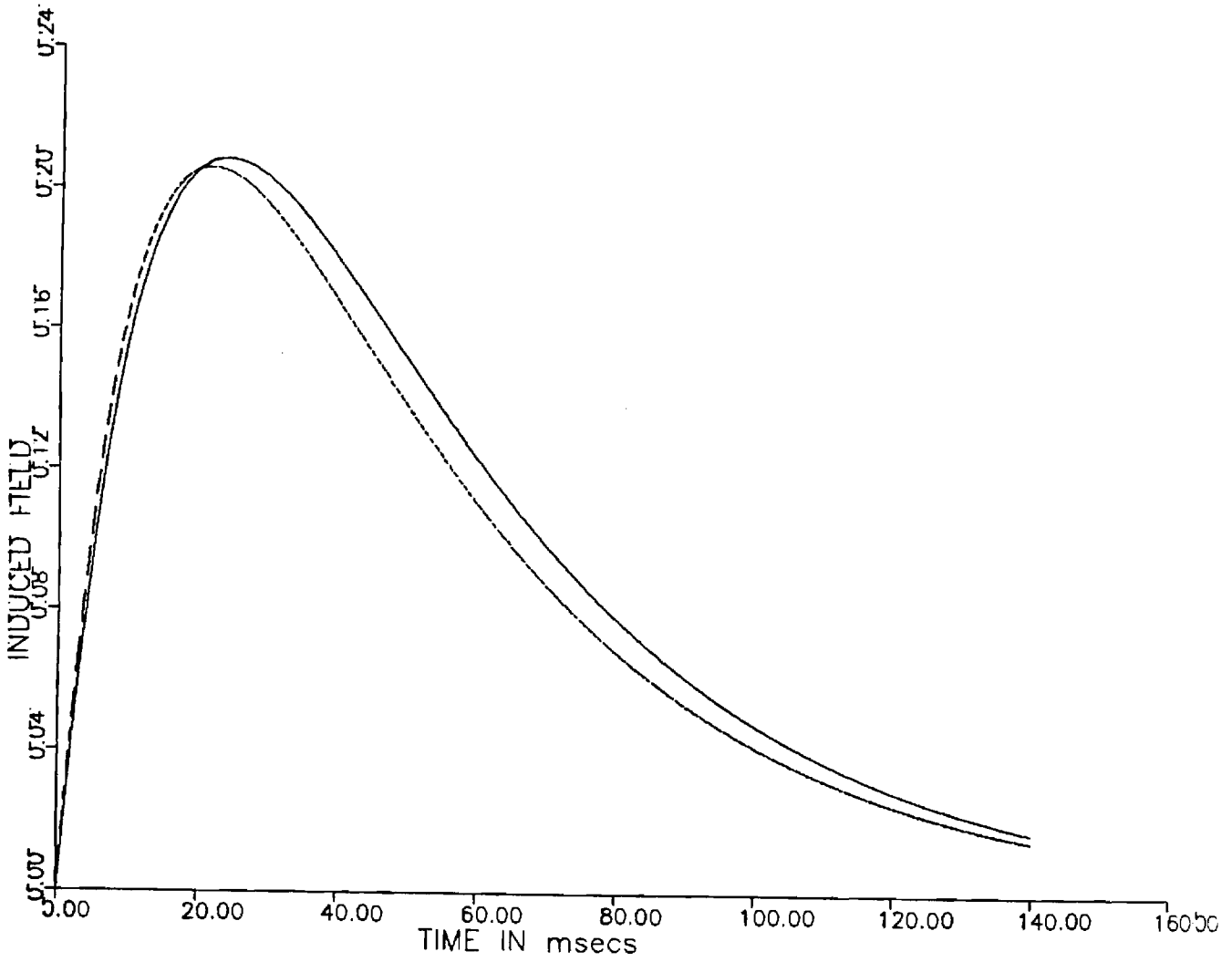

FIGURE 33. ONE TIME CONSTANT FOR 1ST MODE WITH NORMALIZED INPUT FIELD, TIME CONSTANT = 39.68 msec, MEDIUM CYLINDER

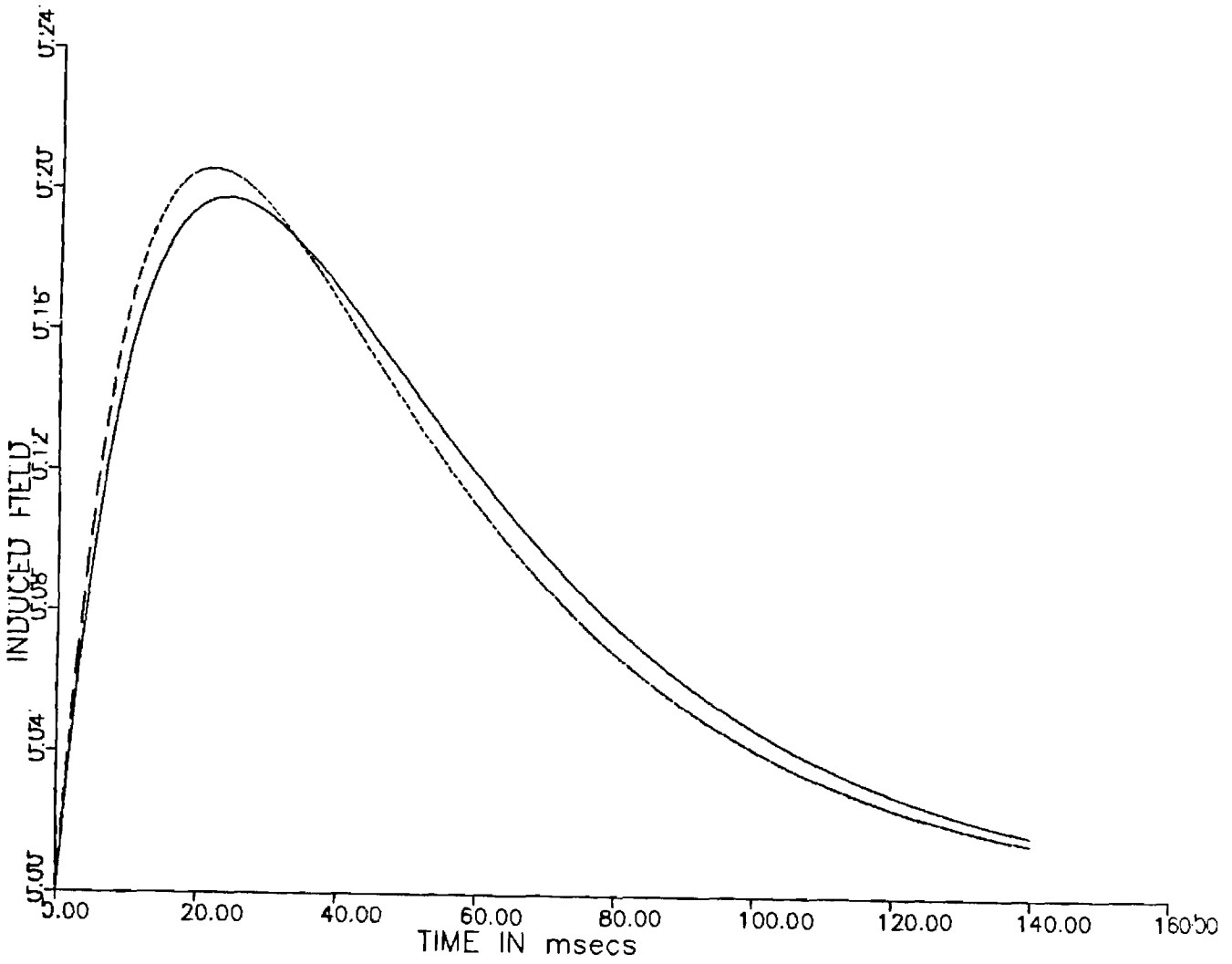

FIGURE 34. TWO TIME CONSTANTS FOR 1ST MODE WITH NORMALIZED INPUT FIELD, TIME CONSTANT = 39.68 msec, MEDIUM CYLINDER

REFERENCES

[1] S. Zhi-ming, et al., "The Finite Element Solution of Transient Axi Symmetrical Nonlinear Eddy Current Field Problems," Fifth Compumag Conference, Fort Collins, Colorado, pp. 241-244, 1985.

[2] B. Aldefeld, "A Numerical Solution of Transient Nonlinear Eddy Current Problems Including Moving Iron Parts," IEEE Trans. Magnetics, Vol. MAG-14, No. 5, pp. 371-373, 1978.

[3] A. Kameari and Y. Suzuki, "Eddy Current Analysis by the Finite Element Circuit Method," 7th Symposium on Engineering Problems in Fusion Research, Knoxville, Tennessee, pp. 1386-1392.

[4] S. Tandon, A. Armor, and M. V. K. Chan, "Nonlinear Transient Finite Element Field Computation for Electrical Machines and Devices," IEEE Trans. Power App. Sys., Vol. PAS-102, pp. 1089-1096, May 1983.

[5] W. F. Praeg, et al., "Felix, An Experimental Facility to Study Electromagnetic Effects for First Wall, Blanket, and Shield Systems," Proc. 9th Symp. on Engineering Problems in Fusion Research, IEEE Pub. No. 81, Ch. 1715, pp. 1763-1766, 1981.

[6] L. R. Turner, et al., "Felix Construction Status and Experimental PRogram," Nucl. Technol./Fusion, Vol. 4, No. 2, Pt. 2, pp. 745-750, 1983.

[7] L. R. Turner, et al., "Results from the Felix Experiments on Electromagnetic Effects in Hollow Cylinders," Fifth Compumag Conference, Fort Collins, Colorado, pp. 356-359, 1985.

[8] P. Hammond, "Use of Potentials in Calculation of Electromagnetic Fields," IEE Proceedings, Vol. 129, Part A, No. 2, pp. 106-112, 1982.

[9] W. R. Smythe, Static and Dynamic Electricity, McGraw Hill, pp. 285, 369, 1978.

[10] C. Emkin, W. Trowbridge, and J. Simkin, "Further Developments in Three Dimensional Eddy Current Analysis," IEEE Trans. Magnetics, Vol. MAG-21, No. 6, pp. 2231-2234, November 1985.

[11] R. Shaw and G. Tai, "Time Harmonic Acoustic Radiation from Nonconcentric Circular Cylinders," J. Acoust. Soc. Am., Vol. 56, No. 5, pp. 1437-1443, May 1974.

GEORGIA INSTITUTE OF TECHNOLOGY
SCHOOL OF ELECTRICAL ENGINEERING
ATLANTA, GEORGIA 30332

TELEPHONE: (404) 894-7337

October 7, 1985

Ms. Dianne Hutchinson
Senior Contract Specialist
Argonne National Laboratory
4700 South Cass Ave.
Argonne, IL 60439

SUBJECT: Contract No. 31-109-ENG-38, Project Director - Dr. K. R. Davey, Final Report

Dear Ms. Hutchinson:

Enclosed please find the Final Report for the period 7/15/85 - 9/30/85 for the above referenced project per contract specifications (Georgia Tech contract E-21-638). If you have any questions, please contact Dr. Kent R. Davey at 404-894-2925.

Sincerely,

Pam Majors
Staff Assistant

pm

Enclosures

cc: OCA (2)

CALCULATIONS OF TRANSIENT FIELDS IN THE FELIX EXPERIMENTS AT ARGONNE USING HULL FIELD INTEGRATED TECHNIQUES

By

Kent R. Davey
School of Electrical Engineering
Georgia Institute of Technology
Atlanta, Georgia 30332-0250

Submitted to:

Argonne National Laboratory
4700 South Cass Avenue
Argonne, IL 60439

Final Report

Contract No. 31-109-ENG-38

September 30, 1985

ABSTRACT

The transient eddy current problem is characteristically computationally intensive. The motivation for this research was to realize an efficient, accurate, solution technique involving small matrices via an eigenvalue approach. Such a technique is indeed realized and tested using the null field integral technique. Using smart (i.e., efficient, global) basis functions to represent unknowns in terms of a minimum number of unknowns, homogeneous eigenvectors and eigenvalues are first determined. The general excitatory response is then represented in terms of these eigenvalues/eigenvectors. Excellent results are obtained for the Argonne Felix cylinder experiments using a 4 x 4 matrix. Extension to the 3-D problem (short cylinder) is set up in terms of an 8 x 8 matrix.

Introduction

Approaches to transient eddy current solutions to date tend to fall into one of two categories [4-7]:

(1) Time domain developed by forward difference albeit explicit or implicit. Spatial discretizations are pursued in much the same way as present time harmonic problems.

(2) Time domain developed via the characteristic eigenvalues/eigenvectors of the system. The spatial domain is characteristically pursued via either finite difference or finite element techniques.

The first approach is computationally intensive, involving the solution of the entire spatial domain recursively throughout the time period of interest. The second approach is theoretically more efficient, but is frought with many other problems. To obtain an accurate spatial discretization, one must necessarily employ a sufficiently large number of nodal points. For every modal point there will result an eigenvalue and related eigenvector. It is the author's experience that most real world problems have only a handful of dominant eigenvalues; by far most of the eigenvalues generated by a finite element technique are both spurious and (hopefully) subdominant. High accuracy in the spatial field representation is bought with the price of generating a host of important eigenvalues, a potential source of considerable error. It is with the intent of capitalizing on the positive features of the eigenvalue approach while minimizing the size of matrices (and thus number of eigenvalues) that the present research was undertaken.

The general theory involving the use of the null field integral equations in determining eigenvalues is first developed. The theory is applied to the Argonne Felix cylinder experiments [1-3]. Predictions are compared to the

exact analytical expressions for the problem. Extension of the technique to the short cylinder is discussed briefly, such an extension being realized through an 8 x 8 matrix rather than through the 4 x 4 matrix used for the long cylinder.

General Theoretical Development

The solution of the general matrix equation

$$\underline{X}' = \underline{\underline{A}}\,\underline{x} + \underline{b} \tag{1}$$

is found by first assuming

$$\underline{x} = e^{\lambda t} \tag{2}$$

and solving the homogeneous eigenvalue problem

$$\underline{\underline{A}}\,\underline{x} = \lambda\,\underline{x} \tag{3}$$

for eigenvalues $\underline{\underline{\lambda}}$ and eigenvectors $\underline{\underline{u}}$, where

$$\underline{\underline{\lambda}} = \begin{bmatrix} \lambda_1 & & & \\ & \lambda_2 & & \\ & & \ddots & \\ & & & \lambda_N \end{bmatrix}$$

$$\underline{\underline{u}} = \begin{bmatrix} \underline{x}_1 & \underline{x}_2 & \cdots & \underline{x}_N \end{bmatrix}$$

$\underline{x}_n$ = nth eigenvector

The temporal solution is written in terms of the particular solution $\underline{x}_p(t)$ as

$$\underline{x}(t) = \sum_{i=1}^{N} C_i \underline{x}_i e^{\lambda_i t} + \underline{x}_p(t) \ , \tag{4}$$

the C_i's being chosen to satisfy initial conditions.

Assuming temporal dependence $e^{-\lambda t}$ for all unknowns, the source-free magnetoquasistatic vector Helmholtz equation becomes

$$\nabla^2 \vec{A} + k^2 \vec{A} = 0 \tag{5}$$

where $k^2 = \lambda\mu\sigma$.

It is convenient from a pedagogical perspective to focus attention on the two dimensional object shown in Fig. 1, which has only a z-directed vector potential (the vector/subscript on $\vec{A}$ being henceforth dropped). The integral equation for A in each region can be written

$$\oint \left(\frac{\partial A_1'}{\partial n} G_1 - A_1' \frac{\partial G_2}{\partial n}\right) ds' = \begin{cases} A(r) & ; \ r \in \text{Domain 1} \\ A(r)/2 & ; \ r \text{ interface} \\ 0 & ; \ r \in \text{Domain 2} \end{cases} \tag{6}$$

$$-\oint \left(\frac{\partial A_2'}{\partial n} G_2 - A_2' \frac{\partial G_2}{\partial n}\right) ds' = \begin{cases} A(r) & ; \ r \in \text{Domain 2} \\ A(r)/2 & ; \ r \text{ interface} \\ 0 & ; \ r \in \text{Domain 1} \end{cases} \tag{7}$$

where

$G_1 = -\frac{j}{4} H_o^{(2)}(kr)$

$G_2 = -\ln(r)/2\pi$

$H_o^{(2)}$ = modified Hankel function of second kind, order zero.

Solution is realized by first assuming values for A_1 and $\partial A_1/\partial n$ in terms of a global basis set.

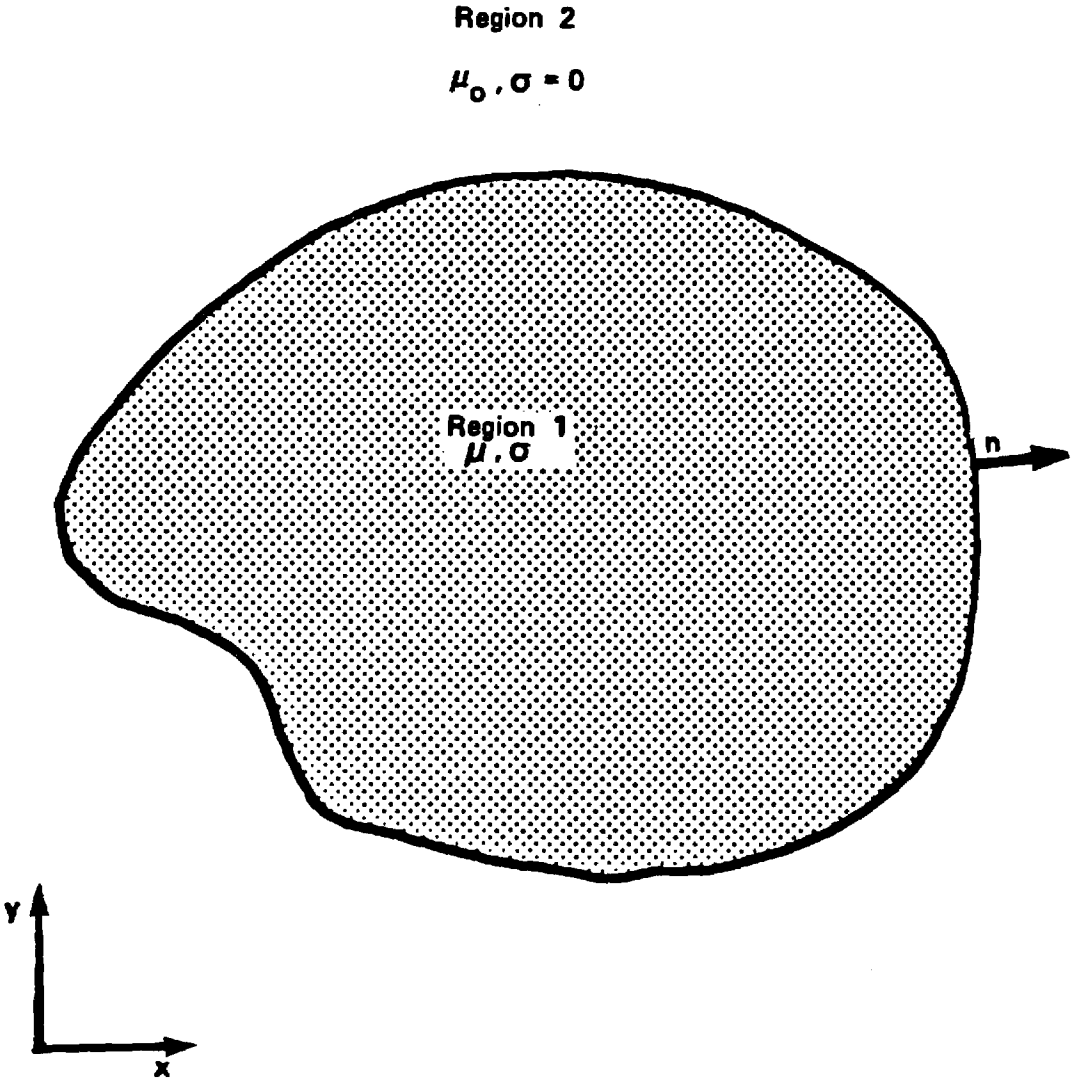

Figure 1. General two dimensional object characterized by a z - directed vector vector potential.

$$A_1 = \sum_{i=1}^{N} C_i \psi_i(\vec{r}) \tag{8}$$

$$\frac{\partial A_1}{\partial n} = \sum_{i=1}^{N} D_i \psi_i(\vec{r}) \tag{9}$$

(The basis functions in (8) and (9) will in general be identical but need not be for the analysis.) Boundary conditions on tangential $\vec{H}$ and normal $\vec{B}$ dictate that

$$A_1 = A_2 \tag{10}$$

$$\frac{1}{\mu} \frac{\partial A_1}{\partial n} = \frac{1}{\mu_o} \frac{\partial A_2}{\partial n} \tag{11}$$

so (8) and (9) characterize the problem entirely. The real advantage to the above approach comes about in the intelligent choice of $\psi_i(\vec{r})$. The more intelligent this choice, the smaller will be the determination matrix and thus the set of eigenvalues governing the problem. This choice can be adopted by analytical insight or experimental data taken, for instance, at $t = 0$, $t = t_{final}/2$, and $t = t_{final}$ (in which case $N = 3$).

Solution proceeds by arbitrarily choosing "N" points inside and outside the body. The "N" points outside the body are then used to write "N" null field equations using (6c) and the "N" points inside are used with (7c) to yield "N" more. These "2N" equations result in a matrix as follows:

$$\begin{bmatrix} -\int \psi_1 \frac{\partial G_1}{\partial n} & -\int \psi_2 \frac{\partial G_1}{\partial n} & \cdots & \int \psi_1 G_1 \\ \cdots & \cdots & \cdots & \cdots \\ \int \psi_N \frac{\partial G_2}{\partial n} & \cdots & -\int \psi_n \frac{\partial G_2}{\partial n} & \end{bmatrix} \begin{matrix} C_1 \\ \vdots \\ C_N \\ D_1 \\ \vdots \\ D_N \end{matrix} \equiv \underline{\underline{F}} \begin{matrix} \underline{C} \\ \underline{D} \end{matrix} = 0 \tag{12}$$

The eigenvalues of the system immediately drop out as those values of k for which the determinant of the matrix $\underline{\underline{F}}$ in (12) is zero. These must be found of several nonlinear root solving techniques (e.g., Newton Raphson, Secant, etc.). Once the zero determinant values of ($\underline{\underline{F}}$) are known, a new matrix $\underline{\underline{F}}$ can be defined

$$\underline{\underline{F}}' = \underline{\underline{F}} + \underline{\lambda} \tag{13}$$

The eigenvectors $\underline{u}$ of $\underline{\underline{F}}'$, and thus of the original system, can be obtained via several numerical packages (e.g., QR algorithm, Jacobi iteration, etc.). The interfacial unknowns for all time is written in terms of the system eigenvectors $\underline{x}_1, \underline{x}_2, \cdots, \underline{x}_{2N}$ and the eigenvalues $\lambda_1, \lambda_2, \cdots, \lambda_{2N}$ as

$$\begin{matrix} C_1 \\ \vdots \\ C_N \\ D_1 \\ \vdots \\ \\ D_N \end{matrix} = \begin{matrix} \underline{C} \\ \underline{D} \end{matrix} = \sum_{i=1}^{2N} g_i e^{\lambda_i t} \underline{x}_i + \underline{x}_p(t) \tag{14}$$

where the g_i's are obtained from initial conditions. Typically, the field inside a conductor is known at $t = 0^+$ (identical to that before the transient); $\underline{x}_p(t)$ is the normal steady state solution. The interfacial unknowns are easily determined using "N" equations from (6a) and "N" null field equations (7c) to give a matrix equation for initial unknowns which is <u>not</u> homogeneous.

The Felix Cylinder Experiments

The methodology is now implemented for a 2-D, three region problem (Fig. 2). The Felix cylinder experiments involved three cylinders, one of which will be examined here. The cylinder is slit down its length. At t = 0, an external vertical field is allowed to collapse with time constant τ = 39.68 msec. We wish to predict the self-generated fields for all time. There is in addition an externally applied z-directed field. As will be shown, the length is long enough that for measurements in the center of the cylinder (at z = 0), the finite length, horizontal slits, and z-directed external field have no effect on the self-excited x-y field. The infinite cylinder with no slits will show an indiscernible difference in eddy current field at z = 0. Finite length effects must be considered when L < π/first eigenvalue "k" (this is roughly when L ≈ 3 * diameter).

The solution proceeds as follows. First, recognize that the following basis set satisfies all boundary constraints on A

$$A(r = a) = C \sin \theta \tag{15}$$

$$\frac{\partial A}{\partial r}(r = a) = D \sin \theta \tag{16}$$

$$A(r = b) = E \sin \theta \tag{17}$$

$$\frac{\partial A}{\partial r}(r = b) = F \sin \theta \tag{18}$$

Next evaluate 4 null field equations

$$0 = \int_0^{2\pi} \left\{D \sin \theta \, G_1 - C \sin \theta \frac{\partial G_1}{\partial r}\right\} a \, d\theta \; ; \; r > a \tag{19}$$

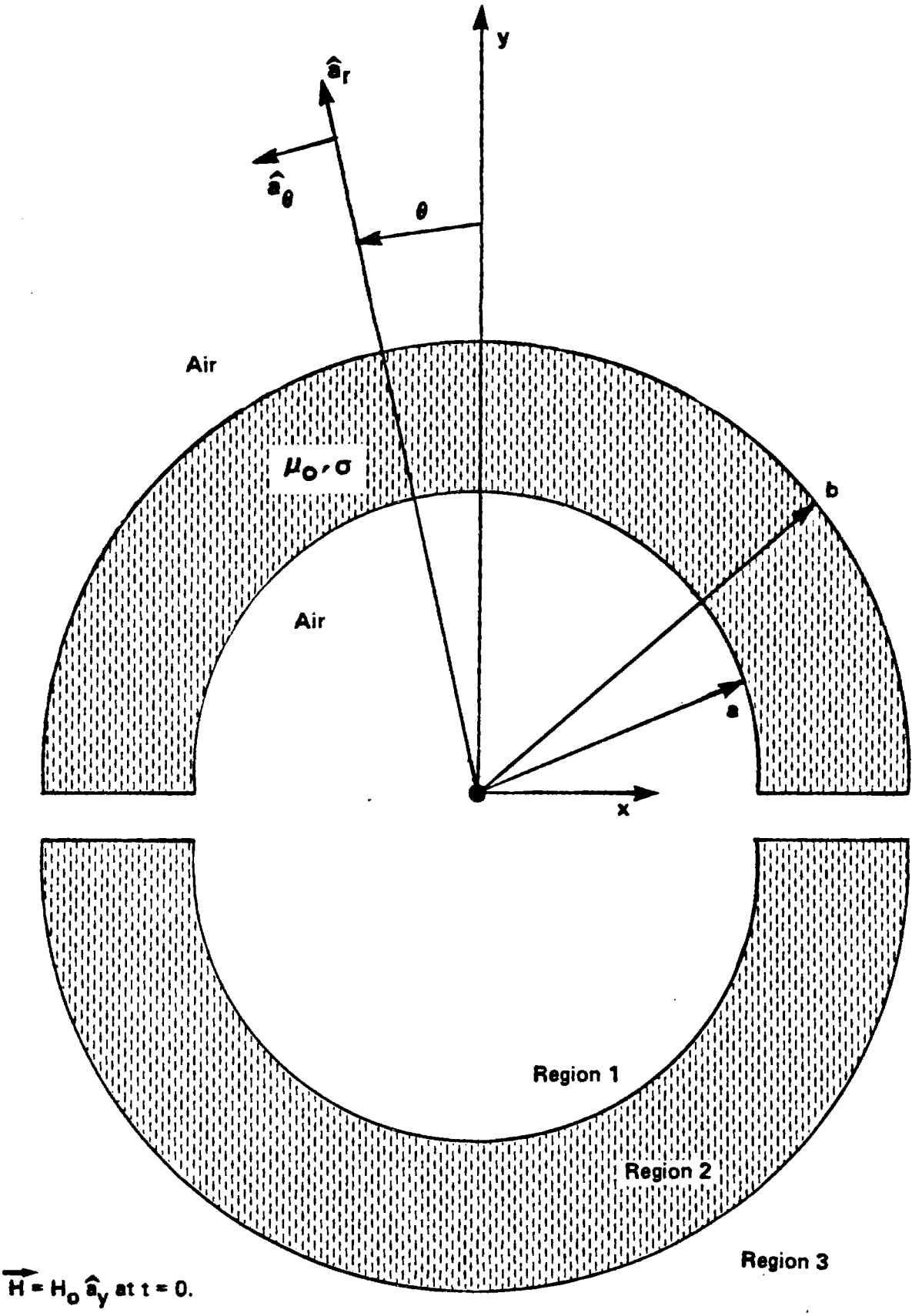

Figure 2. Felix Cylinder Experiment. Slit cylinder is immersed in a homogeneous field $\vec{H} = H_o \hat{a}_y$ at t = 0; a = 25.4mm, b = 50.8mm, length = 600mm, $\sigma = 2.538 \times 10^7$ mho/m; field collapses with time constant $\tau = 39.68$m sec.

$$0 = -\int_0^{2\pi} \left(D \sin\theta\, G_2 - C \sin\theta \frac{\partial G_2}{\partial r}\right) a\, d\theta$$

$$+ \int_0^{2\pi} \left(F \sin\theta\, G_2 - E \sin\theta \frac{\partial G_2}{\partial r}\right) b\, d\theta \; ; \; r < a \tag{20}$$

$$0 = -\int_0^{2\pi} \left(D \sin\theta\, G_2 - C \sin\theta \frac{\partial G_2}{\partial r}\right) a\, d\theta$$

$$+ \int_0^{2\pi} \left(F \sin\theta\, G_2 - E \sin\theta \frac{\partial G_2}{\partial r}\right) b\, d\theta \; ; \; r > b \tag{21}$$

$$0 = -\int_0^{2\pi} \left(F \sin\theta\, G_3 - E \sin\theta \frac{\partial G_3}{\partial r}\right) b\, d\theta \; ; \; r < b \tag{22}$$

where

$$G_1(r,r') = G_2(r,r') = -\frac{\ell n|\bar{r}-\bar{r}'|}{2\pi}$$

$$G_2(r,r') = -\frac{j}{4} H_o^{(2)}\left(k(r-r')\right)$$

$$k = \frac{\lambda}{\mu\sigma}$$

Note, it is necessary to avoid putting null field points along the $\theta = 0$ or $\theta = 180°$ axes or the origin where integration of sin θ terms identically yields zero. Otherwise no restraints are made. The system of equations (19)-(22) are written as the matrix

$$\begin{matrix} * & * & 0 & 0 & C \\ * & * & * & * & D \\ * & * & * & * & E \\ 0 & 0 & * & * & F \end{matrix} = 0 \tag{23}$$

The determinant of (23) is then evaluated for various values of k to determine zeros or eigenvalues. For the short cylinder dimension, as in Figure 2, the first three zeros were found to be 50.2830, 144.1659, 258.9145; a plot of the

determinant of (23) versus k is shown in Fig. 3 (along with the exact prediction which follows). The higher order eigenvalues are well removed from the base temporal decay; these higher order eigenvalues are reflective of the short temporal diffusion of the field across the thickness of the cylinder, a fact made more clear by looking at longer, thinner cylinders. For a medium sized cylinder with a = 57.14 mm, b = 69.85 mm, length = 600 mm, the eigenvalues k were found to be 51.4501, 257.9221, and 500.1842. A still larger cylinder with a = 131.7 mm, b = 136.5 mm, length = 1200 mm, gave eigenvalues k = 56.074, 659.2865, 1311.4041. Notice the increased separation between eigenvalues in each case reflective of the shorter relative diffusion time of the field through the cylinder walls.

As will be shown shortly, to predict the response to any external field drive, it suffices to determine the response to an external field H_o which drops instantaneously to zero; the final field being determined via convolution. Since the response field is dominated entirely by the first eigenvalue ($e^{\lambda_1 t}$), we need only predict C, D, E, and F at $t = 0^+$. At $t = 0^+$, only the field internal to the cylinder ($r < a$) is known to be equal to the value $H_o \hat{a}_y$ (or $A_z = H_o r \sin\theta$), the field at any other position being uncertain. The constants C, D, E, F follow by solving three null field equations in regions 2 and 3, and one inhomogeneous integral equation for region 1.

$$H_o r \sin\theta = \int_0^{2\pi} \left(D \sin\theta\, G_1 - C \sin\theta \frac{\partial G_1}{\partial r}\right) a\, d\theta \; ; \; r < a \tag{24}$$

$$0 = -\int_0^{2\pi} \left(D \sin\theta\, G_2 - C \sin\theta \frac{\partial G_2}{\partial r}\right) a\, d\theta$$

$$+ \int_0^{2\pi} \left(F \sin\theta\, G_2 - E \sin\theta \frac{\partial G_2}{\partial r}\right) b\, d\theta \; ; \; r < a \tag{25}$$

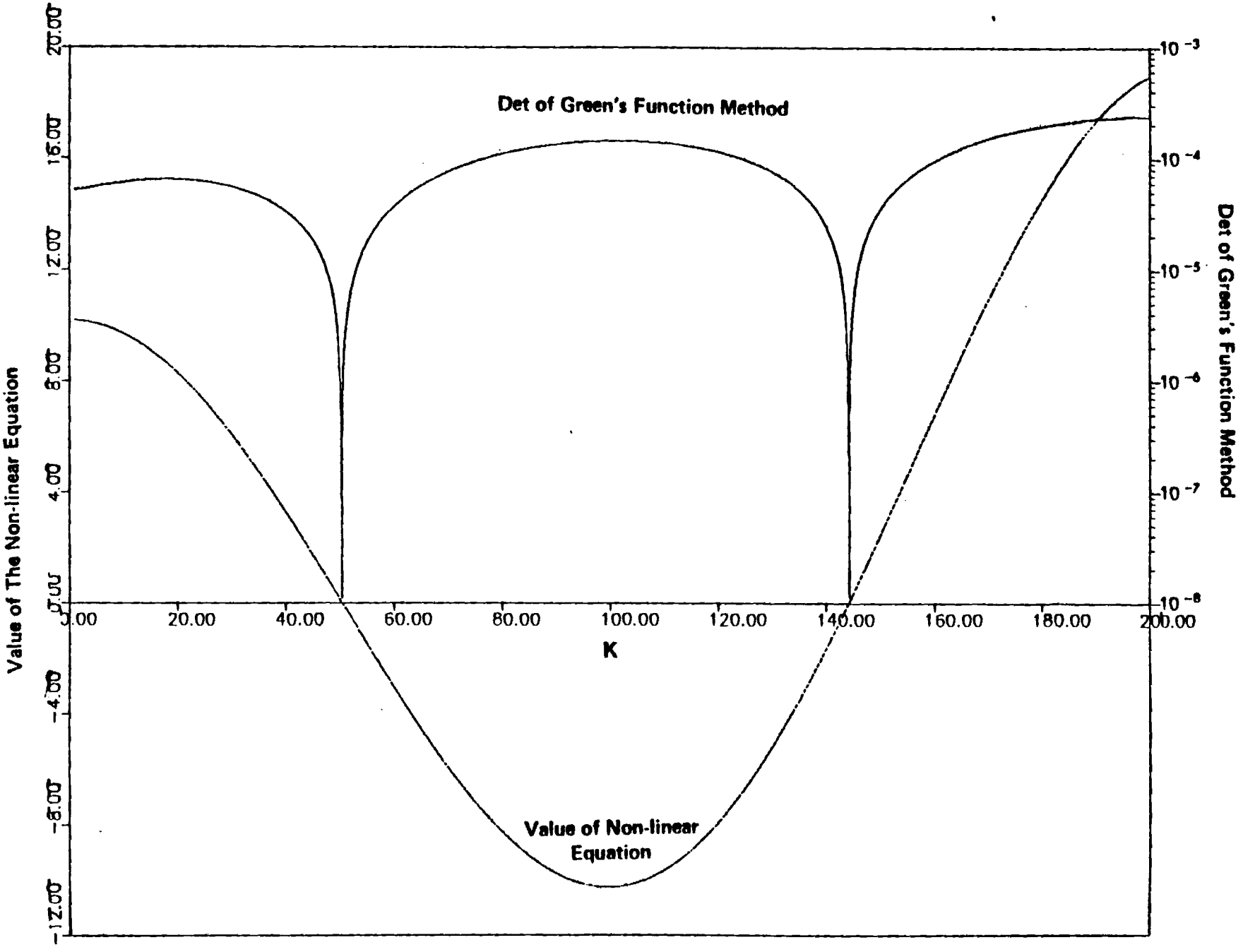

Fig. 3 Eigenvalues from Exact and Null-field Integral Calculations
Zeros of K are the Eigenvalues

$$0 = -\int_0^{2\pi} \left(D \sin\theta\, G_2 - C \sin\theta \frac{\partial G_2}{\partial r}\right) a\, d\theta$$

$$+ \int_0^{2\pi} \left(F \sin\theta\, G_2 - E \sin\theta \frac{\partial G_2}{\partial r}\right) b\, d\theta \;;\; r > b \qquad (26)$$

$$0 = -\int_0^{2\pi} \left(F \sin\theta\, G_3 - E \sin\theta \frac{\partial G_3}{\partial r}\right) b\, d\theta \;;\; r < b \qquad (27)$$

Once the constants are determined, the standard integral equations ((6a) and (7a)) yield the solution everywhere. This procedure has been implemented on a Cyber CDC; the results agree with those predicted by an exact solution to 5 decimal places (.001% error). These results are shown in the next section, where the exact solution is derived for comparison.

Analytical Formulation of the Eddy Current (Step Response) Field

In the exact analytical formulation possible in this test case, one begins by performing a separation of variables on $\nabla^2 A + k^2 A = 0$. The result for regions 1, 2, and 3 is

$$A_1 = Cr \sin\theta\, e^{-\frac{k^2}{\mu\sigma} t} \qquad (28)$$

$$A_2 = \left[AJ_1(kr) + BY_1(kr)\right] \sin\theta\, e^{-\frac{k^2}{\mu\sigma} t} \qquad (29)$$

$$A_3 = \frac{D}{r} \sin\theta\, e^{-\frac{k^2}{\mu\sigma} t} \qquad (30)$$

Enforcing the boundary conditions on A_2 and its normal derivative at $r = a$ and $r = b$ leads to an eigenvalue equation

$$[2J_1(kb) + kb(J_o(kb) - J_2(kb))][2Y_1(ka) - ka(Y_o(ka) - Y_2(ka))]$$
$$= [2J_1(ka) - ka(J_o/ka) - J_2(ka)][2Y_1(kb) + kb(Y_o(kb) - Y_2(kb))] \quad (31)$$

The numerical plot of (31) is shown in Fig. 3 to yield the same eigenvalues as those predicted by the integral technique.

By requiring the field internal to the cylinder to be H_o at $t = 0^+$ as above, we determine the constants A, B, C, D to be respectively (normalized to H_o)

Small Cylinder

A = 0.05899

B = 0.009081

C = 1

D = 0.001524

Medium Cylinder

A = 0.04878

B = 0.1281

C = 1

D = 0.004045

Large Cylinder

A = 0.2491

B = -0.3827

C = 1

D = 0.01798

These are again within 0.001% of the results found from the integral technique.

Total Transient Solution

So far we have found only the self-field due to the cylinder in response to step change in external field.

$$Hy = H_o - H_o u_{-1}(+) \tag{32}$$

The actual source field is

$$Hy = H_o - H_o u_{-1}(+) + H_o e^{-\alpha t} u_{-1}(+) \tag{33}$$

where

α = 39.68 msec.

The total response field is realized through a convolution of $(-dH_y/dt)$ with $e^{-\lambda t}$, i.e.,

$$\begin{aligned} H_{response} &= \int_0^t \left(-\frac{d}{dt}(H_y)_{t=\tau}\right) e^{-(t-\tau)} d\tau \\ &= \int_0^t \alpha H_o e^{-\alpha\tau} e^{-\frac{k^2}{\mu\sigma}(t-\tau)} d\tau \\ &= \frac{\alpha e^{-\frac{k^2}{\mu\sigma}t}}{\frac{k^2}{\mu\sigma} - \alpha} \left(e^{(\frac{k^2}{\mu\sigma} - \alpha)t} - 1\right) \end{aligned} \tag{34}$$

The total field is found as the response field (34) plus the source field $H_o e^{-\alpha t} \hat{a}_y$. Recalling that $H_r = \frac{1}{r}\frac{\partial A_z}{\partial \theta}$ and $H_\theta = -\frac{\partial A_z}{\partial r}$, it is a simple matter to construct the following solution table (Table I) for the total field. A plot of the response field and total field in region 2 (or 3) at r = b of the small cylinder is shown in Figs. 4 and 5 (H_r and H_θ).

The reader should note that the cylinder current density $\underline{J} = -\nabla^2 \underline{A}$ does not change its spatial character with time unless secondary and tertiary eigenvalues are significant in the problem. The current distribution through-

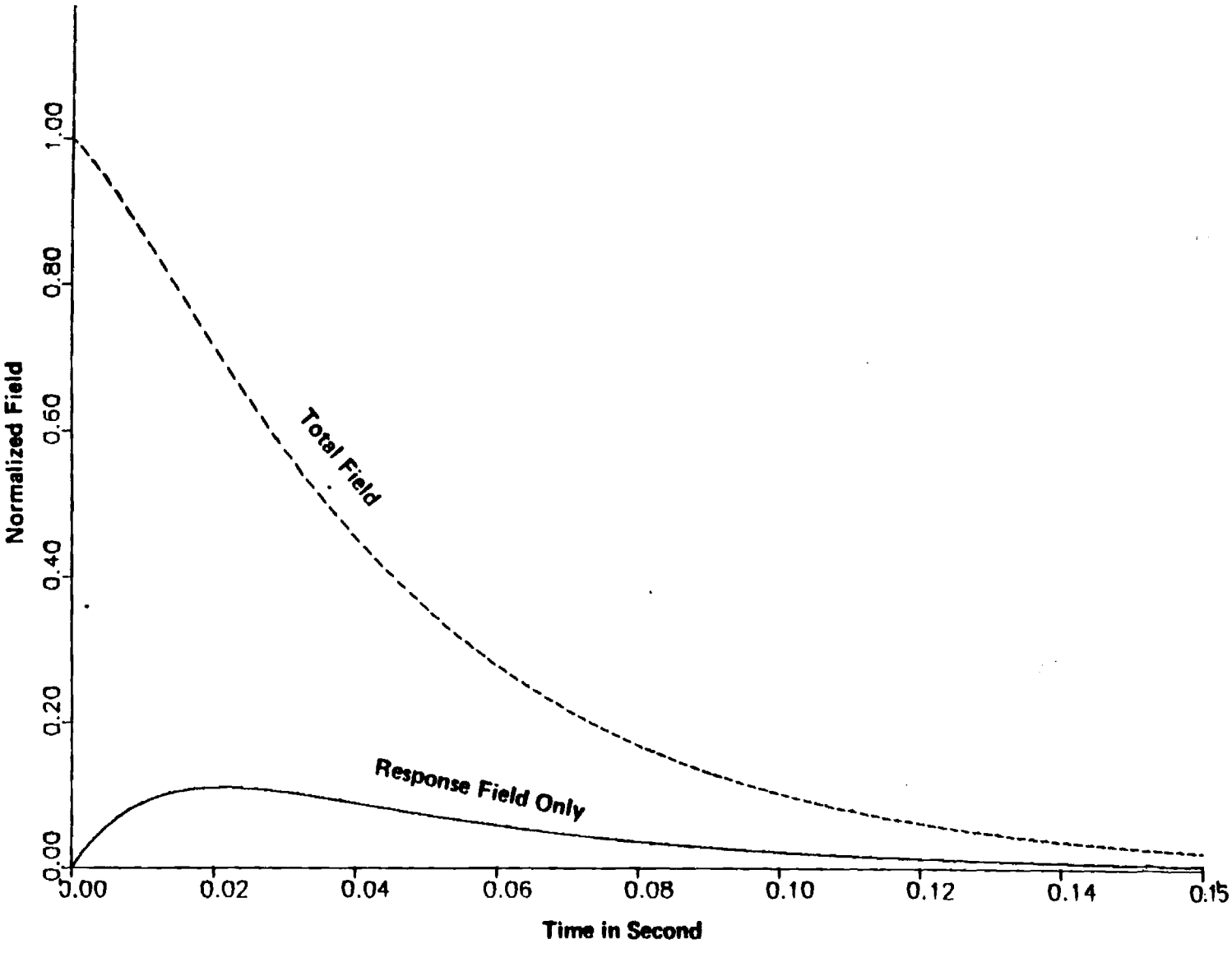

Fig. 4 R Component of Region(2) at Outer Radius

Outer Diameter 0.1016 meter, Thickness 0.0254 meter

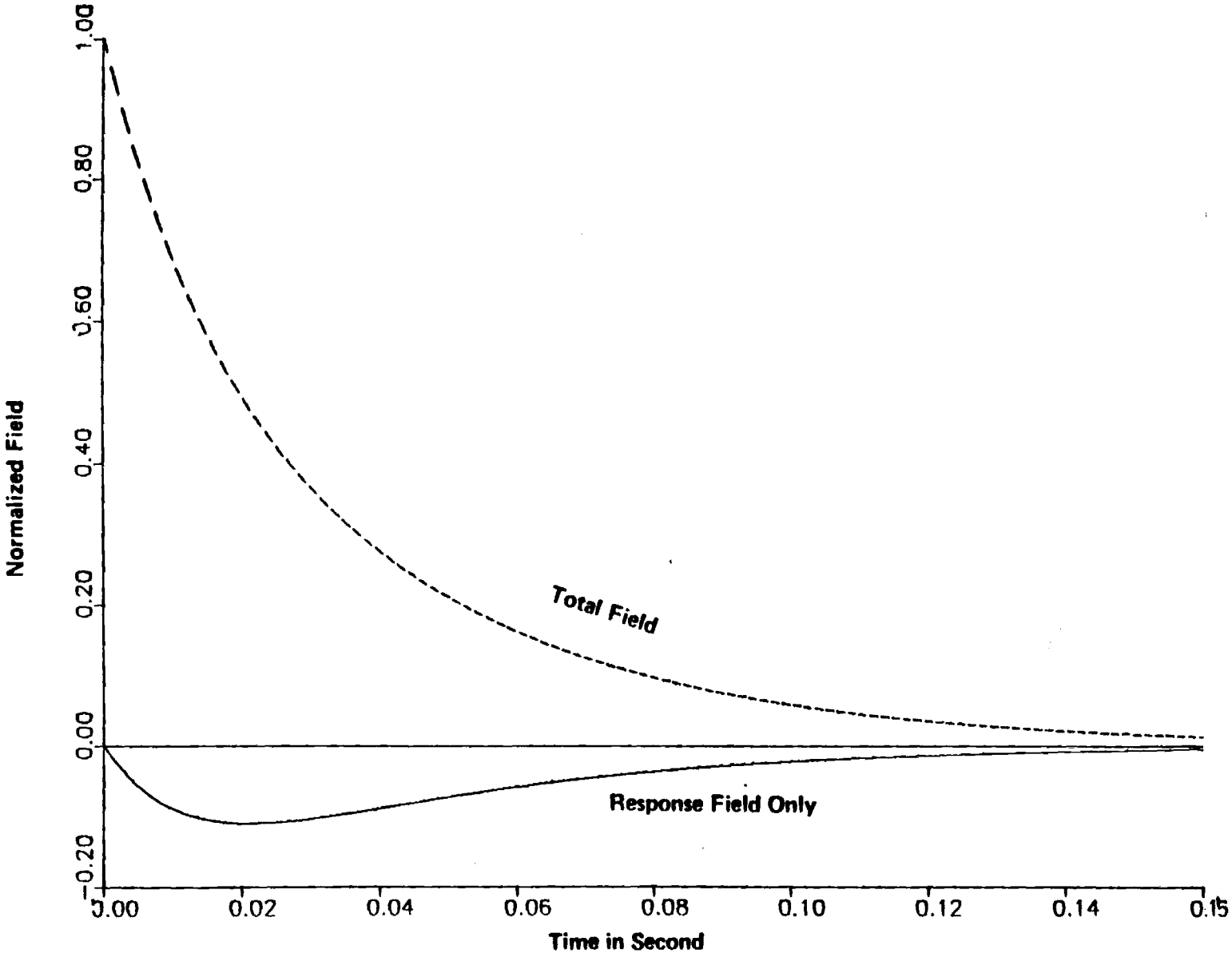

Fig. 5 Theta Component of Region(2) at Outer Radius

Outer Diameter 0.1016 meter, Thickness 0.0254 meter

Table 1. Total H field Response in the Cylinder

Component	Region	H
H_r	(1)	$H_o \cos\theta \left(e^{-\alpha t} + T(t)\right)$
	(2)	$H_o \cos\theta\, e^{-\alpha t} + \frac{H_o}{r}\left[AJ_1(kr) + BY_1(kr)\right]\cos\theta\, T(t)$
	(3)	$H_o \cos\theta\, e^{-\alpha t} + \frac{H_o D}{r^2}\cos\theta\, T(t)$
H_θ	(1)	$-H_o \sin\theta \left[e^{-\alpha t} + T(t)\right]$
	(2)	$-H_o \sin\theta \left(e^{-\alpha t} - \left[\frac{kA}{2}\left(J_o(kr) - J_2(kr)\right)\right.\right.$ $\left.\left. + \frac{kB}{2}\left(Y_2(kr)_o - Y_2(kr)\right)T(+)\right]\right)$
	(3)	$-H_o \sin\theta \left[e^{-\alpha t} - \frac{D}{r^2}T(t)\right]$

where $T(t) = \alpha \dfrac{e^{-\frac{k^2}{\mu\sigma}t}}{\left(\frac{k^2}{\mu\sigma} - \alpha\right)}\left(e^{\left(\frac{k^2}{\mu\sigma} - \alpha\right)t} - 1\right)$

out the cylindrical annulus is depicted in Fig. 6 by x's and o's whose size is indicative of the current density strength. Fig. 7 gives a more analytical picture of the current density radial distribution for θ = 0°, 22.5°, 45°, 67.5°, and 90°.

The large (R = 136.5 mm) and medium (R = 69.8 mm) cylinder eigenvalues are shown in Figs. 8 and 9; plotted in each is the analytical expression (31). These zeros agree to five decimal places with those predicted from the integral technique. Figures 10 and 11 show the large cylinder predicted versus experimental B_z fields for the total and induced fields, respectively. The dots indicate field data measured at the center of the cylinder. Figures 12 and 13 show the same B_z fields for the medium cylinder. The dots, however, are B_z field data 20 cm along the axis of the cylinder. These data points would be expected to be only slightly lower than those at the center. The agreement in all four curves is very reasonable.

Finite Length Effects

A first refinement taken to account for finite length effects is obtained by reconsidering the governing equation, $\nabla^2 A - \mu\sigma \frac{\partial A}{\partial t} = 0$. As before, we first separate into space and time, letting

$$A_z = U(\vec{r})e^{-\lambda t} = R(r)Z(z)\Theta(\theta)e^{-\lambda t}$$

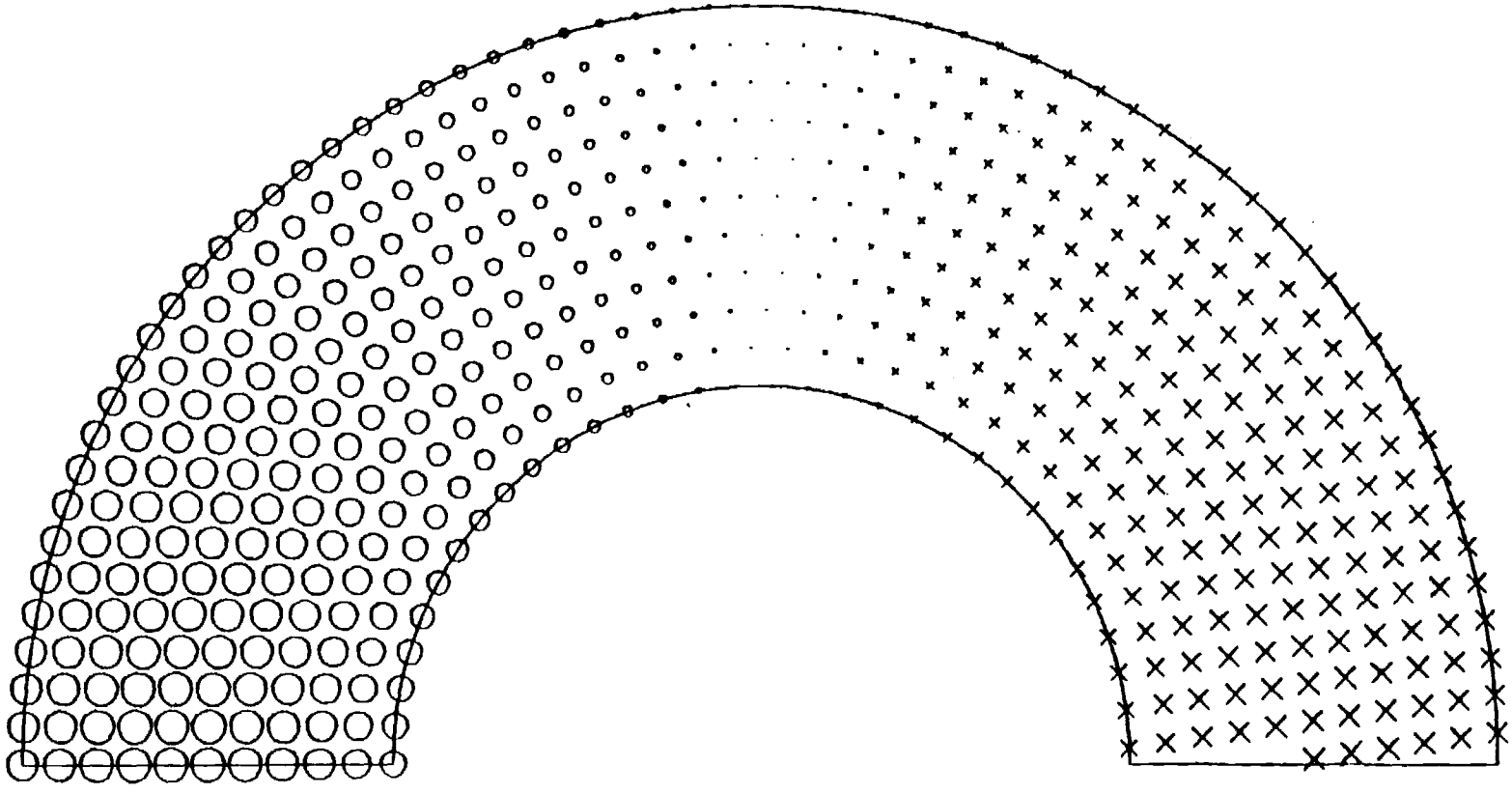

Fig. 6 Distribution of Current in the Annular Region

Magnitude of Current Density is Represented by the Size of X—O

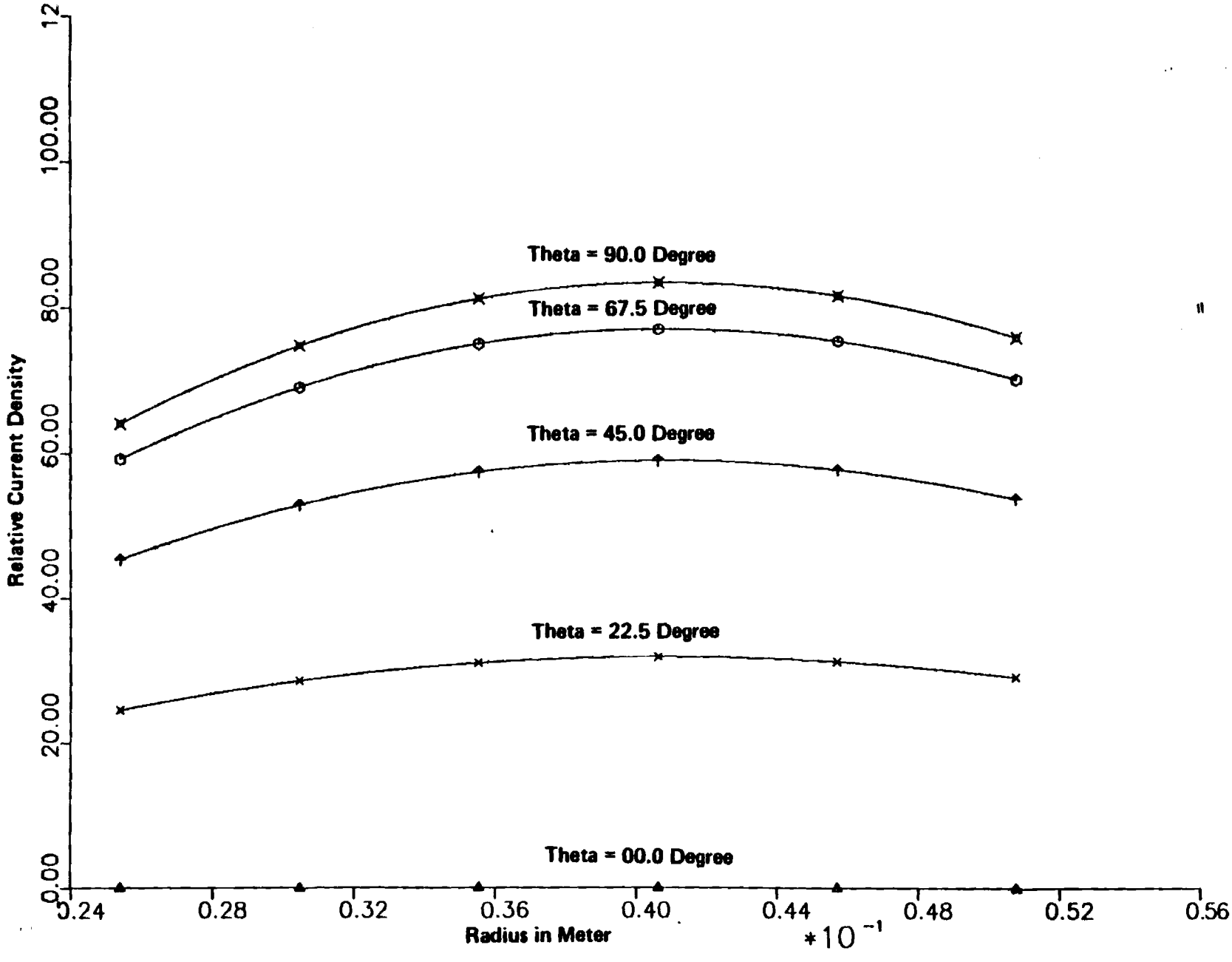

Fig. 7 **Distribution of Current**

Outer Diameter 0.1016 m, Thickness 0.0254 m

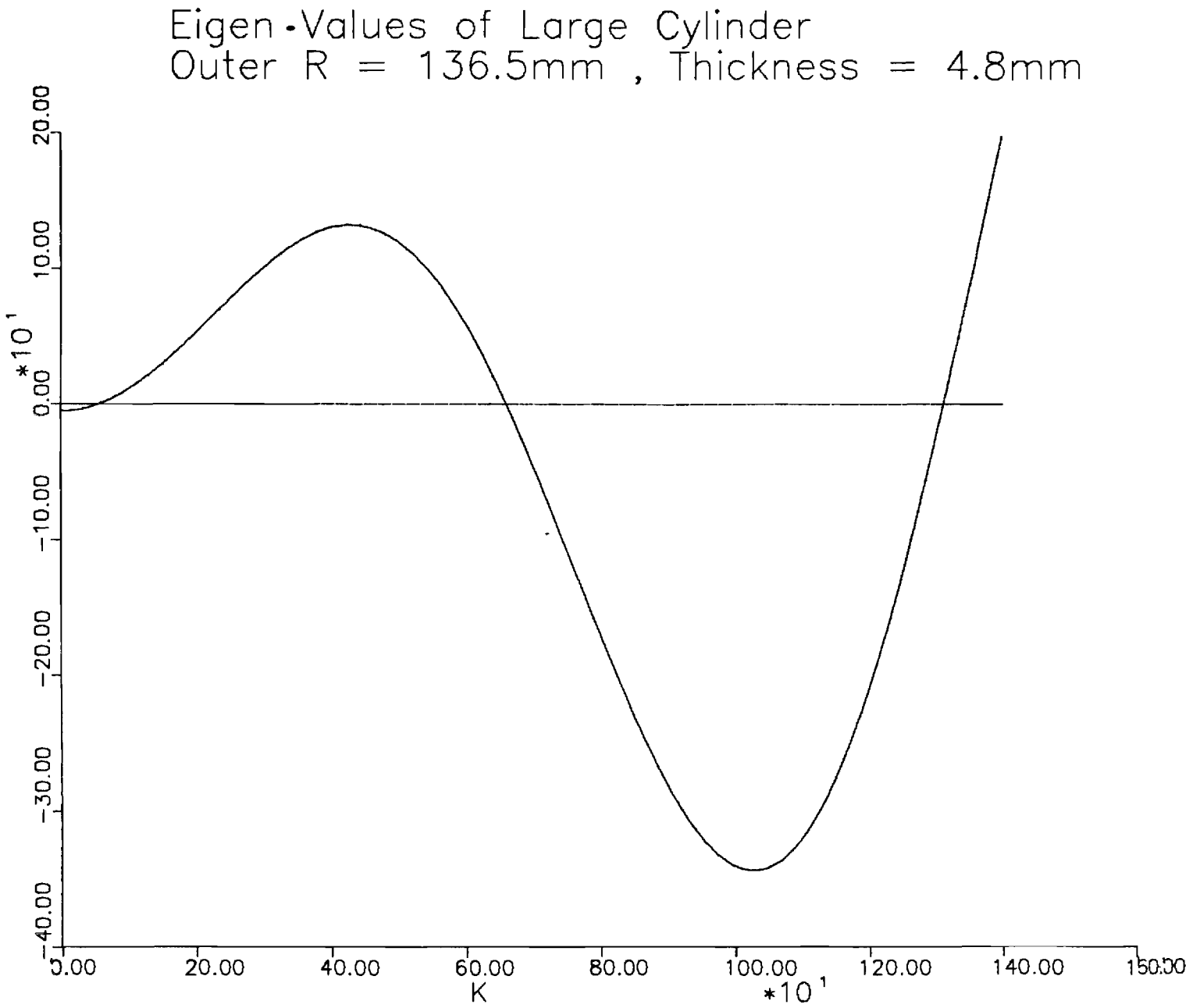

Fig. 8 Plot Eq.(31) versus k; the zero crossings show the eigenvalues expected for the large cylinder.

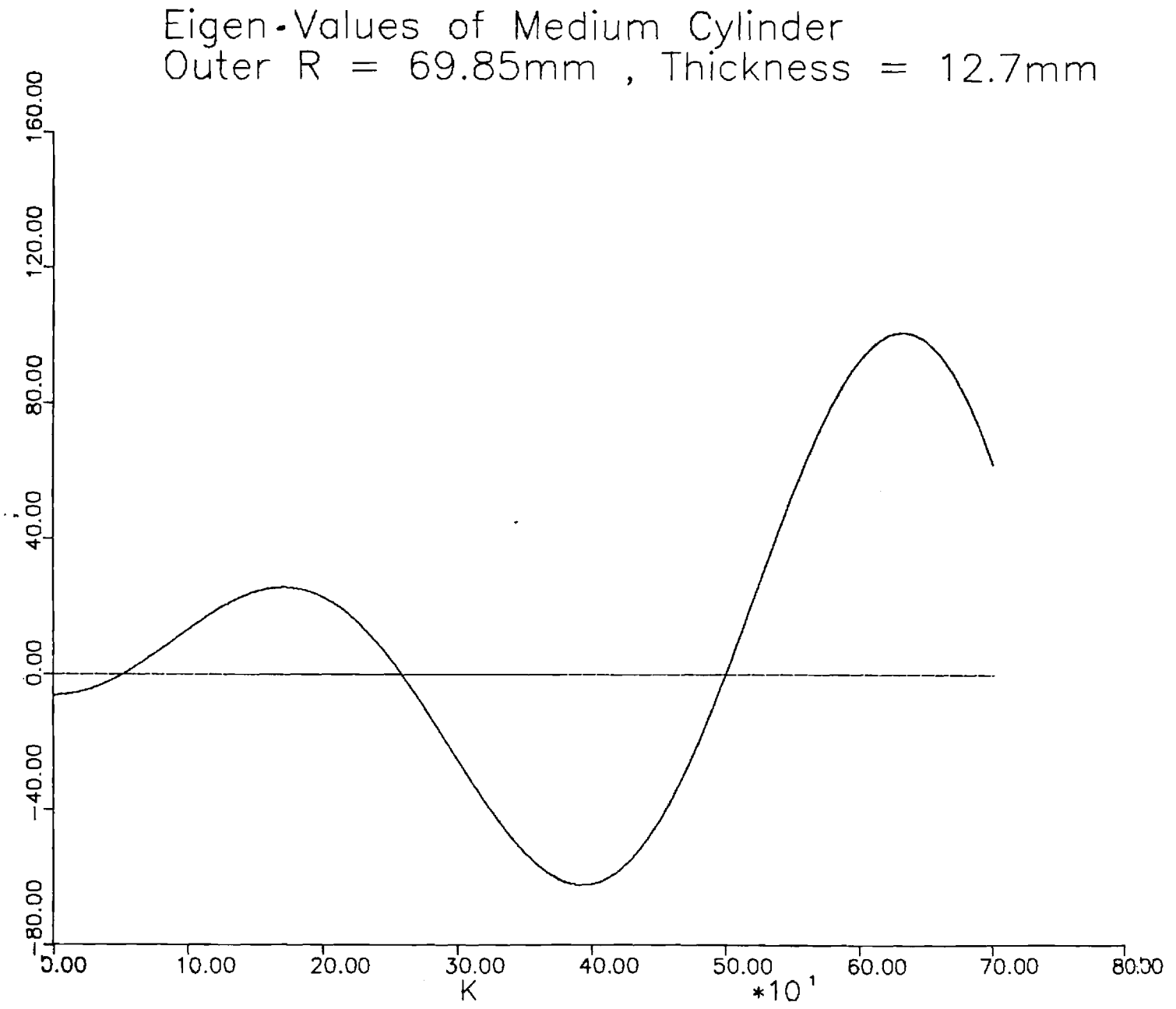

Fig. 9 Plot of Eq.(31) versus k for the medium cylinder; the zero crossings indicate the eigenvalues.

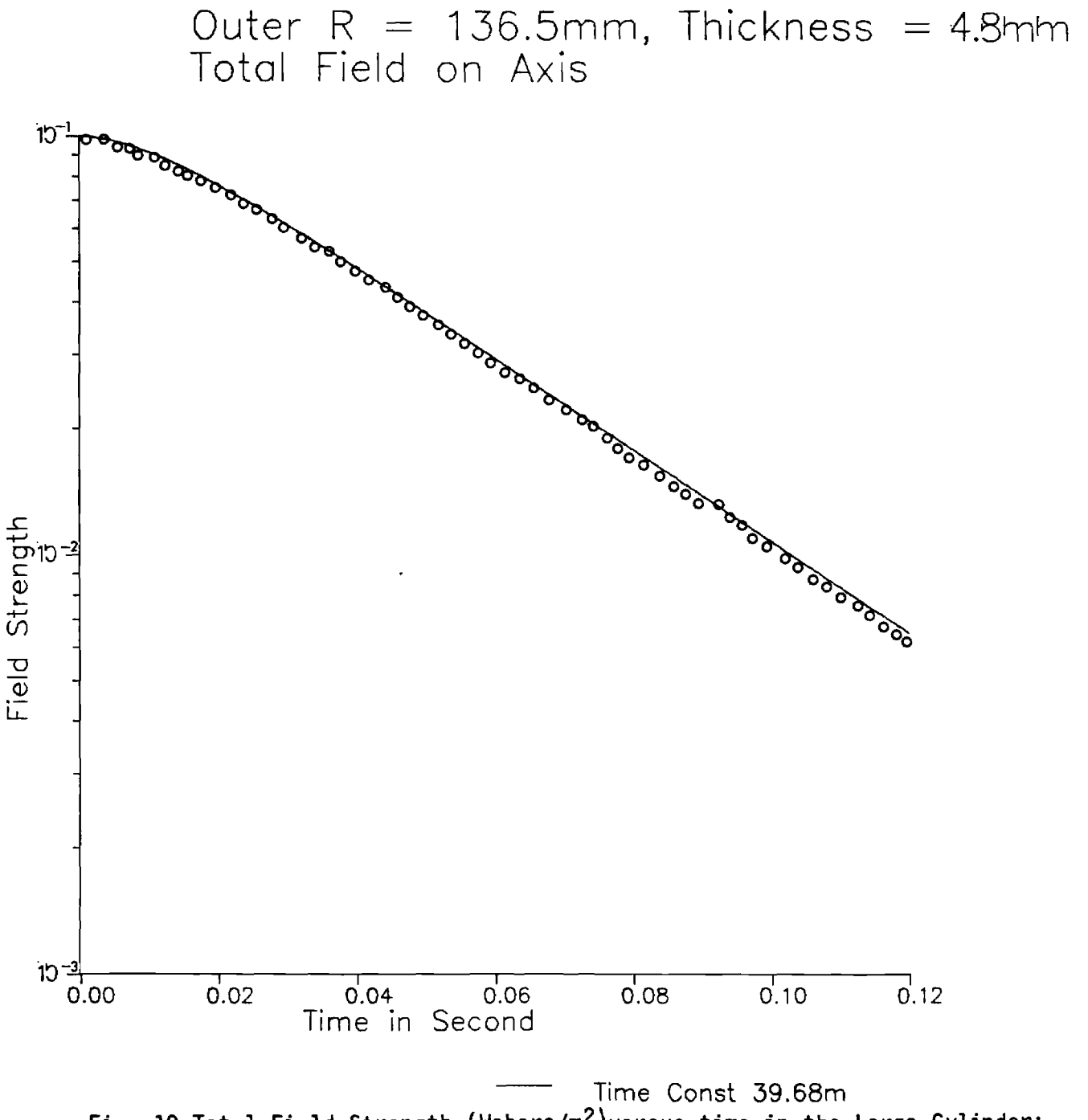

Fig. 10 Total Field Strength (Webers/m^2)versus time in the Large Cylinder; external field constant 39.68 msec. The dots indicate experimental values at the center of the cylinder.

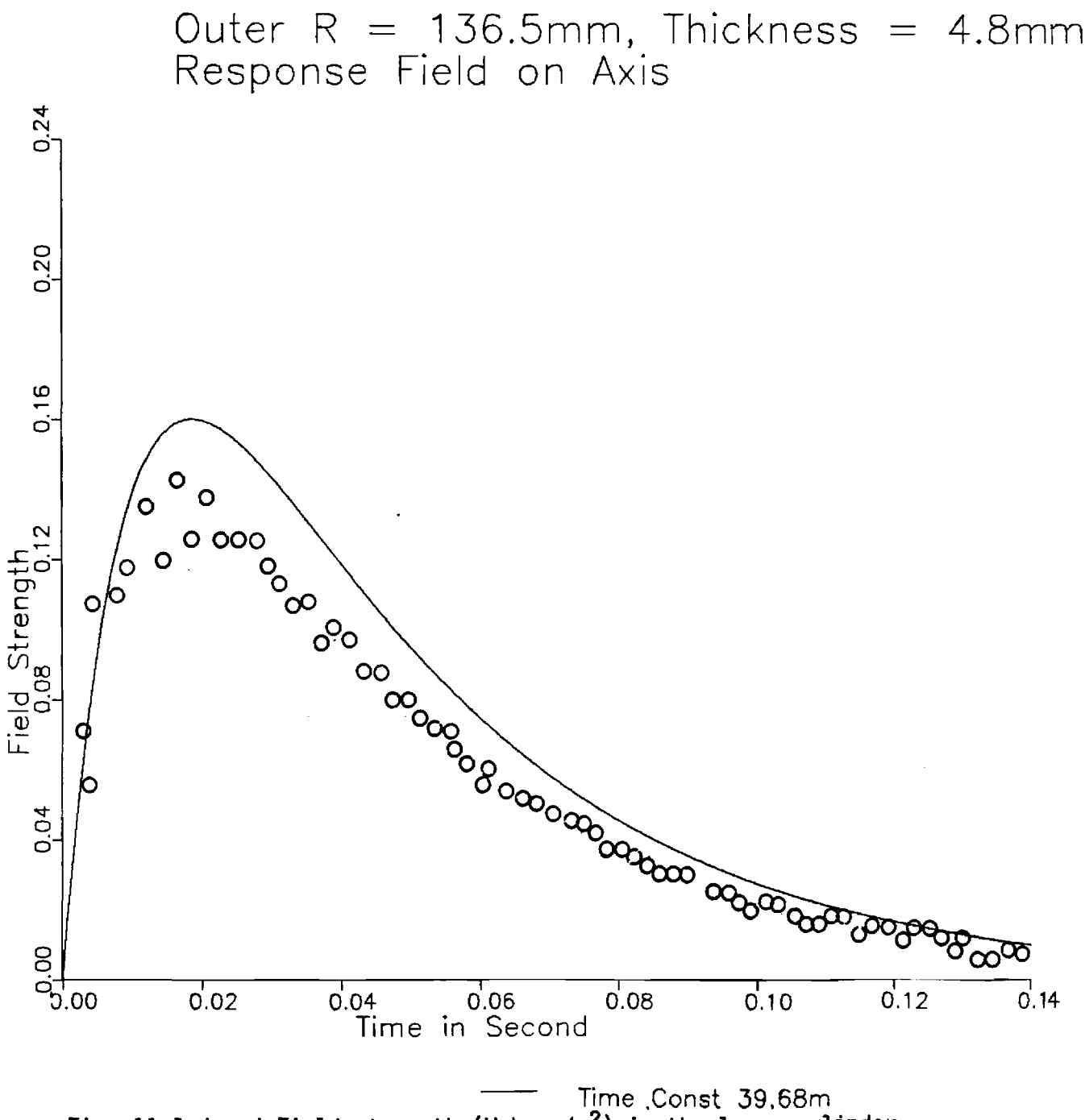

Fig. 11 Induced Field strength (Webers/m^2) in the large cylinder versus time; main field time constant is 39.68 msec. Dots indicate experimental data at the center of the cylinder.

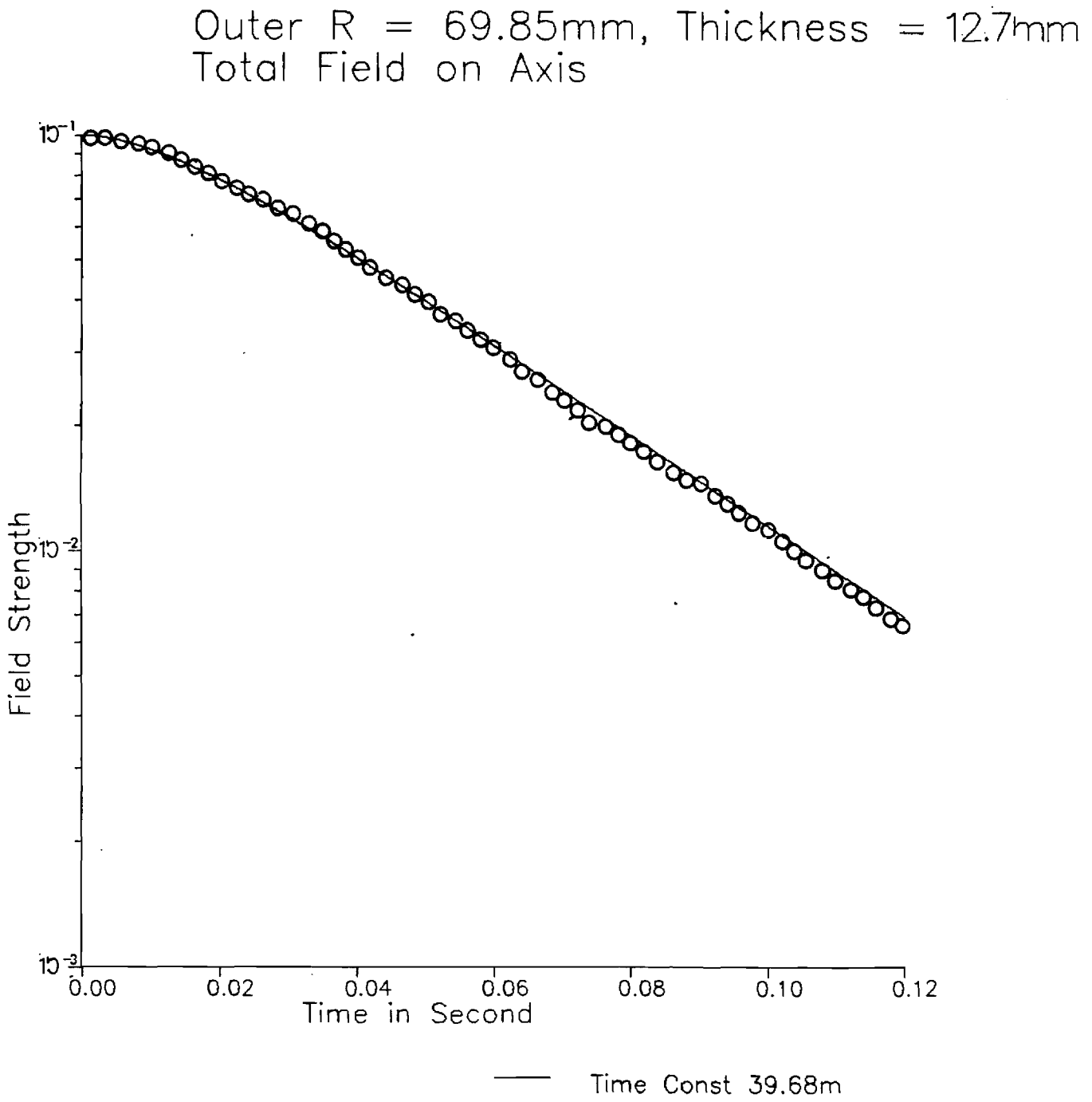

Fig. 12 Total Field response (Webers/m^2) versus time in the medium cylinder; main field time constant is 39.68. Dots indicate experimental data 20 cm from the center of the cylinder along the z axis.

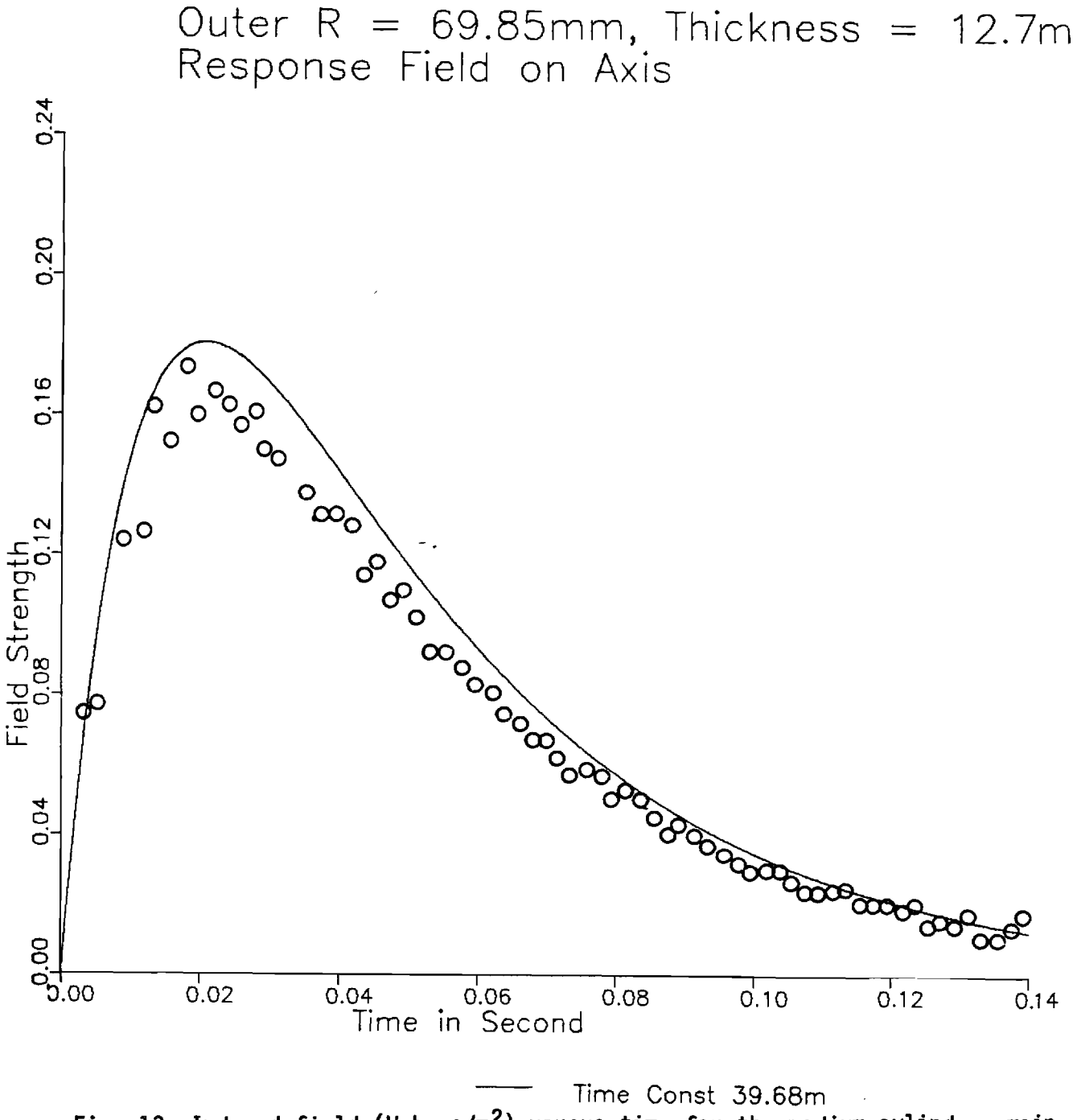

Fig. 13 Induced field (Webers/m^2) versus time for the medium cylinder; main field time constant is 39.68 msec. Dots indicate experimental values 20 cm from the center of the cylinder along the z axis.

Then with $k'^2 = \mu\sigma\lambda$, it follows that

$$\frac{1}{r}\frac{d}{dr}\left(r\frac{dR}{dr}\right) + \left[\left(k'^2 - \ell^2\right) - \frac{m^2}{r^2}\right]R = 0 \tag{35}$$

$$\frac{d^2\theta}{d\theta^2} + m^2\theta = 0 \tag{36}$$

$$\frac{d^2Z}{dz^2} + \ell^2 Z = 0 \tag{37}$$

For our problem meaningful solutions result when $m = 1$, $\ell = n\pi/L$ (i.e., $A \sim \sin\left(\frac{n\pi}{L} z\right)$ where L = total length). From (35) we find a new eigenvalue $k'^2 = k^2 + \ell^2 = k^2 + \left(\frac{n\pi}{L}\right)^2$ with a modified reciprocal time constant $\lambda = \frac{k^2 + (n\pi/L)^2}{\mu\sigma}$. Even for the short cylinder in Felix, the dominant eigenvalues with n = 1 have virtually no length modifications since k is so much larger than π/L.

Discussion and Conclusions

The null field integral technique offers a rather simple method of predicting transient eddy current solutions using small determination matrices. The salient features of the technique revolve around the intelligent choice of interfacial basis functions. These basis functions can be inferred as perturbations from known solutions or from experimental tests. For example, one might conceivably construct a set of basis sets by looking at interfacial field data at t = 0, half way through the process, and near the end of a process.

An extension of the method to the short cylinder considering the 3-D nature of the field can be obtained by constructing the following basis sets for both A_z and A_θ

$$A_z, \frac{\partial A_z}{\partial n} \simeq \sin\theta \cos\frac{\pi}{L} z \tag{38}$$

$$A_\theta, \frac{\partial A_\theta}{\partial n} \simeq \cos\theta \sin\frac{\pi}{L} z \tag{39}$$

where z = 0 is set at the midpoint (L/2) on the cylinder. Using these basis functions will necessitate the construction of an (8 x 8) determination matrix rather than the (4 x 4) used above. Of course, odd multiples of $(\frac{\pi}{L})$ can be used, but these only yield higher order perturbations to the base system eigenvalues.

REFERENCES

[1] W. F. Praeg, et al., "Felix, An Experimental Facility to Study Electromagnetic Effects for First Wall, Blanket, and Shield Systems," Proc. 9th Symp. on Engineering Problems in Fusion Research, IEEE Pub. No. 81, Ch. 1715, pp. 1763-1766, 1981.

[2] L. R. Turner, et al., "Felix Construction Status and Experimental Program," Nucl. Technol./Fusion, Vol. 4, No. 2, Pt. 2, pp. 745-750, 1983.

[3] L. R. Turner, et al., "Results from the Felix Experiments on Electromagnetic Effects in Hollow Cylinders," Fifth Compumag Conference, Fort Collins, Colorado, pp. 356-359, 1985.

[4] S. Zhi-ming, et al., "The Finite Element Solution of Transient Axi Symmetrical Nonlinear Eddy Current Field Problems," Fifth Compumag Conference, Fort Collins, Colorado, pp. 241-244, 1985.

[5] B. Aldefeld, "A Numerical Solution of Transient Nonlinear Eddy Current Problems Including Moving Iron Parts," IEEE Trans. Magnetics, Vol. MAG-14, No. 5, pp. 371-373, 1978.

[6] A. Kameari and Y. Suzuki, "Eddy Current Analysis by the Finite Element Circuit Method," 7th Symposium, Knoxville, Tennessee, pp. 1386-1392.

[7] S. Tandon, A. Armor, and M. V. K. Chan, "Nonlinear Transient Finite Element Field Computation for Electrical Machines and Devices," IEEE Trans. Power App. Sys., Vol. PAS-102, pp. 1089-1096, May 1983.

GEORGIA INSTITUTE OF TECHNOLOGY
SCHOOL OF ELECTRICAL ENGINEERING
ATLANTA, GEORGIA 30332

TELEPHONE: (404) 894-7337

December 11, 1987

Ms. Dianne Hutchinson
Senior Contract Specialist
Argonne National Laboratory
4700 South Cass Avenue
Argonne, IL 60439

RE: Contract No. 51772401 under Prime Contract 31-109-ENG-38 (DOE)
Project Director: K. R. Davey

Dear Ms. Hutchinson:

Enclosed please find copies of the Final Report on the above referenced contract, "Transient Electromagnetic Analysis."

If you have any questions, please feel free to contact me.

Sincerely,

Pam Majors
Research Administrator

pm
Enclosures

THE USE OF TIME SPACE GREEN'S FUNCTIONS IN THE COMPUTATION OF TRANSIENT EDDY CURRENT FIELDS*

by

Kent Davey
School of Electrical Engineering
Georgia Institute of Technology
Atlanta, Georgia 30332-0250

and

Larry Turner
Argonne National Labs
9700 South Cass Avenue
Argonne, Illinois 60439

October 1987

*Work supported by the U.S. Department of Energy.

ABSTRACT

The utility of integral equations to solve eddy current problems has been born out by numerous computations in the past few years. This paper attempts to examine the applicability of the integral approaches in both time and space for the more generic transient problem. The basic formulation for the time space Green's function approach is laid out. A technique employing Gauss-Leguerre integration is employed to realize the temporal solution. The technique is then applied to the FELIX cylinder experiments in both two and three dimensions. It is found that quite accurate solutions can be obtained using rather coarse time steps and very few unknowns; the three-dimensional field solution worked out in this context used basically only four unknowns. The solution appears to be somewhat sensitive to the choice of time step, a consequence of a numercial instability imbedded in the Green's function.

INTRODUCTION

In recent years, there has been increasing use of integral equations in solving eddy current problems [1-6]. Because only the surfaces of conducting regions need discretization, these methods sharply reduce the number of unknowns compared to finite element or finite difference methods. Integral methods are particularly useful involving problems with unbounded regions. They have recently been applied successfully to nonlinear problems [7].

Application of integral equation methods to transient problems has generally employed eigenvalue or Laplace transform techniques [8]. A. Nicolas [9] has suggested an approach using time and space Green's functions. This paper develops and applies Nicolas's method in which the solution is found by integrating both over the interfaces of conducting bodies and over the time interval characterizing the problem.

Theoretical Development

The equation that characterizes the vector potential in a linear piecewise homogeneous region with time variant fields is

$$\nabla^2 A - \mu_o \sigma \frac{\partial A}{\partial \tau} = -\mu_o J_s \ . \tag{1}$$

The development of the governing integral equations in time and space is approached by writing the counterpart of Equation (1) with the Green's function in space and time.

$$\nabla^2 G + \mu_o \sigma \frac{\partial G}{\partial \tau} = -\delta (r_p - r_q, t-\tau) \tag{2}$$

The solution proceeds as follows: First, multiple Equation (1) by the Green's function, Equation (2) by vector potential A, and subtract Equation (2) from Equation (1). The result is as follows:

$$\int_{\tau}\int_{V_q} \nabla\cdot(G\nabla A) - \nabla\cdot(A\nabla G)\,dV_q\,d\tau$$

$$-\int_{\tau}\int_{V_q} (\nabla G\cdot\nabla A - \nabla A\cdot\nabla G)\,dV_q\,d\tau$$

$$-\mu_o\sigma \int_{V_q}\int \frac{d}{d\tau}(AG)\,d\tau\,dV_q$$

$$= -\int_{\tau}\int_{V_q} \mu_o J_s(r_q)G\,dV_q\,d\tau + \varepsilon A(r_p,t)\ , \qquad (3)$$

where ε is unity if the point r_p lies within the volume of interest, one-half if the point lies on the interface of a smooth region boundary, or zero if the point lies outside of the volume of integration. Note that the third integral is a complete integral of the differentiated product AG. Thus, after evaluating this time integral and rearranging terms, one arrives at the following equation:

$$\varepsilon A(r_p,t) = \iint \mu_o J_s(r_p)G\,dV_q\,d\tau + \iint 0\left(\frac{\partial A}{\partial n}(r_q,\tau)G - A(r_q,\tau)\frac{\partial G}{\partial n}\right)dS_q\,d\tau$$

$$-\mu_o\tau\int (AG)\Big]_{t_o}^{t} dV_q \qquad (4)$$

Before proceeding any further, we must consider what Green's functions apply to this problem. The Green's functions satisfying Equation (2) for two,

three, and N dimensional problems are shown in Equations (5) through (7), respectively.

$$G = \frac{1}{4\pi(t-\tau)} \exp\left(\frac{-\mu_o \sigma r^2}{4(t-\tau)}\right) \quad , \quad \text{2D} \tag{5}$$

$$G = \frac{\sqrt{\mu_o \sigma}}{8[\pi(t-\tau)]^{3/2}} \exp\left(\frac{-\mu_o \sigma r^2}{4(t-\tau)}\right) \quad , \quad \text{3D} \tag{6}$$

$$G = \frac{1}{\mu\sigma} \left\{\frac{\sqrt{\mu\sigma}}{2\sqrt{\pi(t-\tau)}}\right\}^n \exp\left(\frac{-\mu_o \sigma r^2}{4(t-\tau)}\right) \quad , \quad \text{n dimensions} \tag{7}$$

where

$$r = |\vec{r}_p - \vec{r}_q| \ .$$

Of significance is the value that G takes as τ approaches the upper limit t. There are two singularities: one going as $\frac{1}{t-\tau}$ and the other going exponentially as $\frac{1}{t-\tau}$. The exponential variation is dominant and forces the upper limit of the third integral expression in Equation (4) to zero. The final expression for the time space Green's function integral becomes:

$$\varepsilon A(r_p,t) = \int_{t_o}^{t} \int \mu_o J_s(r_p) G dV_q d\tau + \int_{t_o}^{t} \oint \left(\frac{\partial A}{\partial n}(r_q,\tau)G - A(r_q,t)\frac{\partial G}{\partial n}\right) dS_q d\tau$$

$$+ \mu_o \sigma \int A(r_q,t_o) G dV_q \tag{8}$$

The use of Equation (8) encounters at least two problem areas. First, two of the three terms on the right-hand side involve a volume integral. The third integral in (8) can be expressed in terms of the interfacial values of A. There are two ways to proceed. The first is to fix the starting time, t_o. Then the last integral in (8) need be evaluated only once. This turns out to be a rather poor choice because it requires the identification matrix,

which one uses to solve for the unknowns embedded in the surface integral, to be reevaluated at every time step. A much more effective approach is to slide the starting time, t_o, along as one progresses through the problem, i.e., to keep $t - t_o$ constant. This forces a new calculation of the volume term in the third integral of (8), but keeps the identification matrix, i.e., the surface integral term, constant throughout the problem. For the test problem chosen in this research, the volume integral could be expressed generically in terms of the interfacial values, thus this integration was accomplished quite quickly at every time step.

The second difficulty results from the nature of the Green's functions in (5) through (7). It is apparent that one cannot choose a simple finite difference approach in a time domain. The value of the integrand, that is of G, is zero at the upper limit of $\tau = t$, the very place that one is seeking the new value of the unknown A, or $\partial A/\partial n$, at any time step. The approach adopted here is to choose A and $\partial A/\partial n$ at the time step t as the unknowns. The value at any intermediate position between t_o and t is assumed to be linear. We employ the Gauss-Laguerre integration quadrature formula to compute the value of this time integration over this very sensitive region. The way in which this is accomplished will now be explained.

Consider a three-dimensional problem and the computation of the second term in the surface integral of (8), i.e., $A\partial G/\partial n$. Let us designate the temporal integral of $A\partial G/\partial n$ as I. The integral that must be performed before the surface integral is:

$$I = \int_0^t A(\tau) \frac{\mu\sigma(\vec{r}\cdot\hat{n})/2}{(4\pi)^{3/2}(t-\tau)^{3/2}} \exp\left(\frac{-\mu\sigma r^2}{4(t-\tau)}\right) d\tau \qquad (9)$$

The integration proceeds by first making the substitution:

$$u = \frac{1}{t - \tau} \tag{10}$$

With this substitution, the integral becomes:

$$I = \frac{\mu\sigma(\vec{r}\,\hat{n})/2}{(4\pi)^{3/2}} \int_{1/t}^{\infty} A\left(t - \frac{1}{u}\right) u^{1/2} \exp\left(\frac{-\mu\sigma r^2 u}{4}\right) du \ . \tag{11}$$

Next, we make the substitution:

$$\beta = \frac{\mu\sigma r^2}{4} u \tag{12}$$

After this substitution, we have:

$$I = \frac{\mu\sigma(\vec{r}\,\hat{n})/2}{(4\pi)^{3/2}} \int_{\frac{\mu\sigma r^2}{4t}}^{\infty} A\left(t - \frac{\mu\sigma r^2}{4\beta}\right)\left(\frac{4}{\mu\sigma r^2}\right)^{3/2} \sqrt{\beta}\, \exp(-\beta)\, d\beta \ . \tag{13}$$

Lastly, let:

$$\lambda = \beta - \frac{\mu\sigma r^2}{4t} \ . \tag{14}$$

The integral becomes:

$$I = \frac{|\vec{r}\,\hat{n}|\, \exp\left(\frac{-\mu\sigma r^2}{4t}\right)}{2r^3\pi^{3/2}} \int_0^{\infty} A\left(t - \frac{1}{\frac{1}{t} + \frac{4\lambda}{\mu\sigma r^2}}\right) \sqrt{\lambda + \frac{\mu\sigma r^2}{4t}}\, e^{-\lambda} d\lambda \ . \tag{15}$$

Note that the integral now runs from zero to infinity; over this range, the index for the vector potential ranges from zero to t. This, of course, is just what we started with, but it allows us to use an accurate integration procedure for determining I. For reference, we include the comparable expressions for the integral of $\frac{\partial A}{\partial n} G$:

$$I \text{ for } \int \frac{\partial A}{\partial n} G = \frac{1}{4(\pi)^{3/2} r} \exp\left(\frac{-\mu\sigma r^2}{4t}\right) \int_0^{\infty} \frac{\partial A}{\partial n}\left(t - \frac{1}{\frac{1}{t} + \frac{4\lambda}{\mu\sigma r^2}}\right) \frac{\exp(-\lambda)}{\sqrt{\lambda + \frac{\mu s \sigma r^2}{4t}}} dA \qquad (16)$$

Their two-dimensional counterparts are:

$$I_{2D} = \int_0^{\infty} \frac{\partial A}{\partial n}\left(t - \frac{1}{\frac{1}{t} + \frac{4\lambda}{\mu\sigma r^2}}\right) \frac{\exp\left(\frac{-\mu\sigma r^2}{4t}\right)}{4\pi\left(\lambda + \frac{\mu\sigma r^2}{4t}\right)} \exp(-\lambda) d\lambda \qquad (17)$$

$$I_{2D}\left(A \frac{\partial G}{\partial n}\right) = \int_0^{\infty} A\left(t - \frac{1}{\frac{1}{t} + \frac{4\lambda}{\mu\sigma r^2}}\right) \frac{(\vec{r}\,\hat{n}) \exp\left(\frac{-\mu\sigma r^2}{4t}\right)}{2\pi r^2} \exp(-\lambda) d\lambda \ . \qquad (18)$$

The advantage of transforming the equations to the above form is realized through the Gauss-Laguerre quadrature integration formula. It basically states that the integration of a function with an exponential multiplier is written as:

$$\int_0^{\infty} f(\lambda) e^{-\lambda} d\lambda = \sum_{i=1}^{N} f(\lambda_i) w_i \ . \qquad (19)$$

Assuming a linear fit between the starting values at t_o and the unknowns at time t allows us, using (19), to write a rather accurate expression for the time integral based on starting and end values only. The contributions from the sum are additive; those involving the starting value become the drive of the right-hand side of the matrix equation. Rather large time steps yield a

reasonably accurate solution. The number of unknowns can be minimized by incorporating basis functions building in some a priori knowledge of the field dependence where possible.

Two and Three-Dimensional Field Conditions for the FELIX Cylinder

The technique was applied to the transient generated by the collapse of an external field stressing a hollow conducting cylinder (the FELIX cylinder experiments [10]). The geometry is shown in Figure 1. In two dimensions, the vector potential is z-directed and takes the form of an unknown constant having a $\sin(\theta)$ dependence. There are thus four unknowns: A and its normal derivative on the inner radius, and the vector potential A and its normal derivative on the outer radius. At time t = 0, A has the following form:

$$A = -H_o r \sin\theta \, \hat{a}_z \, . \tag{20}$$

In three dimensions, the magnetic field must be represented with care. In the air regions, the H field is represented as the gradient of a scalar:

$$\vec{H} = -\nabla\psi \, . \tag{21}$$

In the conductor, the vector potential A has three components, but the radial component and the radial current are small, roughly 10% of the θ and z components. With little loss in accuracy, we represent a vector potential A as:

$$\vec{A} = A_z(r,\theta,z)\hat{a}_z + A_\theta(r,\theta,z)\hat{a}_\theta \tag{22}$$

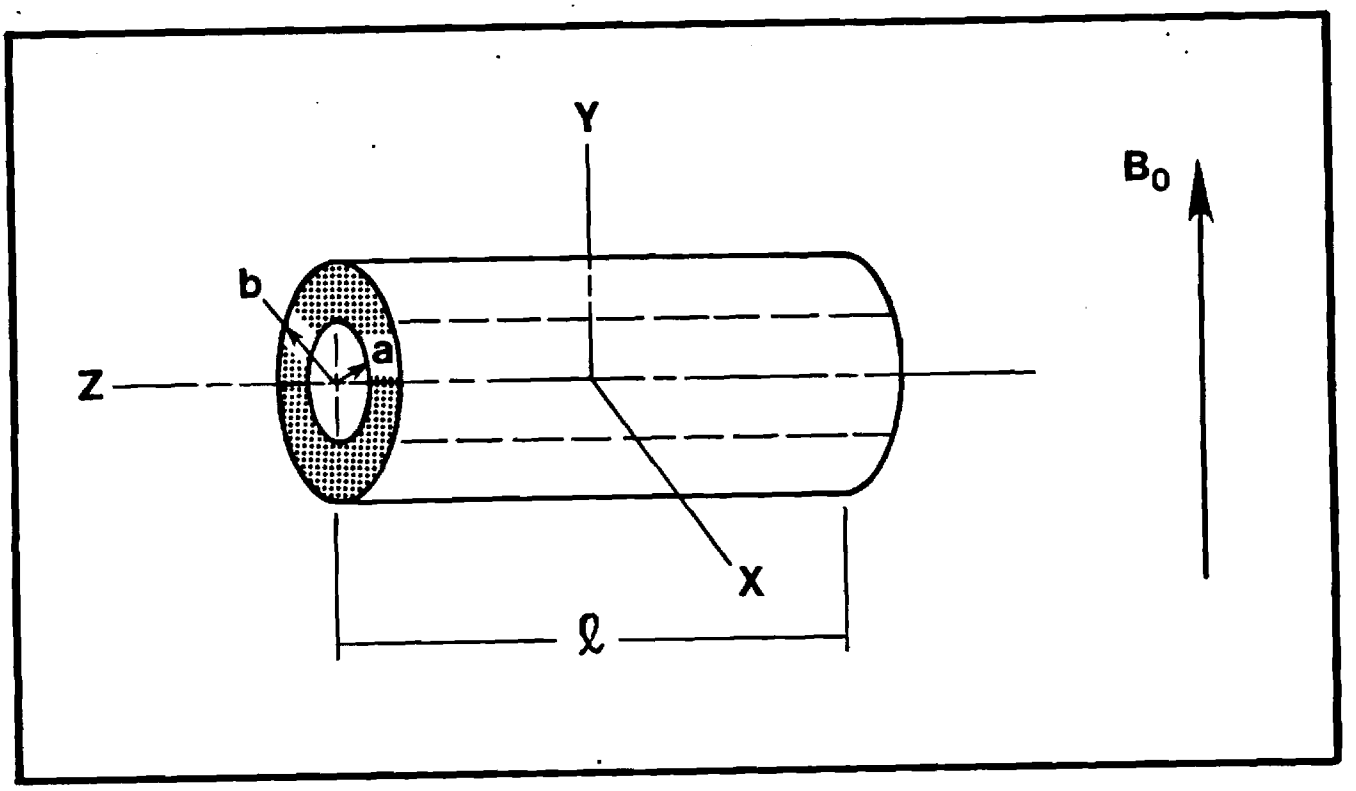

Figure 1. Felix Cylinder stressed by a vertical B field; inner radius a, outer radius b

The current requirements at the end of the cylinder (which has a length ℓ) and the external magnetic field dependence argue for sinusoidal field dependence in both axial and azimuthal directions. The scalar potential, the vector potential components, and the normal derivatives at the inner radius take the following form:

$$\psi(r=a) = \sum_n C_n \cos\theta \cos \frac{n\pi}{\ell} z \tag{23}$$

$$\frac{\partial \psi}{\partial n}(r=a) = \sum_n D_n \cos\theta \cos \frac{n\pi}{\ell} z \tag{24}$$

$$A_z(r=a) = \sum_n E_n \sin\theta \cos \frac{n\pi}{\ell} z \tag{25}$$

$$\frac{\partial A_z}{\partial n}(r=a) = \sum_n F_n \sin\theta \cos \frac{n\pi}{\ell} z \tag{26}$$

$$A_\theta(r=a) = \sum_n I_n \cos\theta \sin \frac{n\pi}{\ell} z \tag{27}$$

$$\frac{\partial A_\theta}{\partial n}(r=a) = \sum_n J_n \cos\theta \sin \frac{n\pi}{\ell} z \tag{28}$$

Boundary conditions are employed to relate the unknowns at the interface $r = a$. The requirement that the normal component of B be continuous implies a connection between the E_n, I_n, and D_n as follows:

$$\frac{\partial A_z}{r\partial\theta} - \frac{\partial A_\theta}{\partial z} = -\frac{\partial \psi}{\partial r} + \frac{E_n}{a} - I_n \frac{n\pi}{\ell} = -D_n \,. \tag{29}$$

The requirement that the θ directed component of H be continuous implies a connection between C_n and F_n:

$$H_\theta = -\frac{\partial A_z}{\partial n} = -\frac{1}{r}\frac{\partial \psi}{\partial \theta} + \frac{C_n}{a} = -F_n \ . \tag{30}$$

Finally, the requirement that the z component of H be continuous implies a connection between the C_n and J_n:

$$H_z = -\frac{\partial A_\theta}{\partial n} = -\frac{\partial \psi}{\partial z} + C_n \frac{n\pi}{\ell} = J_n \ . \tag{31}$$

In addition, we note that the divergence of J is zero in the conductor. This yields an additional relation between E and I which enables us to collapse the problem to only four unknowns at any one time:

$$\nabla \cdot \bar{J} = 0 \rightarrow -E_n \frac{n\pi}{\ell} = \frac{I_n}{r} + E_n\left(\frac{1}{a} + \left(\frac{n\pi}{\ell}\right)^2 a\right) = -D_n \ . \tag{32}$$

In summary, the unknowns at the inner radius r = a involving the vector potentials A_z, A_θ, and their normal derivatives can each be related to the unknowns characterizing the scalar potential, i.e., C and D.

The solution proceeds by noting first the relationship on ψ, i.e., that it satisfies the Laplacian equation:

$$\nabla^2 \psi = 0 \tag{33}$$

The corresponding integral equation:

$$\varepsilon\psi(p) = \oint \left(\frac{\partial \psi}{\partial n} G_{air} - \psi \frac{\partial G_{air}}{\partial n}\, dS_q\right) \tag{34}$$

where

$$G_{air} = \frac{1}{4\pi |\vec{r}_p - \vec{r}_q|}$$

For purposes of nomenclature, we will let the scalar potential ψ and its normal derivative be represented by:

$$\psi(r=b) = \sum_r M_n \cos\theta \cos\frac{n\pi}{\ell} z \tag{35}$$

$$\frac{\partial\psi}{\partial n}(r=b) = \sum_r N_n \cos\theta \cos\frac{n\pi}{\ell} z \,. \tag{36}$$

Thus, for the three-dimensional problem, we have for any one set of eigenmodes n, four unknowns at every time step. The solution proceeds by setting up a matrix equation for these unknowns. The first two equations of the matrix are those for the air, Equation (34), the first with point P on the inner radius and the second with point P on the outer radius. The second two equations are those for the conductor, Equation (8), with a time and space Green's function employed; again, the first with P on the inner radius and the second with P on the outer radius. Only the latter two equations yield nonzero drive terms. These drive terms, which are the only components that change at any given time step, result from two sources.

$$\begin{vmatrix} \text{Air Eqn (34) with P on inner radius} \\ \text{Air Eqn (34) with P on outer radius} \\ \text{Conductor Eqn (8) with P on inner radius} \\ \text{Conductor Eqn (8) with P on outer radius} \end{vmatrix} \begin{vmatrix} C_n \\ D_n \\ M_n \\ N_n \end{vmatrix} = \begin{vmatrix} 0 \\ 0 \\ \text{Contributions from surface terms at time } t_o \text{ from Gauss} \\ + \\ \text{Laquerre and volume terms } \int AGdV \end{vmatrix} \tag{37}$$

As shown in the above equation, the first two contributions come from the surface integral components involving A and its normal derivative at time t_o from the Gauss-Laguerre summation, and the second from the volume integration of AG at the beginning of the time step. It was found that both contributions could be worked out generically in terms of their values at any arbitrary time on the interfaces. Thus, a temporal evolution of the field could be realized rapidly since the matrix equation need be generated only once. A similar approach is adopted for the two-dimensional problem. The 2-D problem is simplified by the fact that there are no higher order modes n to be evaluated. In 3-D, one must calculate a solution for every choice of n and then by superposition get the correct solution.

RESULTS

In the FELIX cylinder, the external applied field decays with a characteristic time constant of 39.68 ms. The distribution of the field at time t = 0 was nearly flat for the medium and small cylinders. A Fourier decomposition of this shape shows that only odd harmonics at N space need be considered, each falling off as $\frac{4}{n\pi}$ with alternating signs. It was found to be more convenient to assume the field decayed instantly from its value at time t_o to zero so as to avoid the integration of currents J_s over the volume, i.e., the first term on the right-hand side of Equation (8). The exact solution is simply calculated as a convolution of the field so determined by the instantaneous decay with the actual field decay of 39.68 ms as described in an earlier paper [11]. Figure 2 shows the results of a two-dimensional prediction of the transient induced field for the large FELIX cylinder having inner radius 13.17 cm, outer radius 13.65 cm, and length 1.2 m in the actual experiment. The results of the two-dimensional calculation are larger than

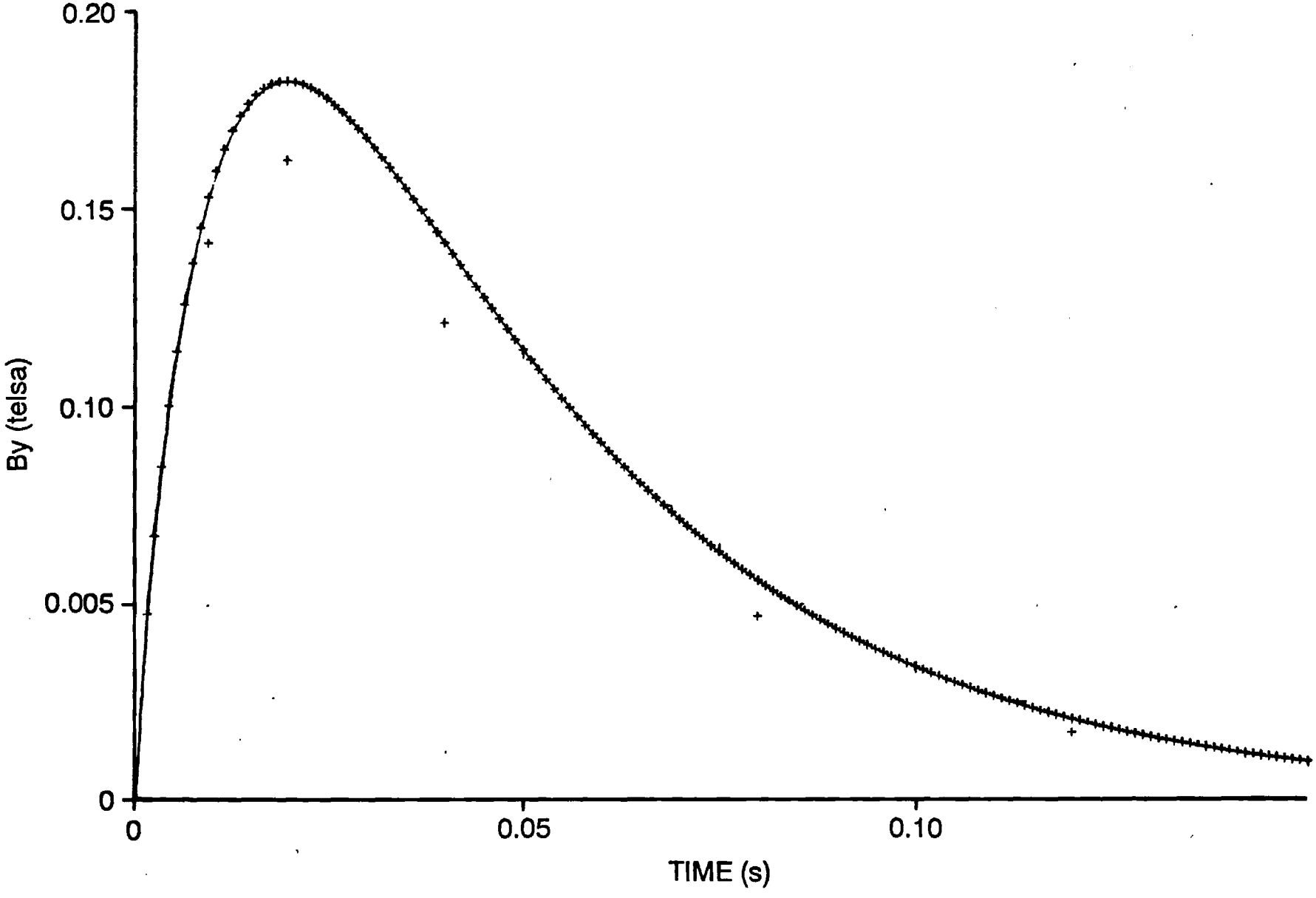

FIG. 2 TWO DIMENSIONAL FIELD PREDICTION USING DELTA T = 1ms COMPARISON TO WORKSHOP CODE-2D PREDICTION (G. RUBINNACCI) FOR THE LARGE FELIX CYLINDER (a = .1317m, b = .1365m, l = 1.2m, EXCITING FIELD TIME CONSTANT = 39.68ms).

those measured in the actual cylinder. They are compared to conventional two-dimensional codes for comparison purposes.

The performance of the three-dimensional code was examined by comparing predicted results to experimental results in a smaller cylinder, the so-called FELIX medium cylinder having an inner radius of 5.7 cm, an outer radius of 6.985 cm, and length of 0.6 m. The conductivity is 2.538×10^7 S/m. The induced field is predicted using the first 13 harmonics and comparing to those measured at the center of the cylinder, $z = 0$ (Figure 3). As would be expected, keeping only the first harmonic yields roughly a 10% deviation from the more exact calculation. The time step for this calculation is 4 ms. By comparison, we also show the predictions for the fields 20 cm along the length, that is 10 cm from the end in Figure 4.

These calculations were performed on a personal computer (Hewlett-Packard 310) and require approximately 4 to 5 minutes for the two-dimensional fields and 15 minutes for the three-dimensional fields (one harmonic only). A 48 point Gauss-Legendre integration was used for all spatial surface integrals and a 15 point Gauss-Laguerre quadrature formula for the time integrals. The accuracy with such a few number of unknowns and rather coarse time steps speaks strongly for the efficacy of this technique.

One negative feature of the approach appears to revolve around the choice of the size of the time step. With the linearity assumed of the field between steps, too large a step quite naturally yields a considerable error in the field prediction. The problem inherent in this procedure is that making the time step too small also results in error. The reason for this centers on the singularity in the Green's functions listed in Equations (5) through (7). A small time step crowds a large number of the Gauss-Laguerre quadrature points close to the singularity of $t = \tau$. Figure 5 illustrates the sensitivity of

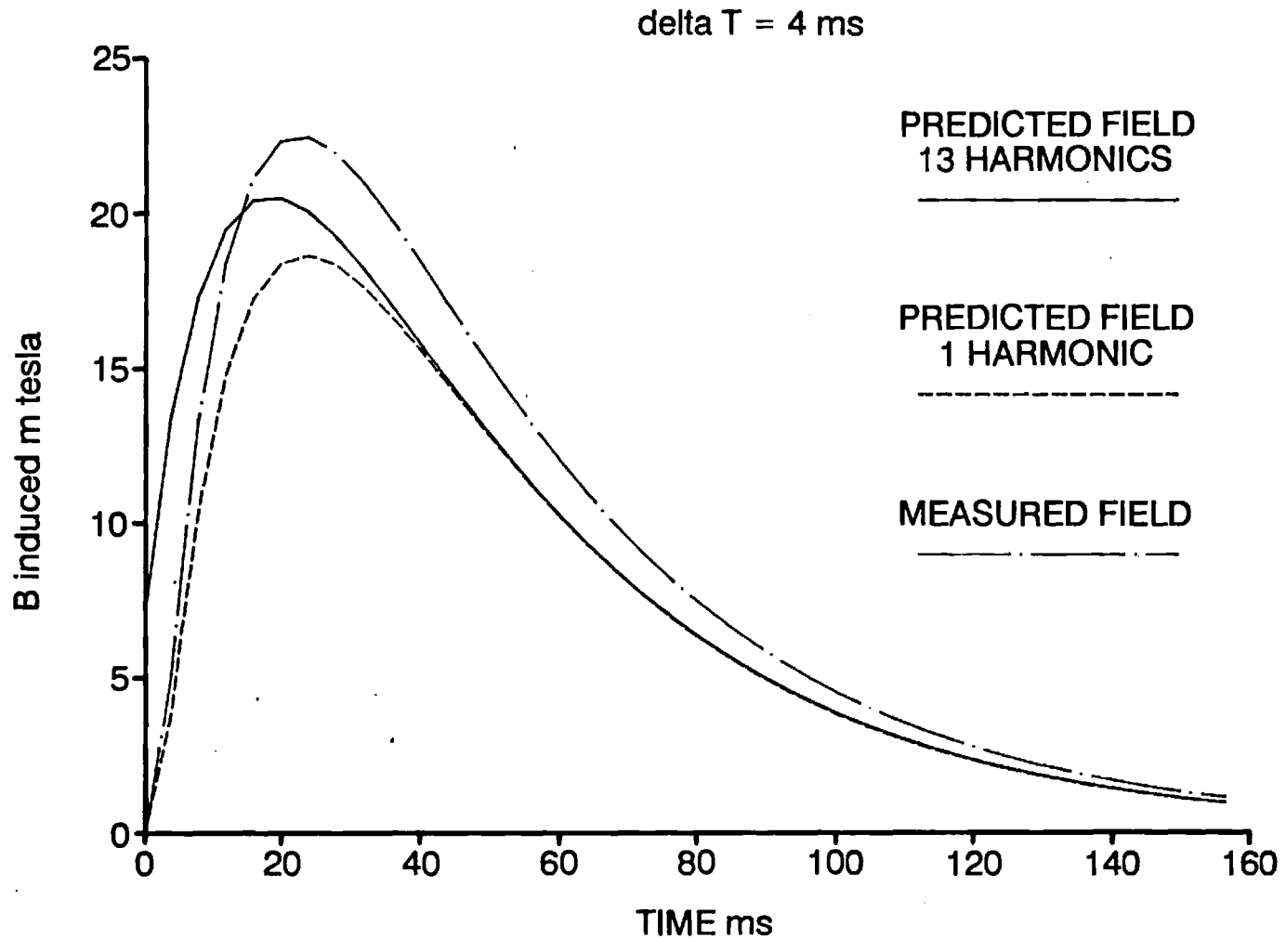

FIG. 3 INDUCED FIELD PREDICTION FOR THE MEDIUM FELIX CYLINDER AT Z = 0 cm.

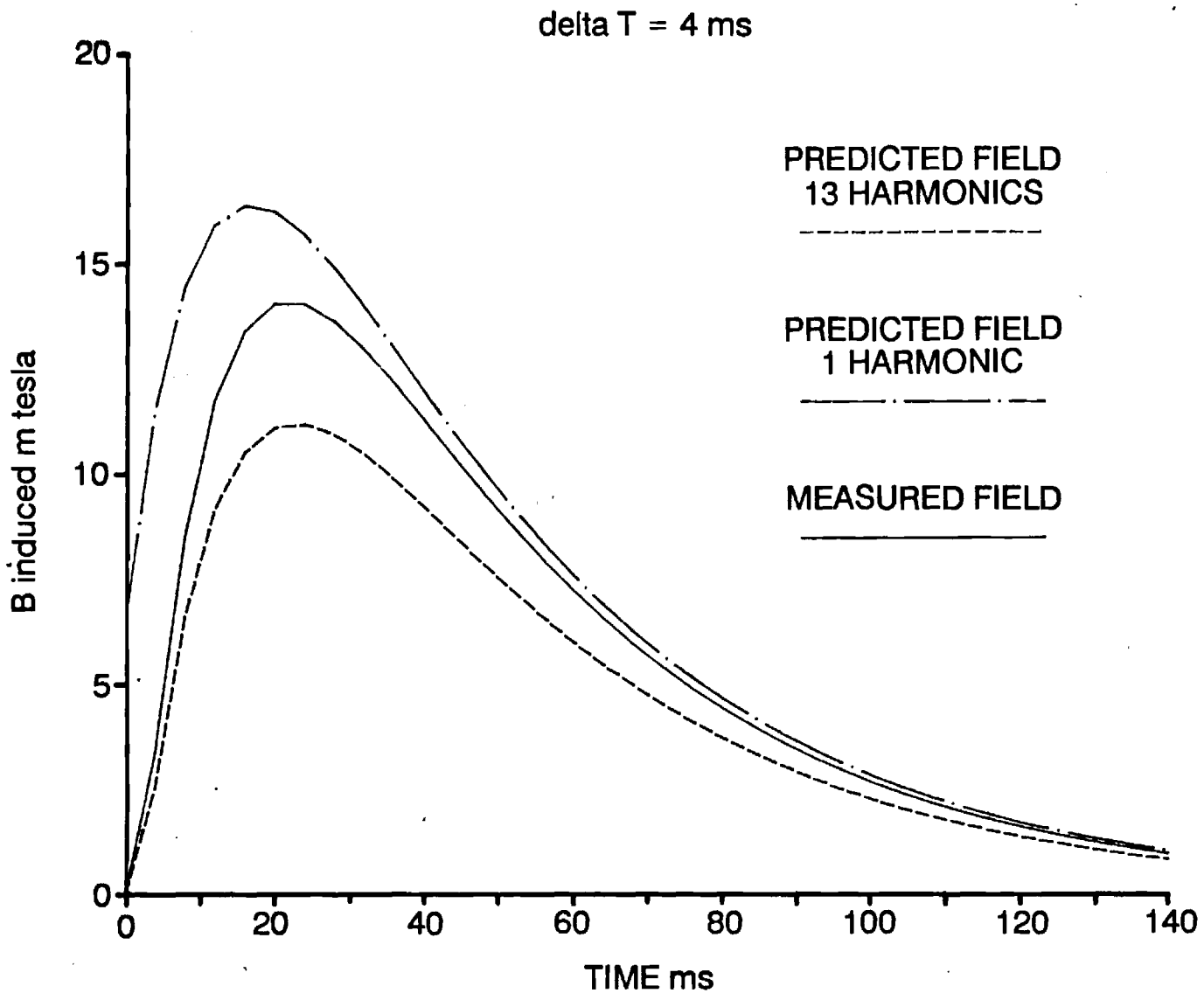

FIG. 4 INDUCED FIELD PREDICTION FOR THE MEDIUM FELIX CYLINDER AT Z = 20 cm.

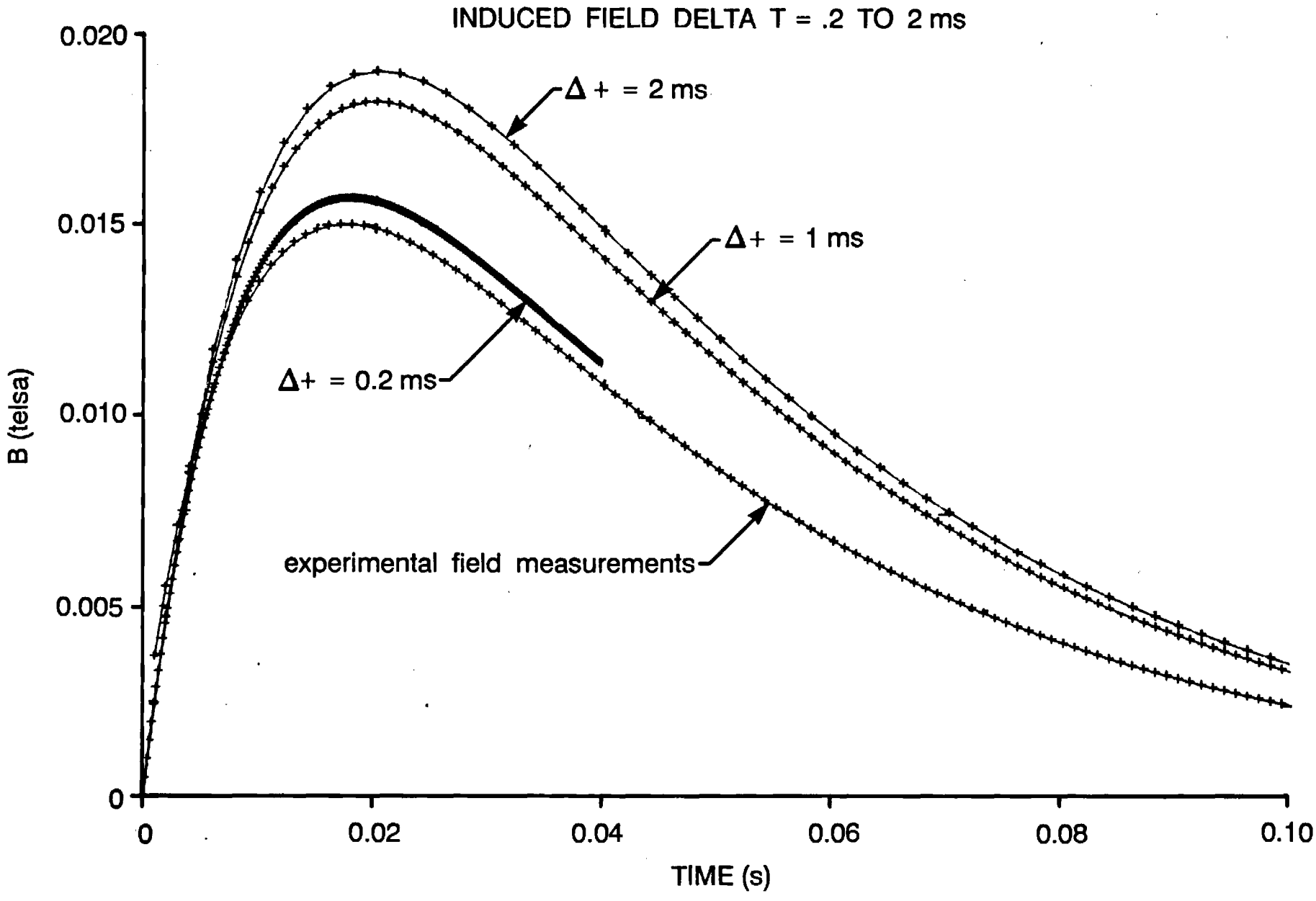

FIG. 5 COMPARISON OF THE 2-D FIELD PREDICTION ON THE LARGE FELIX CYLINDER FOR VARIOUS TIME STEPS t.

the solution to the choice of time step. Here the two-dimensional field prediction is shown for various choices of step size, Δt. A rule of thumb found useful in this regard was to make the step size roughly equal to the smallest time constant generic to the problem, which in this case was the time for the field to diffuse through the thickness of the cylinder, $\tau = \mu\sigma *$ (the thickness of the cylinder)^2.

CONCLUSION

The time space Green's function approach has been applied in two and three dimensions to the FELIX cylinder transient experiments. Reasonably good agreement with experiment and published results were realized. The technique appears to provide one with a useful tool capable of delivering results with very few unknowns and time steps. The technique as proposed is efficient allowing the calculation of governing matrices only once. Additional work should be performed to examine the nature of the singularities involved in the Green's function and their influence on solution accuracy for more complicated shapes.

ACKNOWLEDGEMENT

The work was supported by the U.S. Department of Energy.